

Low energy analysis of $\pi N \rightarrow \pi N$

T. Becher^a and H. Leutwyler^b

^a Newman Laboratory of Nuclear Studies, Cornell University,
Ithaca, NY 14853, USA

^b Institute for Theoretical Physics, University of Bern,
Sidlerstr. 5, CH-3012 Bern, Switzerland

Abstract

We derive a representation for the pion nucleon scattering amplitude that is valid to the fourth order of the chiral expansion. To obtain the correct analytic structure of the singularities in the low energy region, we have performed the calculation in a relativistic framework (infrared regularization). The result can be written in terms of functions of a single variable. We study the corresponding dispersion relations and discuss the problems encountered in the straightforward nonrelativistic expansion of the infrared singularities. As an application, we evaluate the corrections to the Goldberger-Treiman relation and to the low energy theorem that relates the value of the amplitude at the Cheng-Dashen point to the σ -term. While chiral symmetry does govern the behaviour of the amplitude in the vicinity of this point, the representation for the scattering amplitude is not accurate enough to use it for an extrapolation of the experimental data to the subthreshold region. We propose to perform this extrapolation on the basis of a set of integral equations that interrelate the lowest partial waves and are analogous to the Roy equations for $\pi\pi$ scattering.

Contents

1	Introduction	4
2	Kinematics	7
3	Effective Lagrangian	8
4	Tree graphs	10
5	One loop graphs in infrared regularization	13
5.1	Infrared regularization	13
5.2	Comparison with dimensional regularization	15
6	Simplification of the $O(q^4)$ diagrams	16
7	Wave function renormalization	17
8	Chiral expansion of m_N, $g_{\pi N}$ and g_A	19
9	Strength of infrared singularities	21
10	Goldberger-Treiman relation	23
11	Low energy theorems for D^+ and D^-	25
12	Subthreshold expansion	26
13	Chiral symmetry	28
14	Cuts required by unitarity	32
14.1	s -channel cuts	33
14.2	t -channel cuts	34
14.3	Box graph	35
15	Dispersive representation	36
16	Subtracted dispersion integrals	38
17	Dispersion relations versus loop integrals	40
18	Chiral expansion of the amplitude	41
18.1	t -channel cut	42
18.2	s -channel cut	43

18.3 Chiral expansion of the dispersion integrals	45
19 Higher orders	47
20 Values of the coupling constants of $\mathcal{L}_N^{(2)}$	49
21 S-wave scattering lengths	50
22 Total cross section	52
23 Analog of the Roy equations	54
24 Summary and conclusion	58
A Notation	60
B Off-shell πN-amplitude	63
C One-loop integrals	64
D Results for the loop graphs	66
D.1 Loop graphs of $\mathcal{L}^{(1)}$	67
D.2 Loop graphs of $\mathcal{L}^{(2)}$	70
E Renormalization of the effective couplings	72
F Subthreshold coefficients	73
G t-channel partial waves	76
H Imaginary parts of the loop integrals	77
I Low energy expansion of the loop integrals	80
J Low energy expansion of the amplitude	84
K Integral equations for πN scattering	87

1 Introduction

Here, perhaps an accuracy of 5 per cent is more appropriate.

Henley and Thirring ([1], 1962) on the static model.

The description of the pion nucleon interaction in terms of effective fields has quite a long history. The static model represents a forerunner of the effective theories used today. In this model, the kinetic energy of the nucleon is neglected: The nucleon is described as a fixed source that only carries spin and isospin degrees of freedom. For an excellent review of the model and its application to several processes of interest, we refer to the book of Henley and Thirring [1].

The systematic formulation of the effective theory relies on an expansion of the effective Lagrangian in powers of derivatives and quark masses. Chiral symmetry implies that the leading term of this expansion is fully determined by the pion decay constant, F_π , and by the nucleon matrix element of the axial charge, g_A . Disregarding vertices with three or more pions, the explicit expression for the leading term reads

$$\mathcal{L}_{eff} = -\frac{g_A}{2F_\pi} \bar{\psi} \gamma^\mu \gamma_5 \partial_\mu \pi \psi + \frac{1}{8F_\pi^2} \bar{\psi} \gamma^\mu i[\pi, \partial_\mu \pi] \psi + \dots$$

The success of the static model derives from the fact that it properly accounts for the first term on the right hand side – in the nonrelativistic limit, where the momentum of the nucleons is neglected compared to the nucleon mass.

The static model is only a model. In order for the effective theory to correctly describe the properties of QCD at low energies, that framework must be extended, accounting for the second term in the above expression for the effective Lagrangian, for the vertices that contain three or more pion fields, for the contributions arising at higher orders of the derivative expansion, as well as for the chiral symmetry breaking terms generated by the quark masses m_u, m_d . A first step in this direction was taken by Gasser, Sainio and Švarc [2], who formulated the effective theory in a manifestly Lorentz invariant manner. In that framework, chiral power counting poses a problem: The loop graphs in general start contributing at the same order as the corresponding tree level diagrams, so that the loop contributions in general also renormalize the lower order couplings. A method that does preserve chiral power counting at the expense of manifest Lorentz invariance was proposed by Jenkins and Manohar [3], who used a nonrelativistic expansion for the nucleon kinematics. The resulting framework is called “Heavy Baryon Chiral Perturbation Theory” (HBCHPT). It represents an extension of the static

model that correctly accounts for nucleon recoil, order by order in the nonrelativistic expansion (for reviews of this approach, see for instance refs. [4, 5]). In [6, 7], this formalism has been used to obtain an $O(q^3)$ representation for the pion nucleon scattering amplitude. In the meantime, the HBCHPT calculation has been extended to $O(q^4)$ [8].

As pointed out in ref. [9], the nonrelativistic expansion of the infrared singularities generated by pion exchange is a subtle matter. The HBCHPT representations of the scattering amplitude or of the scalar nucleon form factor, for example, diverge in the vicinity of the point $t = 4M_\pi^2$. The problem does not arise in the Lorentz invariant approach proposed earlier [2]. It originates in the fact that for some of the graphs, the loop integration cannot be interchanged with the nonrelativistic expansion.

The reformulation of the effective theory given in ref. [9] exploits the fact that the infrared singular part of the one loop integrals can unambiguously be separated from the remainder. To any finite order of the nonrelativistic expansion, the regular part represents a polynomial in the momenta. Moreover, the singular and regular pieces separately obey the Ward identities of chiral symmetry. This ensures that a suitable renormalization of the effective coupling constants removes the regular part altogether. The resulting representation for the various quantities of interest combines the virtues of the heavy baryon approach with those of the relativistic formulation of ref. [2]: The perturbation series can be ordered with the standard chiral power counting and manifest Lorentz invariance is preserved at every stage of the calculation. The method has recently been extended to the multi-nucleon sector [10].

Previously, this framework has been applied in calculations of the scalar, axial and electromagnetic form factors [9, 11, 12]. In the present paper, we use it to derive a representation for the pion nucleon scattering amplitude which is valid to the fourth order of the chiral expansion. After a comparison of infrared regularization with standard dimensional regularization, we discuss some technical issues in the evaluation of the Feynman diagrams. In sec. 8 we give the chiral expansion of the masses and of the pion nucleon coupling constant $g_{\pi N}$. By comparing the quark mass dependence of the pion and the nucleon mass, we illustrate that the infrared singularities encountered in the baryon sector are considerably stronger than in the Goldstone sector.

In secs. 10–13 we discuss the constraints that chiral symmetry imposes on the scattering amplitude. Using the result for the axial coupling constant g_A obtained by Kambor and Mojžiš [13], we show that the Goldberger-Treiman relation is free of infrared singularities up to and including $O(q^3)$. Our calculation confirms a result obtained in [14]: The difference between the Σ -Term

and the scalar form factor at $t = 2M_\pi^2$ does not involve a chiral logarithm at order q^4 – the chiral expansion of the difference $\Sigma - \sigma(2M_\pi^2)$ starts with a term proportional to the square of the quark masses.

In section 14 we discuss the analytic structure of the amplitude. There are three categories of branch cuts in the one loop amplitude: cuts in the variables s and u due to πN -intermediate states and cuts arising from $\pi\pi$ - and $\bar{N}N$ -intermediate states in the t -channel. The box graph is the only contribution to the amplitude which contains a simultaneous cut in two kinematic variables. Since the $\bar{N}N$ cut only starts at $t = 4m_N^2$, far outside the low energy region, its contribution to the amplitude is well represented by a polynomial. We make use of this fact to simplify the t -dependence of the box graph. Dropping higher order terms suppressed by $t/4m_N^2$, the amplitude is given by the Born-term, a crossing symmetric polynomial of order q^4 and 9 functions of a *single* variable, either s , t or u . These functions are given by dispersion integrals over the imaginary parts of the one loop graphs.

The representation in terms of dispersion integrals contains terms of arbitrarily high order in the chiral expansion. The expansion of the integrals can be carried out explicitly. Truncating the series at $O(q^4)$, we obtain a simple, explicit representation of the scattering amplitude in terms of elementary functions. The result can be compared directly with the representation obtained in HBCHPT, where the chiral expansion of the loop integrals is performed ab initio. In contrast to that approach, our method allows us to examine the convergence of the chiral expansion of the loop integrals. The matter is discussed in detail in section 18, where we point out that the infrared singularities contained in these integrals give rise to several problems. In particular, we show that the kinematic variables must be chosen carefully for the truncated expansion to represent a decent approximation. This leads to considerable complications in the analysis. Our dispersive representation of the scattering amplitude is comparatively simple and is perfectly adequate for numerical analysis.

The representation of the scattering amplitude to $O(q^4)$ neither includes the cuts due to the exchange of more than two stable particles nor the poles on unphysical sheets generated by resonances. It accounts for these effects only summarily, through their contribution to the effective coupling constants. Since the Δ -resonance lies close to the physical threshold it generates significant curvature in that region. In section 19 we discuss the role of the higher order contributions both in the real and the imaginary part of the amplitude.

Using the example of the S -wave scattering lengths, we illustrate that the one loop representation of chiral perturbation theory does not cover a sufficiently large kinematic range to serve as a bridge between the experimentally

accessible region and the Cheng-Dashen point. The problem arises because the one loop amplitude fulfills the unitarity condition only up to higher orders in the chiral expansion and the perturbative series for the amplitude goes out of control immediately above threshold. In sec. 22 we discuss these unitarity violations on the basis of the optical theorem.

We conclude that a reliable extrapolation from the physical region to the Cheng-Dashen point can only be obtained by means of dispersive methods and propose a set of integral equations for the lowest partial waves, similar to the Roy equations [15] for $\pi\pi$ -scattering. Based on partial wave relations [16, 17], they allow for a determination of the S - and P -waves in the elastic region from their imaginary part at higher energies. The structure of the amplitude that underlies these equations matches the representation obtained in chiral perturbation theory, but in contrast to that representation, the lowest partial waves strictly obey the constraints imposed by unitarity. These equations allow us to extend the region where the one loop approximation of chiral perturbation theory provides a reliable description of the scattering amplitude. In the case of $\pi\pi$ scattering, the method has been shown to yield a remarkably accurate representation of the amplitude throughout the elastic region [18, 19]. We expect that the application of this method to πN scattering will lead to a reliable determination of the pion nucleon σ -term.

2 Kinematics

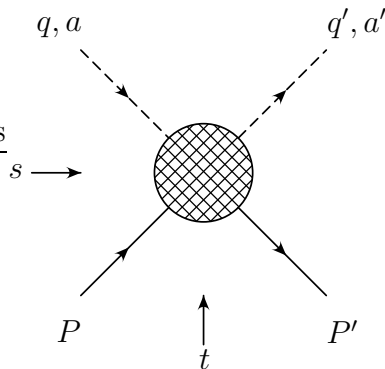


Figure 1: Kinematics of the elastic πN scattering amplitude. P, q (P', q') denote the momentum of the incoming (outgoing) nucleons and pions, and a (a') stands for the isospin index of the incoming (outgoing) pion.

We consider the scattering amplitude on the mass shell,

$$P^2 = P'^2 = m_N^2, \quad q^2 = q'^2 = M_\pi^2.$$

In view of crossing symmetry, it is often convenient to express the energy dependence in terms of the variable

$$\nu = \frac{s - u}{4m_N} .$$

The standard decomposition involves the four Lorentz invariant amplitudes A^\pm, B^\pm :

$$\begin{aligned} T_{a'a} &= \delta_{a'a} T^+ + \frac{1}{2} [\tau_{a'}, \tau_a] T^- \\ T^\pm &= \bar{u}' \left\{ A^\pm + \frac{1}{2} (\not{q}' + \not{q}) B^\pm \right\} u . \end{aligned}$$

This decomposition is not suited to perform the low energy expansion of the amplitude, because the leading contributions from A and B cancel. We replace A by $D \equiv A + \nu B$, so that the scattering amplitude takes the form

$$T^\pm = \bar{u}' \left\{ D^\pm - \frac{1}{4m_N} [\not{q}', \not{q}] B^\pm \right\} u .$$

Our evaluation of the chiral perturbation series to one loop allows us to calculate the amplitudes D^\pm and B^\pm to $O(q^4)$ and $O(q^2)$, respectively.

3 Effective Lagrangian

The variables of the effective theory are the meson field $U(x) \in \text{SU}(2)$ and the Dirac spinor $\psi(x)$ describing the degrees of freedom of the nucleon. The quark mass matrix $m_q = \text{diag}(m_u, m_d)$ only enters the effective Lagrangian together with the constant B that specifies the magnitude of the quark condensate in the chiral limit. As usual, we denote the relevant product by $\chi = 2Bm_q$. The constant B also determines the leading term in the chiral expansion of the square of the pion mass, which we denote by M^2 ,

$$M^2 \equiv (m_u + m_d)B .$$

We disregard isospin breaking effects and set $m_u = m_d$.

The effective Lagrangian relevant for the sector with baryon number equal to one contains two parts,

$$\mathcal{L}_{eff} = \mathcal{L}_\pi + \mathcal{L}_N .$$

The first one only involves the field $U(x)$ and an even number of derivatives thereof. Using the abbreviations

$$u^2 = U , \quad u_\mu = iu^\dagger \partial_\mu U u^\dagger , \quad \Gamma_\mu = \frac{1}{2} [u^\dagger, \partial_\mu u] , \quad \chi_\pm = u^\dagger \chi u^\dagger \pm u \chi^\dagger u ,$$

this part of the Lagrangian takes the form ¹

$$\mathcal{L}_\pi = \frac{1}{4}F^2\langle u_\mu u^\mu + \chi_+ \rangle + \frac{1}{8}l_4\langle u_\mu u^\mu \rangle\langle \chi_+ \rangle + \frac{1}{16}(l_3 + l_4)\langle \chi_+ \rangle^2 + O(q^6) . \quad (3.1)$$

The expression agrees with the one used in ref. [2], but differs from the Lagrangian in ref. [20] by a term proportional to the equation of motion. The difference is irrelevant, because it amounts to a change of the meson field variables. For the physical quantities to remain the same, this change of variables, however, also needs to be performed in the term \mathcal{L}_N – the significance of the effective coupling constants occurring in that term does depend on the specific form used for \mathcal{L}_π [21].

The term \mathcal{L}_N is bilinear in $\bar{\psi}(x)$, $\psi(x)$ and the derivative expansion contains odd as well as even powers of momentum:

$$\mathcal{L}_N = \mathcal{L}_N^{(1)} + \mathcal{L}_N^{(2)} + \mathcal{L}_N^{(3)} + \dots$$

The leading contribution is fully determined by the nucleon mass m_N , the pion decay constant F_π and the matrix element of the axial charge g_A . We denote the values of these quantities in the chiral limit by m , F and g , respectively. With $D_\mu \equiv \partial_\mu + \Gamma_\mu$, the explicit expression then takes the form

$$\mathcal{L}_N^{(1)} = \bar{\psi} (i\not{D} - m) \psi + \frac{1}{2} g \bar{\psi} \psi \gamma_5 \psi ,$$

The Lagrangian of order q^2 contains four independent coupling constants²

$$\begin{aligned} \mathcal{L}_N^{(2)} = & c_1 \langle \chi_+ \rangle \bar{\psi} \psi - \frac{c_2}{4m^2} \langle u_\mu u_\nu \rangle (\bar{\psi} D^\mu D^\nu \psi + \text{h.c.}) \\ & + \frac{c_3}{2} \langle u_\mu u^\mu \rangle \bar{\psi} \psi - \frac{c_4}{4} \bar{\psi} \gamma^\mu \gamma^\nu [u_\mu, u_\nu] \psi . \end{aligned} \quad (3.2)$$

The terms $\mathcal{L}_N^{(3)}$ and $\mathcal{L}_N^{(4)}$ enter the representation of the scattering amplitude to $O(q^4)$ only at tree level. The Lagrangian of order $O(q^3)$ is taken from

¹In the notation of ref. [20], the matrix U stands for $U = U^0 + i \vec{\tau} \cdot \vec{U}$. In the isospin limit, we have $\chi_+ = 2M^2 U^0$, $\chi_- = -2iM^2 \vec{\tau} \cdot \vec{U}$, so that $\langle \chi_- \rangle = 0$, $\langle \chi_-^2 \rangle = \frac{1}{2} \langle \chi_+ \rangle^2 - 4 \langle \chi^\dagger \chi \rangle$.

²We use the conventions of ref. [22]. In this notation, the coupling constants of ref. [2] are given by: $m c_1^{GSS} = F^2 c_1$, $m c_2^{GSS} = -F^2 c_4$, $m c_3^{GSS} = -2F^2 c_3$, $m (c_4^{GSS} - 2m c_5^{GSS}) = -F^2 c_2$ (to order q^2 , the terms c_4^{GSS} and c_5^{GSS} enter the observables only in this combination), while those of ref. [21] read: $16 a_1 = 8 m c_3 + g^2$, $8 a_2 = 4 m c_2 - g^2$, $a_3 = m c_1$, $4 a_5 = 4 m c_4 + 1 - g^2$. In the numerical analysis, we work with $F_\pi = 92.4 \text{ MeV}$, $g_A = 1.267$, $m_N = m_p$, $M_\pi = M_{\pi^+}$.

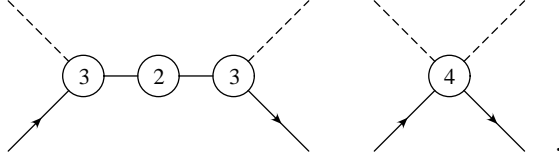
ref. [7]:

$$\begin{aligned}
\mathcal{L}_N^{(3)} = \bar{\psi} \Big\{ & -\frac{d_1 + d_2}{4m} ([u_\mu, [D_\nu, u^\mu] + [D^\mu, u_\nu]] D^\nu + \text{h.c.}) \\
& + \frac{d_3}{12m^3} ([u_\mu, [D_\nu, u_\lambda]] (D^\mu D^\nu D^\lambda + \text{sym.}) + \text{h.c.}) \\
& + \frac{i d_5}{2m} ([\chi_-, u_\mu] D^\mu + \text{h.c.}) \\
& + \frac{i (d_{14} - d_{15})}{8m} (\sigma^{\mu\nu} \langle [D_\lambda, u_\mu] u_\nu - u_\mu [D_\nu, u_\lambda] \rangle D^\lambda + \text{h.c.}) \\
& + \frac{d_{16}}{2} \gamma^\mu \gamma_5 \langle \chi_+ \rangle u_\mu + \frac{i d_{18}}{2} \gamma^\mu \gamma_5 [D_\mu, \chi_-] \Big\} \psi .
\end{aligned}$$

At tree level only five combinations of the coupling constants occurring here enter the scattering amplitude. We do not give an explicit expression for $\mathcal{L}_N^{(4)}$, but characterize this part of the effective Lagrangian through its contributions to the scattering amplitude (sec. 4).

4 Tree graphs

The tree graph contributions to the amplitude have the following structure



The vertex contributions ③ involve the axial coupling g and a quark mass correction to it from the Lagrangian $\mathcal{L}_N^{(3)}$. The quark mass correction can be taken into account by replacing the coupling constant g in $\mathcal{L}^{(1)}$ with $g_2 = g + 2M^2(2d_{16} - d_{18})$. The contributions of type ② represent mass insertions generated by $\mathcal{L}_N^{(2)}$ and $\mathcal{L}_N^{(4)}$ at tree level. They are taken into account by replacing the bare mass m in $\mathcal{L}_N^{(1)}$ with $m_4 = m - 4c_1 M^2 + e_1 M^4$ (we adopt the notation of [9] and denote the relevant coupling constant in $\mathcal{L}_N^{(4)}$ by e_1).

When evaluating the relevant diagrams, we must distinguish between the bare and physical masses of the nucleon. As we are working on the physical mass shell, $P^2 = m_N^2$, we need to use the corresponding Dirac equation for the nucleon spinors, $\not{P} u(P) = m_N u(P)$. The result for the sum of all contributions of type ② and ③ reads (here, the amplitude A is more convenient

than D , because the representation then only involves functions of a single variable):

$$\begin{aligned} A^\pm &= A(s) \pm A(u) & A(s) &= \frac{g_2^2 (m_4 + m_N)}{4 F^2} \left(\frac{s - m_N^2}{s - m_4^2} \right) \\ B^\pm &= B(s) \mp B(u) & B(s) &= \frac{g_2^2 (s + 2 m_4 m_N + m_N^2)}{4 F^2 (m_4^2 - s)}. \end{aligned}$$

The tree graphs of type ④ yield polynomials in ν , t and M^2 . We only list the nonzero contributions. Those from $\mathcal{L}_N^{(1)}$ are given by

$$D^- = \frac{\nu}{2F^2}, \quad B^- = \frac{1}{2F^2},$$

while $\mathcal{L}_N^{(2)}$ generates the terms

$$D^+ = -\frac{4c_1 M^2}{F^2} + \frac{c_2 (16 m_N^2 \nu^2 - t^2)}{8 F^2 m^2} + \frac{c_3 (2M_\pi^2 - t)}{F^2}, \quad B^- = \frac{2c_4 m_N}{F^2}.$$

Note that the coupling constant c_2 gives rise to a contribution proportional to t^2 which is of $O(q^4)$. Quite generally, vertices involving derivatives of the nucleon field may generate contributions beyond the order indicated by chiral power counting.

In the graphs from $\mathcal{L}_N^{(3)}$ and $\mathcal{L}_N^{(4)}$, we may replace the bare constants by the physical ones, because the distinction is beyond the accuracy of our calculation. The term $\mathcal{L}_N^{(3)}$ only shows up in those amplitudes that are odd under crossing:

$$\begin{aligned} D^- &= \frac{2\nu}{F_\pi^2} \{2(d_1 + d_2 + 2d_5) M_\pi^2 - (d_1 + d_2) t + 2d_3 \nu^2\} + O(q^5) \\ B^+ &= \frac{4\nu m_N}{F_\pi^2} (d_{14} - d_{15}) + O(q^3) \end{aligned}$$

Finally, $\mathcal{L}_N^{(4)}$ generates a polynomial that is even under crossing. We identify the coupling constants e_3, \dots, e_{11} with the coefficients of this polynomial:

$$\begin{aligned} D^+ &= \frac{1}{F_\pi^2} \{e_3 M_\pi^4 + e_4 M_\pi^2 \nu^2 + e_5 M_\pi^2 t + e_6 \nu^4 + e_7 \nu^2 t + e_8 t^2\} + O(q^6) \\ B^- &= \frac{m_N}{F_\pi^2} \{e_9 M_\pi^2 + e_{10} \nu^2 + e_{11} t\} + O(q^4) \end{aligned} \quad (4.1)$$

A contribution analogous to $e_3 M_\pi^4 + e_5 M_\pi^2 t$ also occurs in the representation of the scalar form factor to $O(q^4)$ (in [9] the corresponding contribution to $\sigma(t)$ is denoted by $2e_1 M_\pi^4 + e_2 M_\pi^2 t$). The coupling constants are different, because the terms $\langle \chi_-^2 \rangle \bar{\psi} \psi$ and $\langle \chi_+ \rangle \langle u_\mu u^\mu \rangle \bar{\psi} \psi$ of $\mathcal{L}_N^{(4)}$ do contribute to the scattering amplitude, but do not show up in the scalar form factor.

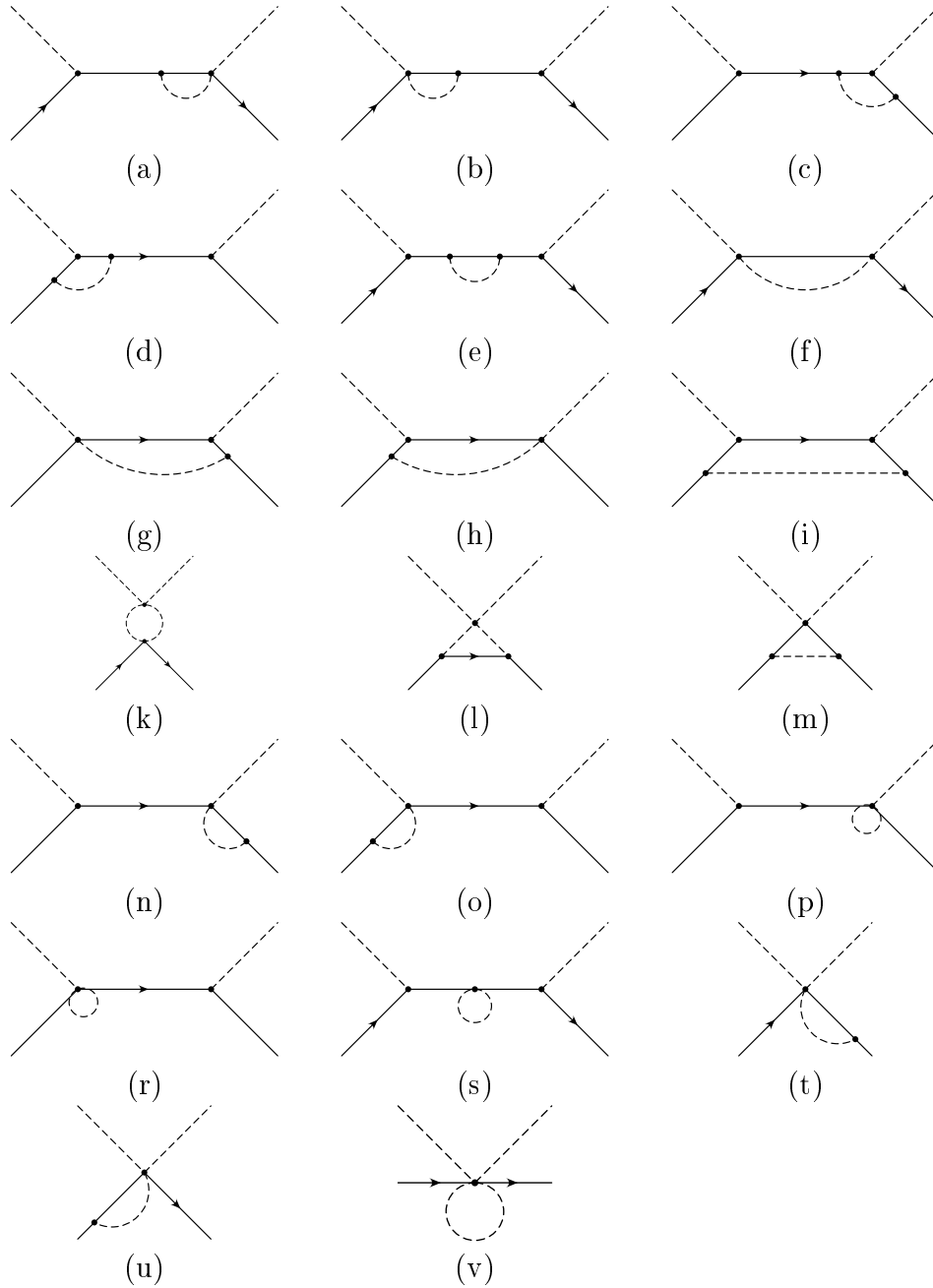


Figure 2: One loop topologies for πN -scattering. Crossed diagrams and external leg corrections are not shown. We do not display topologies involving closed fermion loops since they vanish in infrared regularization.

5 One loop graphs in infrared regularization

To obtain a representation of the scattering amplitude to order q^3 , it suffices to evaluate the one loop graphs of $\mathcal{L}_N^{(1)}$. As we wish to evaluate the scattering amplitude to order q^4 , we in addition need to consider loops containing one vertex from $\mathcal{L}_N^{(2)}$. The various topologies are shown in figure 2. In this figure, we do not differentiate between the vertices of $\mathcal{L}_N^{(1)}$ and those of $\mathcal{L}_N^{(2)}$. Graph (a) for instance describes two different contributions (see figure 3). Since the

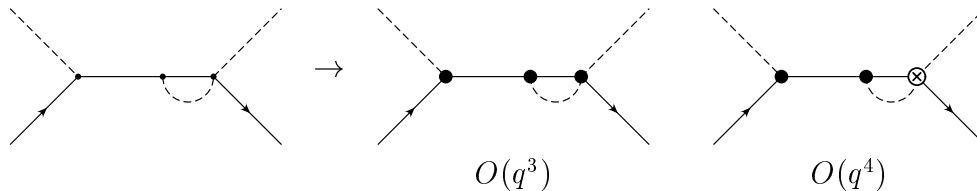


Figure 3: By exclusively inserting vertices from $\mathcal{L}_N^{(1)}$ (drawn as full circles) into topology (a), we obtain a graph of $O(q^3)$. The same topology also occurs if one of the vertices is replaced by one of those in $\mathcal{L}_N^{(2)}$, which involve the coupling constants c_1 , c_2 , c_3 or c_4 (denoted by a circled cross). The resulting graph then starts contributing at $O(q^4)$. Since $\mathcal{L}_N^{(2)}$ exclusively contains vertices with an even number of pions, only the rightmost vertex can be replaced.

second order Lagrangian $\mathcal{L}_N^{(2)}$ only involves couplings with an even number of pions, the topologies (c), (d), (e), (i), (l), (p), (r), (t) and (u) do not give rise to $O(q^4)$ diagrams.

The calculation of the loop diagrams generated by $\mathcal{L}_N^{(1)}$ was carried out quite some time ago by Gasser, Sainio and Švarc [2], using a relativistic Lagrangian and dimensional regularization. As mentioned in the introduction, this approach does not preserve the counting rules. In a recent paper [9], we have set up a variant of dimensional regularization that avoids these difficulties and which we call “infrared regularization”. We now briefly discuss this method.

5.1 Infrared regularization

To explain the essence of the method, we consider the simplest example, the self energy graph shown in figure 4. The corresponding scalar loop integral

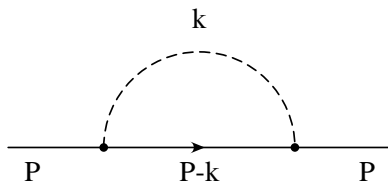


Figure 4: Self energy

has the form

$$H(P^2) = \frac{1}{i} \int \frac{d^d k}{(2\pi)^d} \frac{1}{M^2 - k^2} \frac{1}{m^2 - (P - k)^2} = \frac{1}{i} \int \frac{d^d k}{(2\pi)^d} \frac{1}{a} \frac{1}{b} \quad (5.1)$$

We need to analyze the integral for external momenta in the vicinity of the mass shell: $P = mv + r$, where v is a timelike unit vector and r is a quantity of order q . In the limit $M \rightarrow 0$, the integral develops an infrared singularity, generated by small values of the variable of integration, $k = O(q)$. In that region, the first factor in the denominator is of $O(q^2)$, while the second is of order $O(q)$. Accordingly the chiral expansion of the integral contains terms of order q^{d-3} . The order of the infrared singular part follows from the counting rules at tree level, because it is generated by the region of integration, where the momenta flowing through the propagators are of the same order as in the tree level graphs. The remainder of the integration region does not contain infrared singularities and may thus be expanded in an ordinary Taylor series. An evaluation of the integral at $P^2 = s_+ = (m + M)^2$ nicely shows the two parts:

$$H(s_+) = \frac{\Gamma(2 - \frac{d}{2})}{(4\pi)^{\frac{d}{2}}(d-3)} \left\{ \frac{M^{d-3}}{(m+M)} + \frac{m^{d-3}}{(m+M)} \right\} = I + R$$

The infrared singular part I is proportional to M^{d-3} , while the remainder R is proportional to m^{d-3} and does therefore not contain a singularity at $M = 0$, irrespective of the value of d . Since the regular contribution stems from a region where the variable of integration k is of order m , it violates the tree-level counting rules.

The explicit expression for the loop integral $H(P^2)$ in d dimensions is lengthy, but the splitting into the infrared singular part I and regular part R

is easily obtained in the Schwinger-Feynman representation of the integral.

$$\begin{aligned} H &= \int \frac{d^d k}{(2\pi)^d} \frac{1}{a} \frac{1}{b} = \int_0^1 dz \int \frac{d^d k}{(2\pi)^d} \frac{1}{[(1-z)a + zb]^2} \\ &= \int_0^\infty - \int_1^\infty dz \int \frac{d^d k}{(2\pi)^d} \frac{1}{[(1-z)a + zb]^2} = I + R. \end{aligned}$$

Schwinger-Feynman parametrizations of the infrared singular and regular parts of a general one loop integral are given in [9]. There, the following statements are proven:

- To any given order, the chiral expansion of the infrared regular part of a one loop integral is a polynomial in the quark masses and the external momenta.
- The regular part of the one loop amplitudes is chirally symmetric.

Taken together, the two statements imply that, in a one loop calculation, one may simply drop the regular parts of the loop integrals because the contributions they generate can be absorbed in the coupling constants of the effective Lagrangian. This procedure is called ‘‘infrared regularization’’: The loop graph contributions are identified with the infrared singular parts of the corresponding dimensionally regularized integrals.

5.2 Comparison with dimensional regularization

The calculation of loop graphs in infrared regularization is completely analogous to the evaluation in dimensional regularization. The expressions for the graphs in terms of loop integrals look the same. In dimensional regularization, the contribution of the graph (f) in figure 2 to the isospin even amplitude, for instance, is given by

$$\begin{aligned} T_f^+ &= \frac{1}{16F^4} \bar{u}' \left\{ 4(s - m^2)(2m + \not{q}' + \not{q})H^{(1)}(s) \right. \\ &\quad \left. - (4M^2 H(s) + \Delta_\pi - 4\Delta_N)(\not{q}' + \not{q}) \right\} u \end{aligned}$$

The terms Δ_π and Δ_N stand for the pion and nucleon propagators at the origin, respectively:

$$\Delta_\pi = \frac{1}{i} \int_I \frac{d^d k}{(2\pi)^d} \frac{1}{M^2 - k^2 - i\epsilon}, \quad \Delta_N = \frac{1}{i} \int_I \frac{d^d k}{(2\pi)^d} \frac{1}{m^2 - k^2 - i\epsilon}.$$

The function $H^{(1)}(s)$ may be expressed in terms of the scalar self energy integral $H(s)$, which we considered in the preceding subsection:

$$H^{(1)}(s) = \frac{1}{2s} \{ (s - m^2 + M^2) H(s) + \Delta_\pi - \Delta_N \} .$$

To obtain the corresponding result in infrared regularization, it suffices to replace all loop integrals by their infrared singular parts. Integrals like Δ_π with pion propagators only do not have an infrared regular part, because they do not involve the heavy scale m : In the meson sector, infrared regularization coincides with ordinary dimensional regularization. Nucleon loop integrals like Δ_N , on the other hand, vanish in infrared regularization, because they are infrared regular. Integrals which involve both kinds of propagators do possess a regular and an infrared singular part. These integrals are replaced by their infrared singular part. The result for graph (f) in infrared regularization is thus obtained with the substitution $H(s) \rightarrow I(s)$, $H^{(1)}(s) \rightarrow I^{(1)}(s)$ and $\Delta_N \rightarrow 0$.

The result for the various graphs is given in appendix D. The definitions of the pertinent loop integrals can be found in appendix C. We have checked that our result for the loop graphs of $\mathcal{L}_N^{(1)}$ agrees with the one of Gasser, Sainio and Švarc [2], if we evaluate our loop integrals in dimensional regularization and expand around $d = 4$. Note that we do not display the contributions proportional to loop integrals that exclusively contain nucleon propagators, because these vanish in infrared regularization. Also, the basis used in the decomposition of the vector and tensor integrals differs from the one used by Gasser, Sainio and Švarc – in our basis, the chiral power counting is more transparent.

6 Simplification of the $O(q^4)$ diagrams

The chiral expansion of the loop graphs in general contains terms of arbitrarily high order. Since we need the amplitude only to $O(q^4)$, we can simplify the representation by neglecting terms of $O(q^5)$ or higher. The example of the triangle graph (graph h in fig. 2) shows, however, that the chiral expansion of infrared singularities is a subtle matter [9], which we will discuss in detail later on. The problem arises from the *denominators* that occur in the various loop integrals – the expansion thereof gives rise to an infinite series of terms, which in some cases needs to be summed up to all orders to arrive at a decent representation of the integral. Concerning, the *numerators*, this problem does not arise – the corresponding expansion does not give rise to an infinite series of terms and hence preserves the analytic structure of the

integral, term by term. We exploit this fact to simplify the calculation of those graphs that contain vertices from $\mathcal{L}_N^{(2)}$, which start contributing only at $O(q^4)$ (in the loop graphs generated by $\mathcal{L}_N^{(1)}$, we retain all contributions).

As an illustration, we consider the part of the $O(q^4)$ graph (a) that is proportional to c_2

$$T^+ = \frac{c_2 g_A^2}{4 F^4 m^2} \frac{1}{m^2 - s} \frac{1}{i} \int_I \frac{d^d k}{(2\pi)^d} \frac{1}{(M^2 - k^2)(m^2 - (P + q - k)^2)} \\ \times (k \cdot P' q' \cdot P' + k \cdot (P + q - k) q' \cdot (P + q - k)) \\ \times \bar{u}' (m + \not{P} + \not{q} - \not{k}) \gamma_5 \not{k} (m + \not{P} + \not{q}) \gamma_5 \not{q} u$$

The numerator of the integrand involves terms with up to five powers of the loop momentum. It can explicitly be expressed in terms of the functions $I(s)$, $I^{(1)}(s)$, \dots , that arise in the tensorial decomposition of the generic loop integral with one meson and one nucleon propagator. The resulting expression is rather lengthy, however. As just discussed, we only retain the leading term in the expansion of the numerator:

$$T^+ = \frac{c_2 g_A^2}{4 F^4 m^2} \frac{1}{m^2 - s} \frac{1}{i} \int_I \frac{d^d k}{(2\pi)^d} \frac{1}{(M^2 - k^2)(m^2 - (P + q - k)^2)} \\ \times 2k \cdot P' q' \cdot P' \bar{u}' 2m \gamma_5 \not{k} (m + \not{P}) \gamma_5 \not{q} u + O(q^5) \\ = \frac{c_2 g_A^2}{2 F^4 m} \frac{1}{i} \int_I \frac{d^d k}{(2\pi)^d} \frac{1}{(M^2 - k^2)(m^2 - (P + q - k)^2)} \\ \times k \cdot P' \bar{u}' \not{k} (m - \not{P}) \not{q} u + O(q^5),$$

where we have used $P' = P + O(q)$. The relation $2k \cdot P' = m^2 - (P + q - k)^2 + O(q^2)$ then allows us to remove the nucleon propagator, so that we arrive at

$$T^+ = \frac{c_2 g_A^2}{4 F^4 m} \frac{1}{i} \int_I \frac{d^d k}{(2\pi)^d} \frac{1}{(M^2 - k^2)} \bar{u}' \not{k} (m - \not{P}) \not{q} u + O(q^5).$$

The remaining integral vanishes because the integrand is antisymmetric in k , so that the entire contribution is of $O(q^5)$ and can be dropped.

7 Wave function renormalization

According to the rules of perturbation theory, the scattering amplitude may be evaluated from the connected four-point-function

$$\langle 0 | T N(x') P_{a'}(y') P_a(y) \bar{N}(x) | 0 \rangle_c,$$

where $N(x)$ and $P_a(x)$ are any operators that interpolate between the relevant incoming and outgoing states, so that the matrix elements

$$\langle 0|N(x)|N\rangle = \sqrt{Z_N} u e^{-iPx} , \quad \langle 0|P_a(x)|\pi_b\rangle = \sqrt{Z_\pi} \delta_{ab} e^{-iqx} ,$$

are different from zero (we suppress the spin and isospin quantum numbers of the nucleon). The scattering amplitude $T_{a'a}$ is determined by the residue of the poles occurring in the Fourier transform of this correlation function:

$$\begin{aligned} i \int d^4x' d^4y' d^4y \langle 0|T N(x') P_{a'}(y') P_a(y) \bar{N}(x) |0\rangle_c e^{i(P'x' + q'y' - Px - qy)} \\ = \frac{\sqrt{Z_\pi}}{M_\pi^2 - q'^2} \frac{\sqrt{Z_\pi}}{M_\pi^2 - q^2} \frac{\sqrt{Z_N}}{m_N^2 - P'^2} \frac{\sqrt{Z_N}}{m_N^2 - P^2} u' \bar{u} T_{a'a} + \dots \end{aligned}$$

The result for $T_{a'a}$ does not depend on the choice of the interpolating fields.

In our context, it is convenient to identify the interpolating fields with the variables of the effective theory, $N(x) = \psi(x)$, $P_a(x) = \pi_a(x)$. We emphasize that these are auxiliary quantities that represent the variables of integration in the path integral – the effective fields do not have counterparts in QCD and do thus not represent objects of physical significance. The renormalization of the coupling constants occurring in our effective Lagrangian only ensures that the scattering amplitude remains finite when the regularization is removed, $d \rightarrow 4$. A multiplicative renormalization of the effective fields, $\psi(x) = \sqrt{Z_N} \psi(x)^{ren}$, $\pi_a(x) = \sqrt{Z_\pi} \pi_a(x)^{ren}$, does not suffice to obtain finite correlation functions for these. Note also that the correlation functions depend on the parametrization used for the matrix $U(x)$.

It is easy to see why the correlation functions of the effective fields do not represent meaningful quantities. The corresponding generating functional is obtained by adding source terms to the effective Lagrangian,

$$\mathcal{L}_{eff} \rightarrow \mathcal{L}_{eff} + f^a \pi_a + \bar{g} \psi + \bar{\psi} g .$$

This operation, however, ruins the symmetries of the effective theory, because the representation of the chiral group on $\pi_a(x)$ and $\psi(x)$ involves the pion field in a nonlinear manner. To arrive at finite correlation functions, we would need to add extra counter terms that are not invariant under chiral rotations.

A more physical choice for the interpolating fields is discussed in appendix B. This is of interest, for instance, in connection with the matrix elements relevant for baryon decay. The corresponding correlation functions do have a physical interpretation within QCD. Since the relevant operators carry anomalous dimension, they depend on the running scale of that theory,

but are otherwise free from ambiguities. In our context, the choice of the interpolating fields is irrelevant – the result obtained for the S -matrix by using the fields discussed in appendix B would be the same.

The perturbative calculation of the scattering matrix can be simplified in the familiar manner: It suffices to consider the amputated four-point-function, obtained by (i) discarding all graphs that contain insertions in the external lines and (ii) replacing the free propagators that describe the external lines in the remaining graphs by plane wave factors. Denoting the amputated four-point-function by $\Gamma_{a'a}$, the scattering amplitude is given by

$$T_{a'a} = Z_N Z_\pi \bar{u}' \Gamma_{a'a} u .$$

We have performed our calculations in the so-called sigma parametrization

$$U(x) = \sqrt{1 - \frac{\vec{\pi}(x)^2}{F^2}} + i \frac{\vec{\pi}(x) \cdot \vec{\tau}}{F} .$$

The wave function renormalization constants are then given by [9]

$$\begin{aligned} Z_\pi &= 1 - \frac{2 M^2}{F^2} (\ell_4 + \lambda_\pi) + O(M^4) \\ Z_N &= 1 - \frac{9 M^2 g_A^2}{2 F^2} \left\{ \lambda_\pi + \frac{1}{48 \pi^2} - \frac{M}{32 \pi m} \right\} + O(M^4) , \\ \lambda_\pi &= \frac{M^{d-4}}{(4\pi)^2} \left\{ \frac{1}{d-4} - \frac{1}{2} \left(\ln 4\pi + \Gamma'(1) + 1 \right) \right\} . \end{aligned}$$

The divergences $\propto (d-4)^{-1}$ are contained in the quantity λ_π , which involves the pion mass instead of an arbitrary scale μ – we are in effect identifying the renormalization scale with the pion mass. This is convenient, because it simplifies the formulae: The divergences are always accompanied by a chiral logarithm. Expressed in terms of the usual pole term λ , we have

$$\lambda_\pi = \lambda + \frac{1}{16\pi^2} \ln \frac{M}{\mu} .$$

The effective coupling constants of $\mathcal{L}_\pi^{(4)}$, $\mathcal{L}_N^{(3)}$ and $\mathcal{L}_N^{(4)}$ pick up renormalization. The relevant formulae are listed in appendix E. We have checked that if the scattering amplitude is expressed in the renormalized couplings $\ell_3^r(\mu)$, $\ell_4^r(\mu)$, $d_i^r(\mu)$, $e_i^r(\mu)$ introduced there, it indeed remains finite at $d \rightarrow 4$.

8 Chiral expansion of m_N , $g_{\pi N}$ and g_A

The graphs (e) and (s) in fig. 2 contain a double pole at $s = m_4^2$ and their crossed versions exhibit the analogous singularity at $u = m_4^2$ (we recall that

the mass shifts generated by the tree graphs of $\mathcal{L}_N^{(2)}$ and $\mathcal{L}_N^{(4)}$ are included in the free Lagrangian, so that the nucleons propagating in the loops are equipped with the mass $m_4 = m - 4c_1 M^2 + e_1 M^4$. The double pole disappears as it should if the Born term, which contains the pole due to one-nucleon exchange, is expressed in terms of the physical mass of the nucleon. In the context of the low energy expansion, the standard, pseudoscalar form of the Born term is not convenient, because it corresponds to a scattering amplitude of order q^0 . We instead use the pseudovector form, defined by

$$\begin{aligned} D_{pv}^+(\nu, t) &= \frac{g_{\pi N}^2}{m_N} \frac{\nu_B^2}{\nu_B^2 - \nu^2}, & B_{pv}^+(\nu, t) &= \frac{g_{\pi N}^2}{m_N} \frac{\nu}{\nu_B^2 - \nu^2}, \\ D_{pv}^-(\nu, t) &= \nu B_{pv}^-(\nu, t), & B_{pv}^-(\nu, t) &= \frac{g_{\pi N}^2}{m_N} \frac{\nu_B}{\nu_B^2 - \nu^2} - \frac{g_{\pi N}^2}{2m_N^2}, \\ \nu &= \frac{s - u}{4m_N}, & \nu_B &= \frac{t - 2M_\pi^2}{4m_N}. \end{aligned} \quad (8.1)$$

The Born term exclusively involves the physical values of m_N , $g_{\pi N}$ and M_π . The explicit expression for m_N reads [9]

$$\begin{aligned} m_N &= m - 4c_1 M^2 - \frac{3g^2 M^3}{32\pi F^2} - \frac{3(g^2 - 8c_1 m + c_2 m + 4c_3 m)\lambda_\pi M^4}{2mF^2} \\ &\quad - \frac{3(2g^2 - c_2 m)M^4}{128\pi^2 m F^2} + e_1 M^4 + O(M^5), \end{aligned} \quad (8.2)$$

while the one for the pion-nucleon coupling constant is given by

$$\begin{aligned} g_{\pi N} &= \frac{mg}{F} \left\{ 1 - \frac{l_4 M^2}{F^2} - \frac{4c_1 M^2}{m} + \frac{2(2d_{16} - d_{18})M^2}{g} - \frac{4g^2 \lambda_\pi M^2}{F^2} \right. \\ &\quad \left. - \frac{g^2 M^2}{16\pi^2 F^2} + \frac{(12 + 3g^2 - 16c_3 m + 32c_4 m)M^3}{96\pi m F^2} + O(M^4) \right\}. \end{aligned} \quad (8.3)$$

To order M^2 , the result agrees with the one given in ref. [2] – only the terms of order M^3 are new. The quantity g represents the value of the axial charge in the chiral limit. Kambor and Mojžiš [13] and Schweizer [11] have calculated the physical axial charge g_A to $O(q^3)$, with the result

$$\begin{aligned} g_A &= g \left\{ 1 + \frac{4d_{16} M^2}{g} - \frac{2(2g^2 + 1)\lambda_\pi M^2}{F^2} - \frac{g^2 M^2}{16\pi^2 F^2} \right. \\ &\quad \left. + \frac{(3 + 3g^2 - 4c_3 m + 8c_4 m)M^3}{24\pi m F^2} + O(M^4) \right\}. \end{aligned} \quad (8.4)$$

These expressions are analogous to the well-known representations that describe the dependence of M_π and F_π on the quark masses [20],

$$\begin{aligned} M_\pi^2 &= M^2 \left\{ 1 + \frac{M^2}{F^2} (2l_3 + \lambda_\pi) + O(M^4) \right\} , \\ F_\pi &= F \left\{ 1 + \frac{M^2}{F^2} (l_4 - 2\lambda_\pi) + O(M^4) \right\} . \end{aligned}$$

In all cases, the expansion contains contributions that are not analytic in the quark masses, generated by the infrared singularities. In the meson sector, only the chiral logarithm contained in λ_π occurs, but in the nucleon sector, the expansion in addition involves contributions with $M^3 \propto (m_u + m_d)^{\frac{3}{2}}$.

9 Strength of infrared singularities

The fact that the low energy expansion in the baryon sector contains even as well as odd powers of M implies that the infrared singularities occurring there are stronger than those in the meson sector. We illustrate this with the σ -term matrix element, that is, with the response of the nucleon mass to a change in the quark masses:

$$\sigma = m_u \frac{\partial m_N}{\partial m_u} + m_d \frac{\partial m_N}{\partial m_d} . \quad (9.1)$$

More specifically, we wish to discuss the dependence of this quantity on the quark masses, which is quite remarkable. In this context, the numerical value of σ is not of crucial importance. For definiteness, we use $\sigma = 45$ MeV [23]. The chiral expansion of the σ -term is readily obtained from the formula (8.2), with the result

$$\sigma = k_1 M^2 + \frac{3}{2} k_2 M^3 + k_3 M^4 \left\{ 2 \ln \frac{M^2}{m^2} + 1 \right\} + 2 k_4 M^4 + O(M^5) , \quad (9.2)$$

As discussed above, the term proportional to M^3 arises from an infrared singularity in the self energy of the pion cloud. It lowers the magnitude of the σ -term by $3/2 \times 15$ MeV $\simeq 23$ MeV. The coefficient k_3 can also be expressed in terms of measurable quantities [9]. Numerically the contribution from this term amounts to -7 MeV, thus amplifying the effect seen at $O(M^3)$. Chiral symmetry does not determine all of the effective coupling constants entering the regular contribution $k_4 M^4$, which is of the same type as the correction $\Delta_{CD} = k_{CD} M^4$ to the low energy theorem (11.3). As discussed above, corrections of this type are expected to be very small – we simply

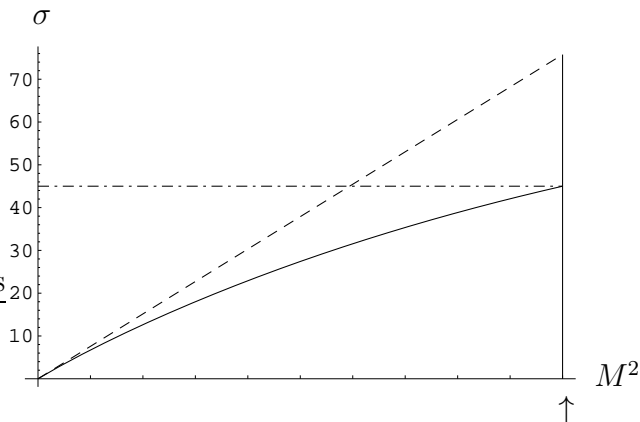


Figure 5: σ -term (in MeV) as a function of the quark masses. The horizontal axis gives the values of $M^2 = (m_u + m_d)B$. The arrow corresponds to the physical value of the quark masses. For definiteness, it is assumed that the physical value of σ is 45 MeV (dash-dotted line). The dashed line depicts the linear dependence that results if the infrared singular contributions proportional to M_π^3 and to $M_\pi^4 \ln M_\pi^2/m_N^2$ are dropped.

drop the term $k_4 M^4$. The value of k_1 is then fixed by the input $\sigma = 45$ MeV for the total, so that we can now discuss the manner in which σ changes when the quark masses are varied.

At leading order, σ is given by $k_1 M^2$. In figure 1 this contribution is shown as a dashed straight line. The full curve includes the contributions generated by the infrared singularities, $k_2 M^3$ and $k_3 M^4 \{2 \ln M^2/m^2 + 1\}$. The figure shows that the expansion of the σ -term in powers of the quark masses contains large contributions from infrared singularities. These must show up in evaluations of the σ -term on a lattice: The ratio $\sigma/(m_u + m_d)$ must change significantly if the quark masses are varied from the chiral limit to their physical values. Note that in this discussion, the mass of the strange quark mass is kept fixed at its physical value – the curvature seen in the figure exclusively arises from the perturbations generated by the two lightest quark masses.

It is instructive to compare this result with the dependence of M_π^2 on the quark masses. In that case, the expansion only contains even powers of M :

$$M_\pi^2 = M^2 + \frac{M^4}{32\pi^2 F^2} \ln \frac{M^2}{\Lambda_3^2} + O(M^6). \quad (9.3)$$

The quantity Λ_3 stands for the renormalization group invariant scale of the effective coupling constant l_3 . The SU(3) estimate for this coupling constant

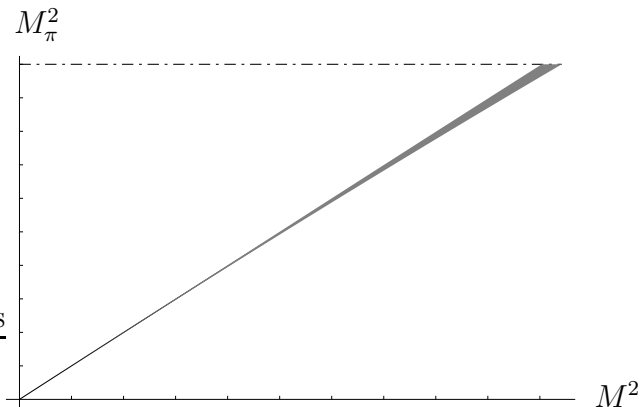


Figure 6: Square of the pion mass as a function of the quark masses. The horizontal axis gives the values of the leading order term $M^2 = (m_u + m_d)B$. The dash-dotted line indicates the physical value of M_π^2 .

given in ref. [24] reads $\bar{l}_3 \equiv -\ln M_\pi^2/\Lambda_3^2 = 2.9 \pm 2.4$. The error bar is so large that the estimate barely determines the order of magnitude of the scale Λ_3 . Figure 2 shows, however, that this uncertainty does not significantly affect the dependence of M_π^2 on the quark masses, because the logarithmic contribution is tiny: the range of \bar{l}_3 just quoted corresponds to the shaded region shown in the figure.

The logarithmic term occurring in the chiral expansion of M_π^2 gets enhanced by about a factor of two if we consider the pion σ -term,

$$\sigma_\pi = \langle \pi | m_u \bar{u}u + m_d \bar{d}d | \pi \rangle = m_u \frac{\partial M_\pi^2}{\partial m_u} + m_d \frac{\partial M_\pi^2}{\partial m_d} . \quad (9.4)$$

We do not show the corresponding curve, because it is also nearly a straight line.

The main point here is that the infrared singularities encountered in the self energy of the nucleon are much stronger than those occurring in the self energy of the pion.

10 Goldberger-Treiman relation

The above expressions for the quantities $g_{\pi N}$, g_A , m_N and F_π allow us to analyze the correction that occurs in the Goldberger-Treiman relation up to and including terms of order M^3 . We write the relation in the form

$$g_{\pi N} = \frac{g_A m_N}{F_\pi} \{1 + \Delta_{GT}\} . \quad (10.1)$$

If the quark masses m_u and m_d are turned off, the strength of the πN interaction is fully determined by g_A and F_π : $\Delta_{GT} = 0$. Inserting the formulae of the preceding section in the ratio $g_A m_N / F_\pi$ and expanding the result to order M^3 , we find that the coefficients of the infrared singular terms proportional to $M^2 \ln M^2 / m^2$ and to M^3 are identical with those in $g_{\pi N}$. Up to and including third order, the correction Δ_{GT} is therefore free of infrared singularities and takes the simple form

$$\Delta_{GT} = -\frac{2d_{18}M^2}{g} + O(M^4). \quad (10.2)$$

As far as the logarithmic terms of $O(M^2)$ are concerned, this result was established a long time ago [2]. What the present calculation adds is that the infrared singularities also cancel at $O(M^3)$, in agreement with ref. [8].

The result shows that in the case of the Goldberger-Treiman relation, the breaking of chiral symmetry generated by the quark masses does not get enhanced by small energy denominators. Chiral symmetry does not determine the magnitude of the coupling constant d_{18} . A crude estimate may be obtained from the assumption that the scale of the symmetry breaking is the same as in the case of F_K / F_π , where it is set by the massive scalar states, $M_S \simeq 1 \text{ GeV}$. This leads to $\Delta_{GT} \simeq M_\pi^2 / M_S^2 \simeq 0.02$. A more detailed analysis based on models and on the SU(3) breaking effects seen in the meson-baryon coupling constants may be found in ref. [25]. Recently the Goldberger-Treiman discrepancy has also been determined from QCD sum rules [26]. Both evaluations confirm the expectation that Δ_{GT} must be very small – a discrepancy of order 4% or more would be very difficult to understand.

Since the days when the Goldberger-Treiman relation was discovered [27], the value of g_A has increased considerably. Also, F_π decreased a little, on account of radiative corrections. The main source of uncertainty is $g_{\pi N}$. The comprehensive analysis of πN scattering published by Höhler in 1983 [28] led to $f^2 = g_{\pi N}^2 M_\pi^2 / (16\pi m_N^2) = 0.079$. With $g_A = 1.267$ and $F_\pi = 92.4 \text{ MeV}$, this value yields $\Delta_{GT} = 0.041$. The data accumulated since then indicate that f^2 is somewhat smaller, numbers in the range from 0.076 to 0.077 looking more likely. This range corresponds to $0.021 < \Delta_{GT} < 0.028$.

We conclude that, within the current experimental uncertainties to be attached to the pion-nucleon coupling constant, the Goldberger-Treiman relation does hold to the expected accuracy. Note that at the level of 1 or 2 %, isospin breaking cannot be ignored. In particular, radiative corrections need to be analyzed carefully. Also, the coupling constant relevant for the neutral pion picks up a significant contribution from $\pi^0 - \eta$ interference.

11 Low energy theorems for D^+ and D^-

The representation of the scattering amplitude to order q^4 also allows us to analyze the corrections occurring in the well-known low energy theorem [29, 30] for the value of the scattering amplitude $D^+(\nu, t)$ at the Cheng-Dashen point, $\nu = 0$, $t = 2M_\pi^2$. The theorem relates the quantity³

$$\Sigma = F_\pi^2 \bar{D}^+(0, 2M_\pi^2) \quad (11.1)$$

to the scalar form factor of the nucleon,

$$\langle N' | m_u \bar{u}u + m_d \bar{d}d | N \rangle = \sigma(t) \bar{u}'u . \quad (11.2)$$

The relation may be written in the form

$$\Sigma = \sigma(2M_\pi^2) + \Delta_{CD} . \quad (11.3)$$

The theorem states that the term Δ_{CD} vanishes up to and including contributions of order M^2 . The explicit expression obtained for Σ when evaluating the scattering amplitude to order q^4 again contains infrared singularities proportional to M^3 and $M^4 \ln M^2/m^2$. Precisely the same singularities, however, also show up in the scalar form factor at $t = 2M_\pi^2$, so that the result for Δ_{CD} is free of such singularities⁴:

$$\Delta_{CD} = \left(-\frac{c_2}{2m^2} - 2e_1 - 2e_2 + e_3 + 2e_5 + 4e_8 \right) M^4 + O(M^5) . \quad (11.4)$$

Equally well, we could replace the bare coupling constants by the renormalized ones: In the combination occurring here, the poles at $d = 4$ contained in e_1, \dots, e_8 cancel. Crude estimates like those used in the case of the Goldberger-Treiman relation indicate that the term Δ_{CD} must be very small, of order 1 MeV.

Unfortunately, the experimental situation concerning the magnitude of D^+ at the Cheng-Dashen point leaves much to be desired (for a recent review, see ref. [32]). The low energy theorem makes it evident that we are dealing with a small quantity here – the object vanishes in the chiral limit. The inconsistencies among the various data sets available at low energies need to be clarified to arrive at a reliable value for $g_{\pi N}$. Only then will it become possible to accurately measure small quantities such as the σ -term.

³At the Cheng-Dashen-point, the amplitude is singular, on account of the Born term. The bar indicates that this term is removed in the pseudovector form specified in eq. (8.1): $\bar{D}^\pm = D^\pm - D_{pv}^\pm$, $\bar{B}^\pm = B^\pm - B_{pv}^\pm$.

⁴The cancellation of the terms of order M^3 was pointed out in ref. [2, 31] and the absence of logarithmic contributions of order M^4 was shown in ref. [14].

There is a low energy theorem also for the isospin odd amplitude: In the chiral limit, the quantity

$$C = 2 F_\pi^2 \frac{\bar{D}^-(\nu, t)}{\nu} \Big|_{\nu=0, t=2M_\pi^2} \quad (11.5)$$

tends to 1. The representation of the scattering amplitude to $O(q^4)$ yields the corrections up to and including $O(M^3)$:

$$\begin{aligned} C &= 1 - \frac{1 + 5 g_A^2}{24 \pi^2 F^2} M^2 \ln \frac{M}{\mu} + k_1 M^2 + k_2 M^3 + O(M^4), \quad (11.6) \\ k_1 &= 16 d_5^r(\mu) - \frac{(14 - 3\pi) + (22 + 3\pi)g_A^2}{288 \pi^2 F^2}, \\ k_2 &= \frac{64 m c_1 + 2 g_A^2(4 + g_A^2) + \sqrt{2} \ln(1 + \sqrt{2}) g_A^2}{32 \pi m F^2}. \end{aligned}$$

Note that the scale dependence of the renormalized coupling constant $d_5^r(\mu)$ cancels against the one of the chiral logarithm.

In contrast to the quantity Δ_{CD} , this expression does contain infrared singularities at the order considered here: A chiral logarithm as well as terms of order M^3 . We will discuss the size of these effects in section 13 – first, we need to establish contact with the available phenomenological representations of the scattering amplitude.

12 Subthreshold expansion

Höhler and collaborators [28] analyze the low energy structure in terms of an expansion of the amplitude around the point $\nu = t = 0$. More precisely, the expansion concerns the difference between the full amplitude and the pseudovector Born term, specified in eq. (8.1). Crossing symmetry implies that the amplitudes $X \in \{D^+, D^-/\nu, B^+/\nu, B^-\}$ are even in ν , so that the expansion takes the form

$$X(\nu, t) = X_{pv}(\nu, t) + x_{00} + x_{10} \nu^2 + x_{01} t + x_{20} \nu^4 + x_{11} \nu^2 t + x_{02} t^2 + \dots$$

At leading order, only the tree graphs from $\mathcal{L}_N^{(1)}$ contribute:

$$d_{00}^+ = O(M^2), \quad d_{00}^- = \frac{1}{2F^2} + O(M^2), \quad b_{00}^- = \frac{1}{2F^2} + O(1).$$

The first two relations may be viewed as a variant of Weinberg's predictions for the S -wave scattering lengths – the two low energy theorems discussed

in section 11 represent yet another version of these relations. The third does not contain significant information, because the coefficient b_{00}^- picks up contributions of the same order also from $\mathcal{L}_N^{(2)}$ – chiral symmetry does predict the values of d_{00}^+ and d_{00}^- for $m_u = m_d = 0$, but does not constrain b_{00}^- .

The representation of the scattering amplitude to $O(q^4)$ is fully determined by the coupling constants of the effective theory. Accordingly, we can calculate the various coefficients in terms of these, to the corresponding order of the chiral expansion. It suffices to expand the loop integrals first around $\nu = t = 0$ and then in powers of M . For d_{00}^- , for instance, the calculation yields

$$d_{00}^- = \frac{1}{2F_\pi^2} \left[1 + M_\pi^2 \left\{ 8(d_1 + d_2 + 2d_5) + \frac{4g_A^4}{3F_\pi^2} \left(\lambda_\pi + \frac{1}{32\pi^2} \right) \right\} - M_\pi^3 \left\{ \frac{8 + 12g_A^2 + 11g_A^4}{64\pi F_\pi^2 m_N} - \frac{4c_1 + (c_3 - c_4)g_A^2}{2\pi F_\pi^2} \right\} + O(M_\pi^4) \right].$$

We have expressed the result in terms of the physical values of F_π , M_π and g_A . The formula represents an exact result: Up to and including terms of $O(m^{\frac{3}{2}})$, the expansion of d_{00}^- in powers of the quark masses is fixed by the coupling constants of the effective Lagrangian specified in section 3. In particular, the result shows that this expansion contains a chiral logarithm at order M_π^2 , as well as a term of $O(M_\pi^3)$. Similar formulae can be given also for the other subthreshold coefficients. These are listed in appendix F. Note that, for some of the coefficients, the expansion starts with M_π^{-1} , indicating that those coefficients diverge in the chiral limit, on account of the infrared singularities required by unitarity.

In the loop integrals, the coupling constants c_1, \dots, c_4 are needed only to leading order. As discussed in detail in ref. [9], we may invert the relations for $d_{00}^+, d_{10}^+, d_{01}^+, b_{00}^-$ and represent these couplings in terms of the subthreshold coefficients:

$$c_1 = -\frac{F_\pi^2}{4M_\pi^2} (d_{00}^+ + 2M_\pi^2 d_{01}^+) + O(M_\pi), \quad c_2 = \frac{F_\pi^2}{2} d_{10}^+ + O(M_\pi), \quad (12.1)$$

$$c_3 = -F_\pi^2 d_{01}^+ + O(M_\pi), \quad c_4 = \frac{F_\pi^2}{2m_N} b_{00}^- - \frac{1}{4m_N} + O(M_\pi).$$

Apart from the Born term, the tree graph contributions to the invariant amplitudes represent polynomials in the momenta. The coefficients of these polynomials involve precisely the same combinations of effective coupling constants as the corresponding subthreshold coefficients – we may trade one set of parameters for the other: Up to and including $O(q^4)$, the scattering amplitude may equally well be expressed in terms of subthreshold coefficients.

13 Chiral symmetry

When parametrizing the scattering amplitude in terms of the subthreshold coefficients, part of the information is lost: Chiral symmetry imposes constraints on these coefficients. In order to identify the constraints, it is useful to split the effective Lagrangian into a chirally symmetric part, \mathcal{L}_s , and a remainder, \mathcal{L}_{sb} , that collects the symmetry breaking vertices. The leading term $\mathcal{L}_N^{(1)}$ does not contain a symmetry breaking piece. In $\mathcal{L}_N^{(2)}$, the term proportional to $c_1 \langle \chi_+ \rangle$ belongs to \mathcal{L}_{sb} , while those involving c_2, c_3, c_4 survive in the chiral limit and hence belong to \mathcal{L}_s . At order q^3 , the coupling constants d_5, d_{16}, d_{18} represent symmetry breaking effects. At $O(q^4)$, we did not specify the Lagrangian, but instead wrote down the corresponding contributions to the scattering amplitude, in eq. (4.1). Concerning D^+ , only those terms in $\mathcal{L}_N^{(4)}$ that contain four derivatives of the meson field belong to the symmetric part. In view of $2q \cdot q' = 2M_\pi^2 - t$ and $4m_N \nu = (P + P') \cdot (q + q')$, the expressions $(t - 2M_\pi^2)^2$, $(t - 2M_\pi^2) \nu^2$ and ν^4 are of this type. Hence the coupling constants e_6, e_7, e_8 , belong to the chirally symmetric part of the Lagrangian, while the combinations $e_3 - 4e_8, e_4 + 2e_7$ and $e_5 + 4e_8$ represent symmetry breaking terms. For the same reason, e_{10}, e_{11} belong to \mathcal{L}_s , while the combination $e_9 + 2e_{11}$ controls the symmetry breaking in the amplitude B^- . The coupling constants e_1 and e_2 , that occur in the chiral expansion of the scalar form factor at first non-leading order, also belong to the symmetry breaking part of the Lagrangian.

If the quark masses are turned off, only the coupling constants of \mathcal{L}_s contribute. One readily checks that, in that limit, the subthreshold coefficients listed in appendix F represent linearly independent combinations of the symmetric coupling constants, except for two constraints: d_{00}^+ vanishes and d_{00}^- is determined by F – precisely the two low energy theorems encountered already at leading order. We conclude that, in addition to the Goldberger-Treiman relation, chiral symmetry only imposes two conditions on the subthreshold coefficients.

As noted above, we can express the amplitude in terms of subthreshold coefficients instead of coupling constants, using the relations (12.1) to eliminate c_1, \dots, c_4 in the contributions from the loops. For the value of $F_\pi^2 D^+$ at the Cheng–Dashen point, we then obtain

$$\begin{aligned}
 \Sigma &= F_\pi^2 (\kappa_1 d_{00}^+ + 2\kappa_2 M_\pi^2 d_{01}^+ + 4M_\pi^4 d_{02}^+ + \kappa_3 M_\pi^2 d_{10}^+) + \Delta^+, \\
 \kappa_1 &= 1 + \frac{19M_\pi^2}{120\pi^2 F_\pi^2} - \frac{3M_\pi^2}{64\pi F_\pi^2}, \\
 \kappa_2 &= 1 + \frac{19M_\pi^2}{96\pi^2 F_\pi^2} - \frac{3M_\pi^2}{64\pi F_\pi^2},
 \end{aligned}
 \tag{13.1}$$

$$\begin{aligned}\kappa_3 &= \frac{19M_\pi^2}{960\pi^2F_\pi^2} - \frac{M_\pi^2}{128\pi F_\pi^2}, \\ \Delta^+ &= \frac{37g_A^2M_\pi^3}{3840\pi F_\pi^2} - \frac{11g_A^2M_\pi^4}{80\pi^2m_NF_\pi^2} + \frac{3g_A^2M_\pi^4}{128\pi m_NF_\pi^2} + O(M_\pi^5).\end{aligned}$$

The only infrared singularity occurring in this relation is the term proportional to M_π^3 . Since the coefficient of this term is very small, the contributions from the loop graphs are tiny: Numerically, we find $\kappa_1 = 1.003$, $\kappa_2 = 1.012$, $\kappa_3 = -0.001$ and $\Delta^+ = 1.1$ MeV. Inserting the values of the subthreshold coefficients from ref. [28], the relation yields $\Sigma = 61$ MeV, in perfect agreement with the value given in that reference.

We conclude that, in the present case, the expansion is rapidly convergent. According to section 11, the term Σ nearly coincides with the value of the scalar form factor at $t = 2M_\pi^2$. The difference between $\sigma(2M_\pi^2)$ and $\sigma \equiv \sigma(0)$ is well understood – the evaluation within chiral perturbation theory [9] confirms the result of the dispersive calculation described in ref. [23]:

$$\sigma(2M_\pi^2) - \sigma(0) = 15.2 \pm 0.4 \text{ MeV} . \quad (13.2)$$

The relation (13.1) may thus be rewritten in the form

$$\sigma = F_\pi^2 (d_{00}^+ + 2M_\pi^2 d_{01}^+ + 4M_\pi^4 d_{02}^+) - \sigma_1 . \quad (13.3)$$

Evaluating the small correction terms with the subthreshold coefficients of ref. [28], we obtain

$$\sigma_1 = 13 \pm 2 \text{ MeV} , \quad (13.4)$$

where the error is our estimate for the uncertainties arising from the correction Δ_{CD} , as well as from the higher order contributions, which our calculation neglects.

For the isospin odd amplitude D^- , the term analogous to Σ is the quantity C , defined in eq. (11.5). The representation in terms of the subthreshold coefficients is of the form

$$C = 2F_\pi^2 (d_{00}^- + 2M_\pi^2 d_{01}^-) + \Delta^- , \quad (13.5)$$

where the correction Δ^- is given by

$$\begin{aligned}\Delta^- &= \frac{(5g_A^2 - 2)M_\pi^2}{72\pi^2F_\pi^2} - \frac{(g_A^2 - 1)M_\pi^2}{96\pi F_\pi^2} - \frac{g_A^2(3g_A^2 + 22)M_\pi^3}{192\pi m_N F_\pi^2} \\ &+ \frac{g_A^2 M_\pi^3}{16\sqrt{2}\pi m_N F_\pi^2} \ln(1 + \sqrt{2}) + O(M_\pi^4) .\end{aligned}$$

The infrared singular terms proportional to M_π^3 are small, of order 0.03. Moreover, they nearly cancel against those of $O(M_\pi^2)$, so that the net correction from the one loop graphs is tiny, $\Delta^- = -0.003 + O(M_\pi^4)$. The contributions of order M_π^4 are more important. In particular, the Δ resonance generates a term of this order, which is enhanced by the third power of the corresponding energy denominator (note that the resonance also contributes to the coefficients d_{00}^- and d_{01}^-):

$$\Delta_\Delta^- = \frac{8F_\pi^2 g_\Delta^2 M_\pi^4}{9 m_N (m_\Delta - m_N)^3} .$$

Numerically, this term amounts to 0.02.⁵ The dispersive analysis of ref. [28] confirms that the resonance contribution dominates. In our opinion, the estimate

$$\Delta^- = 0.02 \pm 0.01 \tag{13.6}$$

covers the uncertainties. We conclude that the relation (13.5) very accurately determines the value of the isospin odd amplitude at the Cheng-Dashen point, in terms of the subthreshold coefficients d_{00}^-, d_{01}^- .

Unfortunately, our knowledge of the coefficient d_{00}^- is not satisfactory. The result obtained for this quantity is very sensitive to the value used for $g_{\pi N}$: The difference $d_{00}^- - g_{\pi N}^2/2m_N^2$ is relatively well known, as it is given by an integral over a total cross section

$$d_{00}^- - \frac{g_{\pi N}^2}{2m_N^2} = \frac{2}{\pi} \int_{M_\pi}^\infty \frac{d\omega}{\omega^2} k \sigma^-(\omega) . \tag{13.7}$$

If the integral is taken known, a shift in $f^2 = g_{\pi N}^2 M_\pi^2/16\pi m_N^2$ from the value $f^2 = 0.079$ [28] to $f^2 = 0.076$ [33] lowers the result for d_{00}^- by $0.08M_\pi^{-2}$, so that C decreases by 0.07. Indeed, the recent evaluations of the subthreshold coefficients by Stahov [34] and Oades [35] confirm that the value of d_{00}^- is lower for the partial wave analyses of the VPI/GW group than for the Karlsruhe analyses. For a precise determination of the value of the isospin odd amplitude at the Cheng-Dashen point, the discrepancy in the value of the pion nucleon coupling constant needs to be resolved.

We can now check whether the phenomenological information is consistent with the low energy theorem (11.6), which predicts the value of C to order M_π^3 , except for the contribution $C_{sb} = 16 M_\pi^2 d_5^r(\mu)$ from the symmetry breaking coupling constant d_5^r . For the reasons given earlier, we expect contributions of this type to be very small, of the order of a few per cent.

⁵ The corresponding contribution to Δ^+ is even smaller, of order 0.1 MeV.

	d_{00}^-	d_{01}^-	C	$16 M_\pi^2 d_5^r(\mu)$
KH80 [28]	1.53 ± 0.02	-0.134 ± 0.005	1.13 ± 0.02	0.04 ± 0.03
KA84 [34]	1.510 ± 0.001	-0.136 ± 0.003	1.11 ± 0.01	0.03 ± 0.01
SP98 [34]	1.468 ± 0.004	-0.138 ± 0.003	1.06 ± 0.01	0.00 ± 0.01
KH80 [35]	1.53 ± 0.02	-0.14 ± 0.03	1.12 ± 0.06	0.04 ± 0.06
SP98 [35]	1.46 ± 0.01	-0.12 ± 0.01	1.09 ± 0.02	0.06 ± 0.02

Table 1: Value of the isospin-odd amplitude at the Cheng-Dashen point. The results for C are obtained with eqs. (13.5) and (13.6). The value of $d_5^r(\mu)$ follows from eq. (11.6) and refers to the running scale $\mu = 1$ GeV.

This is confirmed by the numerical results listed in the last column of table 1 which are obtained by comparing eqs. (11.6) and (13.5) – the relation (12.1) is used to express c_1 in terms of subthreshold coefficients, the running scale μ is set equal to 1 GeV and contributions of order M_π^4 or higher are dropped.

As mentioned above, the Weinberg predictions for the two S -wave scattering lengths represent yet another version of the two energy theorems under discussion. These predictions only hold to leading order of the chiral expansion, but the one loop representation of the amplitude allows us to analyze the corresponding corrections – it suffices to evaluate our representation of the amplitudes $D^\pm(\nu, t)$ at $\nu = M_\pi$, $t = 0$. The expansion of the result in powers of M_π then yields an explicit expression for the S -wave scattering lengths, valid up to and including $O(M_\pi^4)$. In fact, this calculation has been done already, in the framework of HBCHPT [8], and we have verified that our method yields the same result (note that the results given in Appendix A of [8] contain typographical errors).

In the case of the scattering lengths, however, the corrections are by no means small – the first few terms of the chiral expansion only yield a rather poor approximation. This is in marked contrast to the case of $\pi\pi$ scattering, where the chiral expansion of the scattering lengths converges rather rapidly. The main reason is that the distance between the Cheng-Dashen point and threshold is of order M_π and is therefore much larger than for $\pi\pi$ scattering, where the analog of the Cheng-Dashen point occurs at $s = u = M_\pi^2$, $t = 2M_\pi^2$, so that the distance to threshold is of order M_π^2 . Accordingly, the expansion parameter is larger – we cannot expect the chiral representation at threshold to have the same accuracy as in the case of $\pi\pi$ scattering. The problem is accentuated by the fact that the threshold sits on top of the branch point required by unitarity – when considering the scattering lengths, we are in effect analyzing the amplitude at a singular point. In this respect,

the situation is comparable with the case of $\pi\pi$ scattering, where the S -wave scattering lengths also contain chiral logarithms with a large coefficient. As shown in ref. [19], the expansion of the $\pi\pi$ scattering amplitude in the subthreshold region converges much more rapidly than at threshold.

In the variants of the low energy theorems discussed above, these problems did not occur, because we have been comparing the properties of the amplitude at the Cheng–Dashen point, $s = u = m_N^2$, $t = 2M_\pi^2$, with those at $s = u = m_N^2 + M_\pi^2$, $t = 0$. In this region, the amplitude does not contain branch points and the relevant distance is small, of order M_π^2 . This is why the corrections encountered turned out to be rather small.

14 Cuts required by unitarity

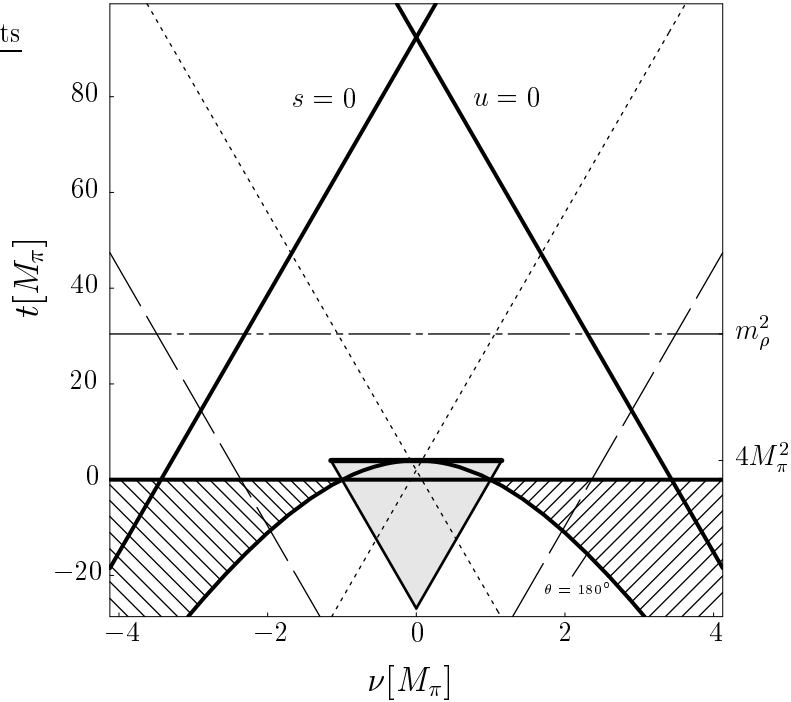


Figure 7: Mandelstam plane. Hatched: Physical regions of πN scattering. In the shaded region $s < (m_N + M_\pi)^2$, $u < (m_N + M_\pi)^2$ and $t < 4M_\pi^2$ the amplitude is real and analytic, once the poles at $s = m_N^2$ and $u = m_N^2$ (thin lines) are subtracted. Dotted: Nucleon poles. Dashed: Δ -resonance. Dot-dashed: ρ -resonance

In the following sections, we examine the energy dependence of the loop graphs in some detail, in order to clarify the problems encountered when extrapolating the chiral representation to threshold or even beyond. For this purpose, we first study the analytic structure of the loop graphs.

In addition to the nucleon pole terms, the scattering amplitude contains branch points at $s = (m_N + M_\pi)^2$, $u = (m_N + M_\pi)^2$ and $t = 4M_\pi^2$. These correspond to the sides of the shaded triangle shown in fig. 7. In the chiral representation of the amplitude, the corresponding cuts are described by the loop integrals. Crossing symmetry relates the discontinuities in the u -channel to those in the s -channel, so that we only need to discuss the s - and t -channel imaginary parts.

We recall that we are absorbing the self energy insertions due to the tree graphs of $\mathcal{L}_N^{(2)}$ and $\mathcal{L}_N^{(4)}$ by replacing the bare nucleon mass with $m_4 = m - 4c_1 M^2 + e_1 M^4$. As far as the loop integrals are concerned, the difference between m_4, M and the physical masses m_N, M_π is beyond the accuracy of our calculation. In the following, we represent these integrals in terms of the physical masses.

14.1 s -channel cuts

The branch cut at $s > (m_N + M_\pi)^2$ is an immediate consequence of the unitarity condition,

$$\langle f | \mathbf{T} | i \rangle - \langle f | \mathbf{T}^\dagger | i \rangle = i \sum_{\{n\}} \langle f | \mathbf{T}^\dagger | n \rangle \langle n | \mathbf{T} | f \rangle . \quad (14.1)$$

At one loop level only πN intermediate states enter this relation – inelastic channels only show up at higher orders. The condition thus exclusively involves the s -channel partial wave amplitudes

$$f_{l\pm}^I(s) = q^{-1} \exp i \delta_{l\pm}^I(s) \sin \delta_{l\pm}^I(s) . \quad (14.2)$$

The lower index specifies the orbital angular momentum l as well as the total angular momentum $J = l \pm \frac{1}{2}$. The upper index refers to the isospin $I = \frac{1}{2}, \frac{3}{2}$ and q stands for the c.m. momentum,

$$q^2 = \frac{1}{4s} \{s - (m_N + M_\pi)^2\} \{s - (m_N - M_\pi)^2\} . \quad (14.3)$$

In this normalization, elastic unitarity takes the form

$$\text{Im } f_{l\pm}^I(s) = q |f_{l\pm}^I(s)|^2 . \quad (14.4)$$

The low energy expansion of the partial waves starts at $O(q)$. The relation (14.4) implies that an imaginary part starts showing up only at $O(q^3)$ – the tree graphs generated by $\mathcal{L}_N^{(1)}$ and $\mathcal{L}_N^{(2)}$ thus suffice to evaluate the imaginary parts of the amplitude to $O(q^4)$. In agreement with the chiral counting rules, the imaginary parts generated by the square of the contributions due to $\mathcal{L}_N^{(2)}$ are of $O(q^5)$ and we can drop these.

We have checked that our representation of the scattering amplitude indeed obeys elastic unitarity. In this respect, there is no difference between infrared and dimensional regularization – the s -channel discontinuities are identical [9]. The real parts are different, however. To any order in the low energy expansion, the difference is a polynomial, but the degree of the polynomial increases with the order.

14.2 t -channel cuts

Some of the graphs contain a branch cut for $t > 4M_\pi^2$. The corresponding discontinuity is determined by the extended unitarity relation

$$\text{Im } f_\pm^J(t) = \{1 - 4M_\pi^2/t\}^{\frac{1}{2}} t_J^I(t)^* f_\pm^J(t), \quad 4M_\pi^2 < t < 16M_\pi^2. \quad (14.5)$$

The quantities $f_\pm^J(t)$ represent the t -channel partial waves of the πN scattering amplitude. The quantum number J stands for the total angular momentum, while the lower index again refers to the spin configuration. There is no need to in addition specify the isospin quantum number, because it is determined by the total angular momentum: J even $\rightarrow I = 0$, J odd $\rightarrow I = 1$. The functions

$$t_J^I(t) = \{1 - 4M_\pi^2/t\}^{-\frac{1}{2}} \exp i \delta_J^I(t) \sin \delta_J^I(t)$$

denote the partial wave projections of the $\pi\pi$ scattering amplitude.

The low energy expansion of the right hand side of (14.5) again starts at $O(q^3)$. In our context, the evaluation of this condition is particularly simple, because the $\pi\pi$ scattering amplitude is needed only to leading order, where it is a polynomial. Hence only the partial waves with $J = 0, 1$ contribute. These are given explicitly in appendix G.

We have checked that, in the region $t < 4m_N^2$, the imaginary parts of our loop integrals do obey the relation (14.5). Note that this relation only accounts for the $\pi\pi$ intermediate states. States with three or more pions do not occur at one loop, but outside the low energy region, the nucleon-antinucleon states yield an additional contribution, which does show up in the box graph and in the triangle graph, fig. 2m, through a branch cut for $t > 4m_N^2$. Because this singularity is absent at any fixed order of the chiral expansion of

the loop integrals, it is not preserved by infrared regularization. Indeed one finds that the regular part of the corresponding loop integrals has a branch cut for $t > 4m_N^2$ so that the imaginary part of the amplitudes in infrared regularization agrees with the one obtained in dimensional regularization only for $t < 4m_N^2$.

14.3 Box graph

The analytic structure of the Box graph (i) is more complicated: The corresponding loop integrals contain a simultaneous cut in the variables s and t and thus contribute to the Mandelstam double spectral function (at one loop level, only the box graph generates such a contribution).

Let us consider the relevant scalar loop integral. In view of the four energy denominators, this integral does not require regularization. It may be represented in terms of the double dispersion relation

$$H_{13}(s, t) = \frac{1}{\pi^2} \int_{s_+}^{\infty} ds' \int_{t_{min}(s')}^{\infty} dt' \frac{\rho_2(s', t')}{(s' - s - i\epsilon)(t' - t - i\epsilon)} .$$

The boundary of the integration region is given by

$$s_{\pm} = (m_N \pm M_{\pi})^2, \quad t_{min}(s) = \frac{4(s - m_N^2 - 2M_{\pi}^2)(m_N^2 s - (m_N^2 - M_{\pi}^2)^2)}{(s - s_+)(s - s_-)},$$

and the explicit expression for the double spectral density reads⁶

$$\rho_2(s, t) = \frac{1}{8\sqrt{t(t - t_{min}(s))(s - s_+)(s - s_-)}} .$$

In view of $t_{min}(s) > 4m_N^2$, we may expand the integral in a Taylor series in powers of t . Because the singularity in the variable t lies far outside the low energy region, the higher order terms in t are strongly suppressed – these contributions are similar to those we dropped when simplifying the integrands of the loop integrals in section 6. The statement also holds in infrared regularization and for the tensor integrals associated with the box graph.

Using the explicit expressions for the box graph in appendix D, we have determined the order to which the t -dependence of the integrals $I_{13}(s, t)$,

⁶The expression for $\rho_2(s, t)$ may be read off from the one given for the imaginary part $\text{Im}_s H_{13}(s, t) = \text{Im}_s I_{13}(s, t)$ in appendix H. The square root occurring in that expression becomes imaginary for $t > t_{min}$. The double spectral density is the discontinuity across the cut generated by this square root.

$I_{13}^{(1)}(s, t)$, $I_{13}^{(2)}(s, t)$ is needed – because of cancellations between the various terms occurring in the representation of the invariant amplitudes in terms of these, the order needed cannot directly be read off. Within the accuracy of our calculation, the box-amplitudes of B^\pm are given by their value at $t = 0$ and the amplitudes D^\pm can be replaced by their first order expansion in t , so that we are allowed to replace the box integrals by their Taylor expansion in t to first order.

The expanded box integrals can be represented in terms of a spectral function with a single variable. In the case of the full scalar integral, for instance, the explicit representation reads:

$$H_{13}(s, t) = \frac{1}{\pi} \int_{s_+}^{\infty} ds' \frac{\rho_1(s')}{s' - s - i\epsilon} \left(1 + \frac{2t}{3t_{min}(s)} + O(t^2) \right) ,$$

$$\rho_1(s) = \frac{\sqrt{(s - s_-)(s - s_+)}}{16\pi(s - m_N^2 - 2M_\pi^2)(m_N^2 s - (m_N^2 - M_\pi^2)^2)} .$$

The formula nicely displays the suppression of the t -dependent part. Since $t_{min}(s)$ is a quantity of order q^0 it is also evident that the t -dependent part is an $O(q^2)$ correction to $H_{13}(s, 0)$.

This shows that, at low energies, the contributions generated by the Mandelstam double spectral function can be described in terms of single variable dispersion integrals.

15 Dispersive representation

With the above simplification of the box graph contribution and after the reduction of the numerators for the diagrams discussed in section 6, all of the loop integrals are of a similar structure: The discontinuities across the s - and u -channel cuts are linear in t , while those across the t -channel cut are linear in ν . Up to higher order corrections, the s -channel imaginary parts thus have the form

$$\begin{aligned} \text{Im}_s D^\pm(s, t) &= \text{Im} D_1^\pm(s) + t \text{Im} D_2^\pm(s) + O(q^5) , \\ \text{Im}_s B^\pm(s, t) &= \text{Im} B_1^\pm(s) + O(q^3) , \end{aligned}$$

while the t -channel discontinuities have the structure (explicit expressions for the functions $\text{Im} D_3^+(t)$, $\text{Im} D_3^-(t)$, $\text{Im} B_2^-(t)$ are given in appendix G)

$$\begin{aligned} \text{Im}_t D^+(\nu, t) &= \text{Im} D_3^+(t) + O(q^5) , & \text{Im}_t D^-(\nu, t) &= \nu \text{Im} D_3^-(t) + O(q^5) , \\ \text{Im}_t B^+(\nu, t) &= O(q^3) , & \text{Im}_t B^-(\nu, t) &= \text{Im} B_2^-(t) + O(q^3) . \end{aligned}$$

We now make use of the fact that an analytic function that asymptotically only grows with a power of the argument is fully determined by its singularities, up to a polynomial. This allows us to establish an alternative representation of the scattering amplitude that also holds to first nonleading order and has two advantages as compared to the one in terms of the explicit expression for the loop integrals: It exhibits the structure of the amplitude in a more transparent manner and only involves the expressions for the imaginary parts. Since unitarity determines the latter in terms of the tree level amplitude, the dispersive representation does not involve any loop integrals.

Explicitly, the dispersive representation reads

$$\begin{aligned}
D^+(\nu, t) &= D_{pv}^+(\nu, t) + D_1^+(s) + D_1^+(u) + t D_2^+(s) + t D_2^+(u) \\
&\quad + D_3^+(t) + D_p^+(\nu, t) + O(q^5), \\
D^-(\nu, t) &= D_{pv}^-(\nu, t) + D_1^-(s) - D_1^-(u) + t D_2^-(s) - t D_2^-(u) \\
&\quad + \nu D_3^-(t) + D_p^-(\nu, t) + O(q^5), \\
B^+(\nu, t) &= B_{pv}^+(\nu, t) + B_1^+(s) - B_1^+(u) + B_p^+(\nu, t) + O(q^3), \\
B^-(\nu, t) &= B_{pv}^-(\nu, t) + B_1^-(s) + B_1^-(u) + B_2^-(t) + B_p^-(\nu, t) + O(q^3).
\end{aligned} \tag{15.1}$$

The functions $D_{pv}^\pm(\nu, t), B_{pv}^\pm(\nu, t)$ represent the pseudovector Born terms of eq. (8.1). The contributions generated by the cuts in the s -, t - and u -channels are described by the functions $D_1^+(s), D_1^+(u), \dots, B_2^-(t)$. The dispersion integrals that determine these in terms of the corresponding imaginary parts are given below. Once the singularities are removed, the low energy representation of the invariant amplitudes reduces to a polynomial. We denote the corresponding contributions by $D_p^\pm(\nu, t), B_p^\pm(\nu, t)$.

A representation of the above type was used already by Gasser, Sainio and Švarc [2, 36]. These authors noted that if the masses occurring in the loop integrals are identified with the physical masses rather than the bare quantities occurring in dimensional regularization, the infrared singularities generated by the cuts are correctly accounted for. As they did not make use of any approximations for the loop integrals, the t -dependence of their s - and u -channel cuts was however more involved. The representation (15.1) shows that, to the accuracy of a one loop calculation, the amplitude may be described in terms of nine functions of a single variable. An analogous representation also holds for the $\pi\pi$ scattering amplitude [37]. In that case three functions of a single variable suffice and the representation is valid even to two loops, that is modulo contributions of $O(q^8)$.

16 Subtracted dispersion integrals

We now specify the functions $D_1^\pm(s), \dots, B_2^\pm(t)$ as suitably subtracted dispersion integrals over their imaginary parts. For this purpose, it is convenient to replace the variable s by the lab energy ω , which is linear in s and independent of t (for $t = 0$, ν coincides with ω),

$$\omega = \frac{s - m_N^2 - M_\pi^2}{2m_N}. \quad (16.1)$$

The number of subtractions is determined by the asymptotic behavior of the imaginary parts and is related to the superficial degree of divergence $\omega(G)$ of the relevant diagram. This quantity is obtained by adding up the powers of the loop momentum k in the region where it is large compared to the masses and to the external momenta: $\omega(G) = 4 + \delta - I_N - 2I_\pi$, where δ is the number of derivatives at the vertices and I_N, I_π stand for the number of nucleon and pion propagators occurring in the loop, respectively. The vertices from $\mathcal{L}_N^{(1)}$ contain one derivative, those of $\mathcal{L}_\pi^{(2)}$ contain two. In $\mathcal{L}_N^{(2)}$, there are up to four derivatives (vertex proportional to c_2). It is important here that we are considering only diagrams with at most one vertex from $\mathcal{L}_N^{(2)}$ – if the unitarity relation is evaluated with the full square of the tree level amplitude, the imaginary part grows more rapidly. Note also that the simplifications discussed in section 6 reduce the degree of divergence.

The imaginary parts occurring in the tensorial decomposition of the loop integrals are listed explicitly in appendix H. These expressions show that the quantities $\text{Im}D_1^\pm(s)$ grow with $s^3 \ln s$, while for the parts linear in t , we have $\text{Im}D_2^\pm(s) \propto s \ln s$. The leading contribution stems from the graphs (g) and (h) and is proportional to c_2 (if only the loops generated by $\mathcal{L}_N^{(1)}$ are considered, we instead obtain $\text{Im}D_1^\pm(s) \propto s^2$ and $\text{Im}D_2^\pm(s) \propto s$). The asymptotic behavior of the B -amplitudes is given by $\text{Im}B_1^+(s) \propto c_2 s \ln s$, $\text{Im}B_1^-(s) \propto s$. We subtract at $\omega = 0$ and write the s -channel dispersion relations in the form

$$\begin{aligned} D_1^\pm(s) &= \frac{\omega^5}{\pi} \int_{M_\pi}^\infty \frac{d\omega' \text{Im}D_1^\pm(s')}{\omega'^5 (\omega' - \omega - i\epsilon)} \\ D_2^\pm(s) &= \frac{\omega^3}{\pi} \int_{M_\pi}^\infty \frac{d\omega' \text{Im}D_2^\pm(s')}{\omega'^3 (\omega' - \omega - i\epsilon)} \\ B_1^\pm(s) &= \frac{\omega^3}{\pi} \int_{M_\pi}^\infty \frac{d\omega' \text{Im}B_1^\pm(s')}{\omega'^3 (\omega' - \omega - i\epsilon)}. \end{aligned} \quad (16.2)$$

The representation (15.1) is manifestly crossing symmetric: The contributions generated by the cuts in the u -channel are obtained from those due to the s -channel discontinuities by the substitution $s \rightarrow u$.

The contributions due to the t -channel cuts may be characterized in the same manner. The dispersion relations take the form

$$\begin{aligned}
D_3^+(t) &= \frac{t^3}{\pi} \int_{4M_\pi^2}^{\infty} \frac{dt' \operatorname{Im} D_3^+(t')}{t'^3 (t' - t - i\epsilon)}, \\
D_3^-(t) &= \frac{t^2}{\pi} \int_{4M_\pi^2}^{\infty} \frac{dt' \operatorname{Im} D_3^-(t')}{t'^2 (t' - t - i\epsilon)}, \\
B_2^-(t) &= \frac{t}{\pi} \int_{4M_\pi^2}^{\infty} \frac{dt' \operatorname{Im} B_2^-(t')}{t' (t' - t - i\epsilon)}.
\end{aligned} \tag{16.3}$$

In the terminology used in ref. [20], the contributions associated with the cuts in the s -, t - and u -channels represent “unitarity corrections”. Together with the explicit expressions for the imaginary parts of the various graphs given in the appendix, these relations unambiguously specify the contributions generated by the cuts.

By construction, the cuts do not contribute to the first few terms in the Taylor series expansion of the amplitude in powers of ν and t , that is to the leading coefficients of the subthreshold expansion, which we discussed in section 12. The polynomials $D_p^\pm(\nu, t)$ and $B_p^\pm(\nu, t)$ account for the following terms of this expansion:

$$\begin{aligned}
D_p^+(\nu, t) &= d_{00}^+ + d_{10}^+ \nu^2 + d_{01}^+ t + d_{20}^+ \nu^4 + d_{11}^+ \nu^2 t + d_{02}^+ t^2, \\
B_p^+(\nu, t) &= b_{00}^+ \nu, \\
D_p^-(\nu, t) &= d_{00}^- \nu + d_{10}^- \nu^3 + d_{01}^- \nu t, \\
B_p^-(\nu, t) &= b_{00}^- + b_{10}^- \nu^2 + b_{01}^- t.
\end{aligned} \tag{16.4}$$

At the order of the chiral expansion under consideration, the higher coefficients exclusively receive contributions from the parts of the amplitude that describe the cuts.

To complete the construction of the dispersive representation, we incorporate the constraints imposed by chiral symmetry. These are:

1. The strength of the πN interaction is determined by g_A , up to corrections from the symmetry breaking part of the effective Lagrangian.
2. In view of the relations (12.1), chiral symmetry and unitarity fix the imaginary parts in terms of the subthreshold coefficients.
3. Finally, as shown in section 13, chiral symmetry subjects the subthreshold coefficients to the two constraints (13.1) and (13.5).

With these supplements, the dispersive representation of the amplitude becomes equivalent to the one in terms of infrared regularized loop integrals. In effect, we made use of these integrals only when analyzing the corrections to the Goldberger-Treiman relation and to the two low energy theorems referred to in point 3.

Note that the dispersive representation does not rely on an expansion of the infrared singularities in powers of the momenta – as mentioned above, this is a subtle matter. In particular, the result depends on the choice of the two independent kinematic variables that are kept fixed when performing the expansion. The above definition of the cut contributions in terms of their absorptive parts precisely serves the purpose of avoiding such problems at this stage. We will give the explicit algebraic representations for the functions $D_1^\pm(s)$, \dots , $B_2^\pm(t)$ that result, for instance, if the expansion is performed by keeping the ratio ω/M_π fixed and discuss the changes occurring if we replace the lab energy ω by the c.m. energy. Also, we will discuss the range of validity of such representations in some detail, but first we wish to describe the result of our calculation without invoking expansions of this sort.

17 Dispersion relations versus loop integrals

The dispersive representation of the loop integrals may be viewed as yet another regularization of the loop graphs that is consistent with power counting. We add a few remarks concerning the comparison of this representation with the one based on infrared regularized loop integrals. For this purpose, we first again consider the scalar self energy integral, for which both of these representations can be given explicitly (compare section 5.1). In dimensional regularization, the relevant integral is given by $H(s)$, while in infrared regularization, only the infrared singular part thereof, $I(s)$, is retained. On the other hand, the dispersive representation of the self energy integral, which we denote by $D(s)$, is determined by the imaginary part of $I(s)$. The relevant dispersion relation involves the minimal number of subtractions required by the asymptotic behaviour:

$$D(s) = \frac{\omega}{\pi} \int_{M_\pi}^{\infty} \frac{d\omega' \operatorname{Im} I(s')}{\omega'(\omega' - \omega - i\epsilon)}.$$

On the interval of interest, $s > (m_N + M_\pi)^2$, we have $\operatorname{Im} I(s) = \operatorname{Im} H(s)$. While the function $H(s)$ is analytic except for the discontinuity on this interval, the function $I(s)$ in addition contains fictitious singularities far outside the low energy region: a pole at $s = 0$, as well as a cut along the negative s -axis. Since by construction, the dispersive representation only contains the right

hand cut, $D(s)$ can differ from the function $H(s)$ only by a polynomial. In fact, the asymptotic behaviour shows that the polynomial is a constant. Hence the explicit expression for $D(s)$ reads

$$D(s) = H(s) - H(m_N^2 + M_\pi^2) .$$

In view of $H(s) = I(s) + R(s)$, the difference between the two representations we wish to compare may be represented as

$$D(s) - I(s) = R(s) - R(m_N^2 + M_\pi^2) - I(m_N^2 + M_\pi^2) .$$

Since the regular part of the self energy integral, $R(s)$, does not contain any infrared singularities, we may replace it by the first few terms in the chiral expansion, which in the present case amounts to a simultaneous expansion in powers of ω and M_π . The resulting representation for $R(s)$ is a polynomial in ω , with coefficients that are polynomials in M_π^2 . We conclude that, to any finite order in the chiral expansion, $D(s) - I(s)$ is a polynomial in ω or, equivalently, in s . Moreover, since all of its coefficients except the constant term only pick up contributions from $R(s)$, they are polynomials in M_π^2 . The constant term, on the other hand, does contain infrared singularities, from $I(m_N^2 + M_\pi^2)$.

The same line of reasoning also applies to the other graphs. When forming the sum of all contributions, the difference also amounts to a polynomial and only the coefficients listed in eq. (16.4) can pick up infrared singularities, from the analogues of the term $I(m_N^2 + M_\pi^2)$ encountered above. As we are explicitly supplementing the dispersion integrals with the relevant polynomial, the result agrees with the representation in terms of infrared regularized loop integrals, up to terms that are beyond the accuracy of a one loop calculation.

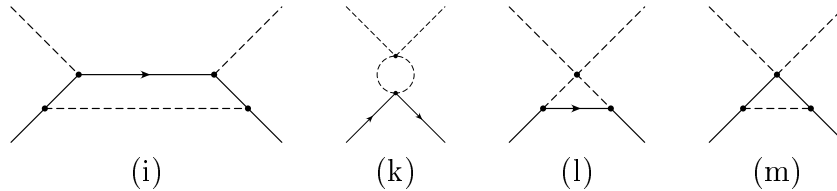
18 Chiral expansion of the amplitude

The dispersive representation given above includes terms of arbitrarily high order in the chiral expansion. It is suitable for numerical analysis, but since the expressions for the imaginary parts are lengthy, an approximate representation that replaces these integrals by elementary functions is useful. Such a representation may be obtained by performing the chiral expansion in the integrand of the loop integrals. The result is very similar to the one obtained in HBCHPT, where the unitarity cuts are described in terms of simple functions such as $\arccos(x)$. In [9], we have proven that this expansion converges for all of the integrals encountered here, at least in part of the low energy region. In the present section, we first briefly comment on the chiral expansion of the integrals associated with the t -channel cut, where the discussion

given in ref. [9] can be taken over without significant complications. Then we analyze the analogous issue for the s -channel and discuss the infrared singularities associated with the corresponding cut in some detail.

18.1 t -channel cut

Only the diagrams belonging to the topologies (i), (k), (l) and (m) develop



an imaginary part for $t > 4M_\pi^2$. For graphs (i) and (m), the t -channel cut only starts at $t = 4m_N^2$. As discussed in section 14, these do not show up at finite orders of the chiral expansion, so that the diagrams (i) and (m) do not contribute. The integrals arising from the graphs (k) and (l) are polynomials in ν . It is convenient to replace the pion mass and the momentum transfer by the two dimensionless variables

$$\alpha = \frac{M_\pi}{m_N}, \quad \tau = \frac{t}{M_\pi^2}.$$

Graph (k) may be expressed in terms of the scalar loop integral with two meson propagators, $J(t)$. We remove the divergence by subtracting at $t = 0$. The remainder, $\bar{J}(t) = J(t) - J(0)$, only depends on the ratio τ and the explicit expression reads

$$\bar{J}(\tau) = \frac{1}{8\pi^2} \left\{ 1 - \sqrt{\frac{4-\tau}{\tau}} \arcsin \frac{\sqrt{\tau}}{2} \right\}.$$

The triangle graph (m) involves integrals with two meson propagators and one nucleon propagator. The chiral expansion of these functions does not cover the entire low energy region: It breaks down in the vicinity of the point $t = 4M_\pi^2$. The matter is discussed in detail in ref. [9], where it is shown that the elementary function

$$g(\tau) = \frac{1}{32\pi\sqrt{\tau}} \ln \frac{2 + \sqrt{\tau}}{2 - \sqrt{\tau}} - \frac{1}{32\pi} \ln \left\{ 1 + \frac{\alpha}{\sqrt{4-\tau}} \right\} \\ + \frac{\alpha}{32\pi^2} \left\{ 1 + \frac{\pi}{\sqrt{4-\tau}} + \frac{2(2-\tau)}{\sqrt{\tau(4-\tau)}} \arcsin \frac{\sqrt{\tau}}{2} \right\}$$

does provide a representation that is valid throughout the low energy region.

18.2 s -channel cut

The dispersive integrals associated with the s -channel cut are polynomials in t with coefficients that depend only on s . The u -channel cut is described by the same integrals. The effective theory concerns the region where $s - m_N^2 = O(q)$. We may for instance consider the expansion of the loop integrals in powers of $\alpha = M_\pi/m_N$ at a fixed value of the ratio $r = (s - m_N^2)/M_\pi$. That expansion, however, necessarily diverges in the vicinity of the branch point $s = (m_N + M_\pi)^2$, because this singularity corresponds to a value of r that depends on the expansion parameter α . A better choice of the variable to be held fixed is the ratio of the pion lab. energy ω to the pion mass, which we denote by

$$\Omega = \frac{s - m_N^2 - M_\pi^2}{2 m_N M_\pi} = \frac{\omega}{M_\pi}.$$

The s -channel cut starts at $\Omega = 1$ and thus stays put when α varies. Indeed, we have shown [9] that the convergence domain of the expansion of the self energy integral $I(s)$ at fixed Ω is $0 < s < 2m_N^2 + 2M_\pi^2$ and thus covers exactly the Mandelstam triangle.

Numerically, the convergence is rather slow, however, already at the threshold. The explicit expression for the self energy integral $I(s)$ involves the factor $m^2/s = (1 + 2\alpha\Omega + \alpha^2)^{-1}$ and some of the loop integrals even contain the third power thereof. At threshold, the expansion of this factor in powers of α is roughly a geometric series with expansion parameter $2\Omega\alpha \simeq \frac{2}{7}$. When the factor appears squared or cubed, the lowest orders do therefore not give a decent approximation.

A more suitable choice is the c. m. energy of the pion

$$\Omega_q = \frac{s - m_N^2 - M_\pi^2}{2M_\pi\sqrt{s}} = \frac{\omega_q}{M_\pi}, \quad (18.1)$$

which maps the interval $0 < s < \infty$ onto $-\infty < \Omega_q < \infty$ and thus pushes the singularity at $s = 0$ away from the threshold at $\Omega_q = 1$. Expressed in terms of this variable, the infrared singular part of the self energy integral is given by

$$I(s) = \frac{M_\pi}{16\pi^2\sqrt{s}} \left\{ -2\sqrt{1 - \Omega_q^2} \arccos(-\Omega_q) + \Omega_q (1 - 32\pi^2\lambda_\pi) \right\}. \quad (18.2)$$

At fixed Ω_q , only the factor $\sqrt{s} = \sqrt{1 + \alpha^2(\Omega_q^2 - 1)} + \alpha\Omega_q$ gets expanded. It has a branch point at $\Omega_q^c = \pm i\sqrt{1 - \alpha^2}/\alpha$. The expansion is convergent for $|\Omega_q| < |\Omega_q^c|$, which corresponds to the range

$$(3 - 2\sqrt{2})(m_N^2 - M_\pi^2) < s < (3 + 2\sqrt{2})(m_N^2 - M_\pi^2).$$

On the left, the convergence range is slightly smaller than the one obtained for the variable Ω , but on the right, the convergence is drastically improved. The point at which the expansion at fixed Ω_q breaks down is six times farther away from threshold than the edge of the Mandelstam triangle, where the expansion at fixed Ω starts to fail.

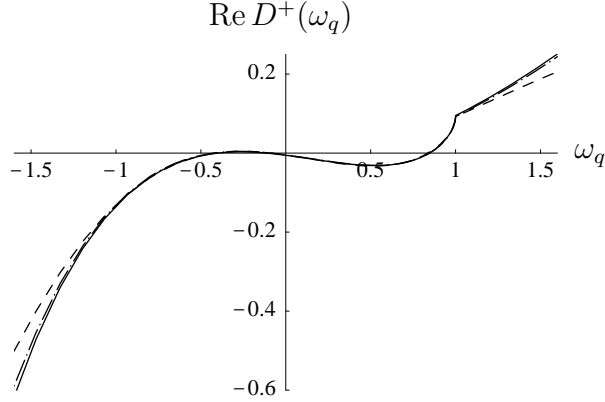


Figure 8: Chiral expansion of the contribution from diagram (f) to the real part of the amplitude D^+ (infrared regularization, scale $\mu = m_N$). Full: relativistic amplitude, dot-dashed: expansion at fixed Ω_q , dashed: expansion at fixed Ω . In all of the figures, dimensionful quantities are given in units of M_π .

We illustrate this with the contribution of graph (f) to the amplitude D^+ at $t = 0$. The corresponding Feynman diagram is shown in fig. 2 and the formulae in appendix D explicitly specify this contribution in terms of the function $I(s)$. In fig. 8, the full line shows the exact result for the renormalized amplitude at $t = 0$, obtained with infrared regularization (for definiteness, we have identified the running scale with the nucleon mass). The dashed line corresponds to the expansion to order α^4 at fixed Ω , while the dash-dotted curve is obtained if we instead keep the variable Ω_q fixed. The figure shows that the chiral expansion at fixed Ω_q describes the result quite accurately.

In fig. 9, we compare the imaginary parts of the loop integrals with the chiral expansion thereof, for the sum of all graphs. Near threshold, these are suppressed by phase space. To make the behavior visible there, we plot the integrand relevant if the variable in the dispersion integrals is identified with the lab momentum $k = \sqrt{\omega^2 - M_\pi^2}$ rather than the lab energy ω . The integrand of the dispersion relation for the value of the amplitude at threshold, $D^\pm(M_\pi, 0) = 4\pi(1 + \alpha)a_{0+}^\pm$, is then given by $n^\pm(k) \text{Im}D_1^\pm(k)$, with

$$n^\pm(k) = \frac{M_\pi^5}{\pi \omega^5} \frac{d\omega}{dk} \left\{ \frac{1}{\omega - M_\pi} \mp \frac{1}{\omega + M_\pi} \right\} = \frac{2M_\pi^5}{\pi k \omega^6} \left\{ \frac{M_\pi}{\omega} \right.$$

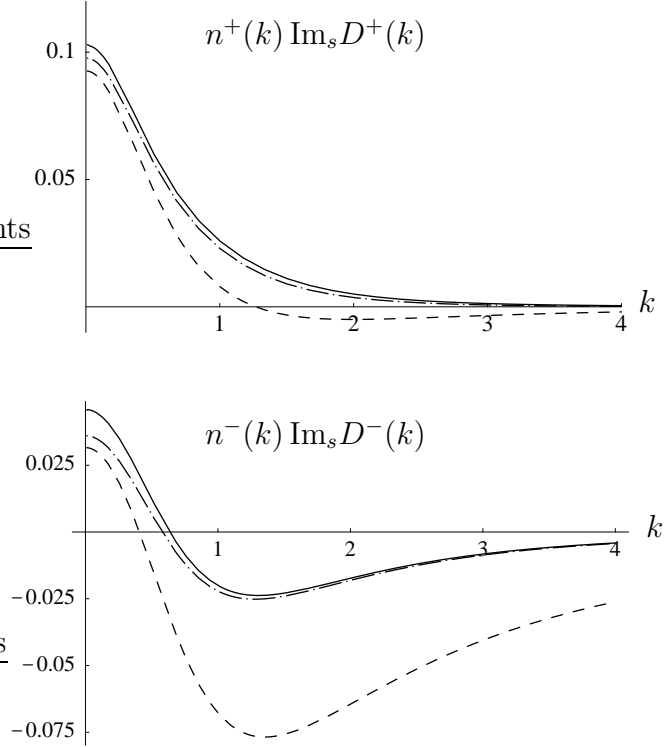


Figure 9: Imaginary part of the D -amplitudes at $t = 0$. The normalization factor $n^\pm(k)$ is chosen such that the area under the curve represents the contribution to the value of the amplitude at threshold. Full: relativistic amplitude, dot-dashed: expansion at fixed Ω_q , dashed: expansion at fixed Ω .

In view of the difference in the weight, the dispersion relation for D^- is more sensitive to the high energy region than the one for D^+ .

18.3 Chiral expansion of the dispersion integrals

The situation changes drastically, however, if we consider the corresponding contribution to the subtracted dispersion integral $D_1^+(s)$, which may be evaluated as follows. We first note that the discontinuity across the right hand cut of the function $I(s)$ coincides with the one of the corresponding dimensionally regularized object, $H(s)$. Moreover, $H(s)$ does not have a left hand cut. Hence the expression obtained by simply replacing $I(s)$ with $H(s)$ does have the same singularities as the dispersive integral we are looking for – the difference is a polynomial in ω . The subtracted dispersion integral is obtained from $H(s)$ by removing the Taylor series expansion to order ω^4 . In fig. 10, the full line represents the exact contribution to $\text{Re}D_1^+(s)$,

while the dot-dashed one depicts the chiral expansion thereof at fixed Ω_q , to $O(\alpha^4)$. Evidently, the truncation of the chiral expansion at $O(\alpha^4)$ very strongly distorts the result.

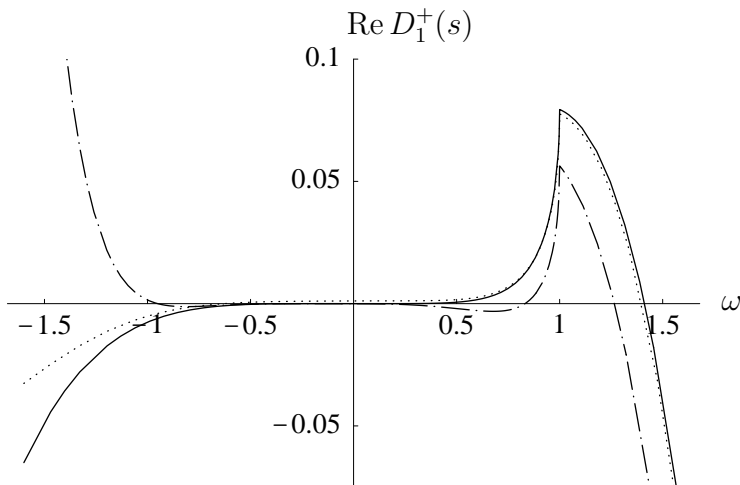


Figure 10: Chiral expansion of the contribution from diagram (f) to the subtracted dispersion integral $D_1^+(s)$.

The reason for this disaster is that the chiral expansion of the Taylor coefficients that specify the subtraction polynomial converges only extremely slowly. The contributions from the s -channel loop graphs to the coefficient d_{20}^+ , for instance, are obtained by evaluating the fourth derivative of the corresponding contributions to D^+ at $\omega = 0$. These quantities are represented very poorly by the leading terms in their chiral expansion. The problem disappears if we keep the Taylor coefficients fixed when performing the chiral expansion (the representation that then results is indicated by the dotted line). When representing the amplitude in the form (15.1), we have absorbed the subtraction polynomial in the coefficients of the subthreshold expansion. This implies that the chiral expansion of the subthreshold coefficients in powers of the quark masses – in particular the one of d_{20}^+ – converges only very slowly.

The physics underneath the phenomenon is readily identified. The coefficient d_{20}^+ may be expressed as an integral over the total cross section. The integral is dominated by the threshold region. If the quark masses are sent to zero, this integral diverges: The explicit formula for d_{20}^+ given in appendix F shows that this constant contains a term that is inversely proportional to M_π . The formula may be viewed as a low energy theorem: The leading term in the expansion of d_{20}^+ in powers of the quark masses is determined by g_A and F_π . At the same time, however, the above discussion shows that this

expansion converges only very slowly, because the terms of higher order pick up important contributions from the same one loop integrals that determine the leading coefficient.

We emphasize that the infrared singularities seen here are perfectly well described by the relativistic loop integrals occurring in our framework. They generate problems only if we attempt to replace the loop integrals by their chiral expansion, as it is done ab initio in Heavy Baryon Chiral Perturbation Theory. The dotted curve in fig.10 indicates that a decent representation of this type may be obtained if (a) the kinematic variables are carefully chosen and (b) the polynomial part of the amplitude is dealt with properly. We do not elaborate further on the chiral expansion of the loop integrals, but now turn to the contributions from the terms of $O(q^5)$ or higher, which our representation does not account for.

19 Higher orders

The representation of the scattering amplitude to $O(q^4)$ incorporates the poles and cuts generated by the exchange of one or two stable particles (nucleons or pions), but accounts for all other singularities only summarily, through their contributions to the effective coupling constants.

The first resonance in the s - and u -channels is the $\Delta(1232)$. In the t -channel, the $\rho(770)$ plays an analogous role. These states generate poles on unphysical sheets of the scattering amplitude. Since we did not include corresponding dynamical degrees of freedom in our effective Lagrangian, we are in effect replacing these singularities by the first few terms of the Taylor series expansion in powers of ν and t .

The ρ -meson pole occurs at $t \simeq 30M_\pi^2$. In the region $|t| \lesssim 10M_\pi^2$, the contribution from this state is well represented by a polynomial, so that the description in terms of effective coupling constants is adequate. The range of validity of this approximation is about the same as the one encountered in $\pi\pi$ scattering.

The situation is different for the Δ -resonance. The curvature caused by this state in the low energy region may be described in terms of a low order polynomial only crudely. A better description of the effects generated by the singularities at $s \simeq m_\Delta^2$, $u \simeq m_\Delta^2$ is obtained from an effective Lagrangian that includes the degrees of freedom of the Δ among the dynamical variables, a procedure followed in many papers on baryon chiral perturbation theory. For details concerning this approach, we refer to the literature [38]. In the following, we make use of the explicit representation for the tree graph contribution to the scattering amplitude associated with Δ exchange given in

appendix D of ref. [9]. We denote this contribution by $D_{\Delta}^{\pm}(\nu, t)$, $B_{\Delta}^{\pm}(\nu, t)$. It involves two parameters: the mass m_{Δ} and the coupling constant g_{Δ} . The Δ -resonance starts contributing at $O(q^2)$. In a calculation to order q^4 the coupling constants of $\mathcal{L}_N^{(2)}$ enter the loop diagrams, so that part of the Δ contribution is absorbed by the loop graphs with one insertion of a vertex from $\mathcal{L}_N^{(2)}$.

For the amplitude D^+ at $t = 0$ the situation is simple, because the contribution of the $\mathcal{L}_N^{(2)}$ -couplings to the dispersion integral $D_1^+(s)$ is of $O(q^5)$ and numerically negligible. We can thus estimate the remaining Δ contribution by subtracting from the Δ tree graph the contribution to the polynomial part D_p^+ . At threshold, the remainder is given by

$$D_{\Delta}^+ = \frac{64 g_{\Delta}^2 m_N^5 M_{\pi}^6 ((m_N + m_{\Delta})^2 - M_{\pi}^2)}{9 m_{\Delta}^2 (m_{\Delta}^2 - m_N^2 - M_{\pi}^2)^5} = O\left(\frac{M_{\pi}^6}{(m_{\Delta} - m_N)^5}\right).$$

It is formally of $O(q^6)$, but numerically enhanced by the small denominator. Inserting the value $g_{\Delta} = 13.0 \text{ GeV}^{-1}$ [28], we obtain $F_{\pi}^2 D_{\Delta}^+ = 2 \text{ MeV}$, indicating that for a determination of the Σ -term, corrections of this type are not entirely negligible. The corresponding contribution to the scattering length is small: $a_{0+\Delta}^+ = 0.0022 M_{\pi}^{-1}$. The effective range of the S -waves or the scattering lengths of the P - and D -waves involve derivatives of the amplitude at threshold, so that the curvature due to the Δ generates more significant effects.

Note that the singularities generated by the Δ do not affect the Goldberger-Treiman relation. In the case of the low energy theorem that relates the scattering amplitude at the Cheng-Dashen point to the σ -term, the higher order terms due to the Δ amount to a correction of order $M_{\pi}^6/(M_{\Delta} - m_N)^3$. The effect is negligibly small: It increases the value of Δ_{CD} by 0.08 MeV. Also, if the effective theory is used only in the threshold region, for instance to study the properties of pionic atoms [39], the contributions generated by the Δ are adequately described by a polynomial – it suffices to replace the Taylor series of the crossing even quantities D^+ , B^+/ν , D^-/ν , B^- in powers of ν by an expansion in powers of $\nu^2 - M_{\pi}^2$. The effective value of d_{00}^+ relevant in that context is the value of D^+ at threshold rather than the one at $\nu = 0$, and analogously for the other coefficients occurring in the polynomial part of our representation. The straightforward identification of these terms with the coefficients of the subthreshold expansion yields an accurate representation in the vicinity of $\nu = t = 0$. It is adequate also at the Cheng-Dashen point, but at threshold, the higher order terms of the subthreshold expansion do become important, quite irrespective of the contributions generated by the branch point that occurs there.

20 Values of the coupling constants of $\mathcal{L}_N^{(2)}$

In the representation of the amplitude specified in section 15, the coupling constants c_1, c_2, c_3, c_4 only enter through the imaginary parts of the dispersion integrals. In section 12, we have fixed these with the leading coefficients of the subthreshold expansion. Numerically, using the values of the subthreshold coefficients of ref. [28], this leads to

$$c_1 = -0.6 m_N^{-1}, \quad c_2 = 1.6 m_N^{-1}, \quad c_3 = -3.4 m_N^{-1}, \quad c_4 = 2.0 m_N^{-1}. \quad (20.1)$$

If we use these values to evaluate the scattering amplitude at threshold, the result differs significantly from what is observed. For the loop integrals to describe the strength of the s - and u -channel threshold singularities, it might be better to fix the couplings of $\mathcal{L}_N^{(2)}$ there, using the values of the amplitude and their first derivatives at threshold as input rather than those at $\nu = 0$. The difference is typical of the higher order effects that our calculation neglects and we now briefly discuss it numerically.

At tree level, the coupling constants c_1, \dots, c_4 only occur in D^+ and B^- . The values and first derivatives of these amplitudes at threshold are related to the scattering lengths of the S -waves, $a_{0\pm}^\pm$, to their effective ranges, $b_{0\pm}^\pm$, and to the scattering lengths of the P -waves, $a_{1\pm}^\pm$ (see appendix A). Expanding the tree graph contributions from $\mathcal{L}_N^{(1)}$ and $\mathcal{L}_N^{(2)}$ around threshold, we thus obtain a representation of the threshold parameters in terms of the effective coupling constants, valid at tree level. Inverting the relation, we arrive at a corresponding representation for the coupling constants:

$$\begin{aligned} c_1 &= \pi F_\pi^2 \left\{ -(4 + 2\alpha + \alpha^2) \frac{a_{0+}^+}{4M_\pi^2} + b_{0+}^+ - 3\alpha a_{1+}^+ \right\} + \alpha^2 c_B, \\ c_2 &= \frac{2\pi F_\pi^2}{1 + \alpha} \left\{ \frac{a_{0+}^+}{2M_\pi m_N} + b_{0+}^+ + 2a_{1+}^+ + a_{1-}^+ \right\} - 8c_B, \\ c_3 &= \frac{2\pi F_\pi^2}{1 + \alpha} \left\{ (1 - \alpha) \frac{a_{0+}^+}{4m_N^2} + \alpha b_{0+}^+ - (2 + 3\alpha + 3\alpha^2) a_{1+}^+ - a_{1-}^+ \right\} + 16c_B \\ c_4 &= -\frac{1}{4m_N} + 4\pi F_\pi^2 \left\{ \frac{a_{0+}^-}{4m_N^2} - a_{1+}^- + a_{1-}^- \right\} - \alpha^2 (4 - \alpha^2) c_B, \\ c_B &= \frac{g_{\pi N}^2 F_\pi^2}{4(4 - \alpha^2)^2 m_N^3}. \end{aligned} \quad (20.2)$$

With Koch's values for the threshold parameters [17], the above representation yields

$$c_1 = -0.9 m_N^{-1}, \quad c_2 = 2.5 m_N^{-1}, \quad c_3 = -4.2 m_N^{-1}, \quad c_4 = 2.3 m_N^{-1}. \quad (20.3)$$

Although, algebraically, the formulae (12.1) and (20.2) differ only through terms of $O(q^2)$, the comparison of the corresponding numerical values in (20.1) and (20.3), shows that the difference

$$\delta c_i = c_i|_{\nu=M_\pi} - c_i|_{\nu=0} \quad (20.4)$$

is quite significant. It mainly arises from the curvature due to the Δ . In leading order of the small scale expansion [38], the shift in the values of c_2 , c_3 and c_4 generated by this state is given by

$$\delta c_2^\Delta = 4\gamma, \quad \delta c_3^\Delta = -2\gamma, \quad \delta c_4^\Delta = \gamma, \quad \gamma = \frac{2g_\Delta^2 F_\pi^2 M_\pi^2}{9(m_\Delta - m_N)^3},$$

and thus involves the third power of the small energy denominator $m_\Delta - m_N$. Inserting the value $g_\Delta = 13 \text{ GeV}^{-1}$ [28], we obtain $\gamma \simeq 0.23 m_N^{-1}$, so that c_2 is increased by about one unit, while $|c_3|$ and c_4 pick up one half and one quarter of a unit, respectively. In c_1 , the singularity does not show up equally strongly: At leading order in the small scale expansion, we have $c_1^\Delta = -(m_\Delta - m_N)/m_N \gamma \simeq -0.07 m_N^{-1}$. The comparison with the numbers given above confirms the claim that the Δ is responsible for the bulk of the difference.

Concerning the t -channel imaginary parts, the role of the coupling constants c_1, c_2, c_3, c_4 and the contributions from the Δ are discussed in detail in ref. [9]. These are not sensitive to the manner in which the coupling constants of $\mathcal{L}_N^{(2)}$ are fixed. As an illustration, we consider the quantity $\Delta_\sigma = \sigma(2M_\pi^2) - \sigma(0)$, relevant for a measurement of the σ -term on the basis of πN data. In ref. [9], we pinned the coupling constants down with the subthreshold expansion and obtained $\Delta_\sigma = 14.0 \text{ MeV}$. If we use the same formulae, but fix the values of the coupling constants with the scattering lengths, this number changes to $\Delta_\sigma = 15.9 \text{ MeV}$. Both of these values agree quite well with the result of the dispersive analysis, $\Delta_\sigma = 15.2 \text{ MeV}$ [23].

21 S -wave scattering lengths

At leading order of the chiral perturbation series, the scattering amplitude is described by the tree graphs from $\mathcal{L}_N^{(1)}$. This leads to Weinberg's prediction for the two scattering lengths: [40],

$$a_{0+}^+ = O(q^2), \quad a_{0+}^- = \frac{M_\pi}{8\pi(1+\alpha)F_\pi^2} + O(q^3).$$

Numerically, Weinberg's formula yields $4\pi(1+\alpha)a_{0+}^- = 1.14 M_\pi^{-1}$, remarkably close to the experimental value.

The one loop representation of the scattering amplitude accounts for the corrections up to and including $O(q^4)$. According to eq. (15.1), the scattering lengths are given by

$$\begin{aligned} 4\pi(1+\alpha)a_{0+}^+ &= D_{pv}^+ + d_{00}^+ + M_\pi^2 d_{10}^+ + M_\pi^4 d_{20}^+ + D_s^+ , \\ 4\pi(1+\alpha)a_{0+}^- &= D_{pv}^- + M_\pi d_{00}^- + M_\pi^3 d_{10}^- + D_s^- , \end{aligned}$$

where D_s^+ and D_s^- collect the contributions from the dispersion integrals at $\nu = M_\pi$, $t = 0$.

In view of the fact that the value of the coupling constant $g_{\pi N}$ plays a significant role, it is not a simple matter to combine the information obtained by different authors [32]. An account of recent work on the low energy parameters may be found in ref. [41]. For the purpose of the present discussion, the precise values of the various experimental quantities do not play a significant role, however – we simply stick to the KA84 solution [42]. The experimental values of the various terms occurring in the above decomposition are listed in the table (all quantities in units of M_π).

	D_{pv}	d_{00}	d_{10}	d_{20}	D_s	total
$4\pi(1+\alpha)a_{0+}^+$	-0.15	-1.49	1.17	0.2	0.15	-0.12
$4\pi(1+\alpha)a_{0+}^-$	0.01	1.51	-0.17	–	-0.035	1.32

The values for D_s^\pm quoted there represent the full dispersion integral rather than the one loop approximation to it, so that the sum of the terms is the value of the physical amplitude at threshold. Evaluating these quantities in one loop approximation, we instead obtain $D_s^+ = 0.08 M_\pi^{-1}$ and $D_s^- = -0.035 M_\pi^{-1}$: While the value for D_s^- agrees with the experimental result, the one for D_s^+ is too small by a factor of two. Although we are discussing small effects here, they do matter at the level of accuracy needed to extract the Σ -term: In the case of D_s^+ , the experimental value is $F_\pi^2 D_s^+ = 9.3 \text{ MeV}$, while the loop graphs yield $F_\pi^2 D_s^+ = 4.9 \text{ MeV}$.

We conclude that the one loop representation of chiral perturbation theory does not cover a sufficiently large kinematic region to serve as a bridge between the experimentally accessible region and the Cheng–Dashen point. A meaningful extrapolation of the data into the subthreshold region can be achieved only by means of dispersive methods – we will outline one such method in section 23. First, however, we wish to identify the origin of the problem, by studying the difference between the full imaginary parts and the one loop representation thereof. We focus on the quantities D_s^\pm , which represent dispersion integrals over total cross sections.

22 Total cross section

The optical theorem relates the imaginary part of the amplitude $D(s, t)$ at $t = 0$ to the total cross section:

$$\text{Im}_s D(s, 0) = k \sigma_{tot} . \quad (22.1)$$

To the order of the low energy expansion we are considering here, the scattering is elastic, so that σ_{tot} is the integral over the differential cross section, given by the square of the scattering amplitude. In the c. m. system, the explicit expression may be written in the simple form

$$\begin{aligned} \frac{d\sigma}{d\Omega} = \frac{m_N^2}{16 \pi^2 s} \left\{ D D^* \left(1 - \frac{t}{4 m^2} \right) \right. \\ \left. + (D B^* + B D^*) \frac{t \nu}{4 m^2} - B B^* \frac{t(t - 4 M^2 + 4 \nu^2)}{16 m_N^2} \right\} . \end{aligned} \quad (22.2)$$

If the chiral perturbation series of the scattering amplitude is truncated at $O(q^3)$, the imaginary part of the loop integrals is given by the square of the tree graphs generated by $\mathcal{L}_N^{(1)}$ (current algebra approximation). Although current algebra does describe the S -wave scattering lengths remarkably well it does not yield a realistic picture for the imaginary parts for two reasons: (a) Since we are now dealing with the square of the amplitude, the deficiencies of the current algebra approximation become more visible and (b) the effects due to the Δ are more pronounced than in the subthreshold region. This is illustrated in fig. 11, where the dotted lines correspond to the current algebra approximation. The full lines show the behaviour of the experimental total cross section, reconstructed from the results of Koch [17] for the amplitudes in the threshold region.

The discrepancy seen near threshold is directly related to the difference between the experimental values of the scattering lengths and the current algebra result: There, the cross section is the square of the scattering length,

$$\sigma^{\frac{1}{2}}_{tot} = 4 \pi (a_{0+}^+ + 2a_{0+}^-)^2 , \quad \sigma^{\frac{3}{2}}_{tot} = 4 \pi (a_{0+}^+ - a_{0+}^-)^2 .$$

These expressions are dominated by a_{0+}^- – the term a_{0+}^+ vanishes at leading order. Although Weinberg's prediction represents a very decent approximation, the difference to the observed scattering lengths generates an effect of order 25 % in the cross section – this explains why, in the vicinity of threshold, the dotted lines are on the low side.

Since the corrections from $\mathcal{L}_N^{(2)}$ do not enter the large scattering length a_{0+}^- , the sum of the contributions from $\mathcal{L}_N^{(1)}$ and $\mathcal{L}_N^{(2)}$ (dot-dashed line) is close

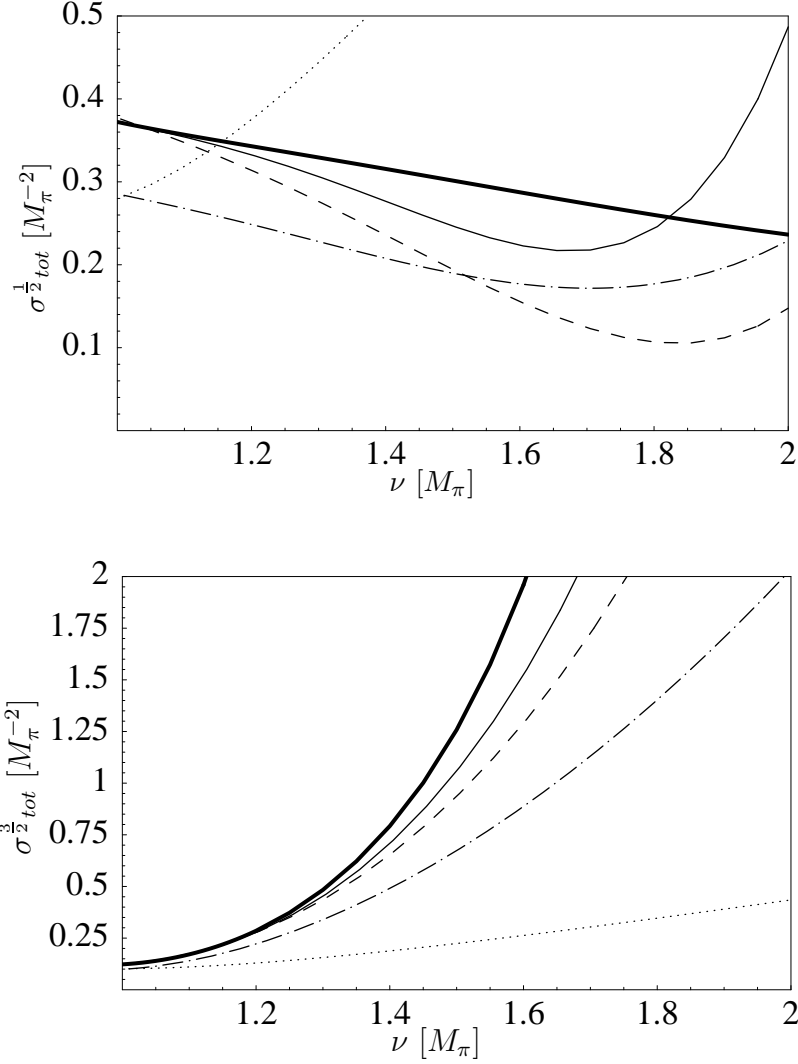


Figure 11: Total cross sections. Dotted: Current algebra. Dot-dashed: Tree graphs from $\mathcal{L}_N^{(1)} + \mathcal{L}_N^{(2)}$. Dashed: CHPT $O(q^4)$, all couplings fixed at $\nu = t = 0$. Thin: CHPT $O(q^4)$, all couplings fixed at threshold. Thick: Experimental values [17].

to the current algebra approximation at threshold. At higher energies the second order terms are however sizeable: The couplings of $\mathcal{L}_N^{(2)}$ pick up large values because of the presence of the Δ resonance. Although the corrections improve the energy dependence, the one loop representation underestimates the cross section, in particular, for $I = \frac{1}{2}$. In the dispersion integral for

D_s^- , which involves the difference $\sigma^{\frac{1}{2}}_{tot} - \sigma^{\frac{3}{2}}_{tot}$, the deficiencies happen to cancel, so that the one loop approximation for this quantity agrees with the full result, but for D_s^+ , where the imaginary part is given by $\sigma^{\frac{1}{2}}_{tot} + 2\sigma^{\frac{3}{2}}_{tot}$, the miracle does not happen – this is why the one loop approximation is too small by a factor of two in that case.

The remaining curves show the cross section obtained with the one loop representation of the scattering amplitude: The dashed lines result if all combinations of the coupling constants c_i, d_i, e_i that enter the amplitudes are determined with the subthreshold coefficients, while for the thin lines, these are evaluated from the scattering lengths. Since in the second case the input parameters are all fixed at threshold, this option yields a somewhat better description at higher energies, but in either case the one-loop results start deviating from the experimental values already at rather low energies. The fact that the dispersive part of the one loop representation is determined by the square of the tree level amplitudes rather than by the square of the one-loop approximation means that this representation obeys unitarity only up to contributions of order q^5 . The difference between the dash-dotted and thin lines shows that the violation of unitarity is numerically quite important, particularly in the case of $I = \frac{1}{2}$. The figure also shows that the perturbative expansion of the amplitude $D^{\frac{1}{2}}$ goes out of control immediately above threshold: The higher order “corrections” exceed the “leading” order contribution.

The approach used in refs. [7, 8] is different. There, the main goal is an analysis of the πN scattering amplitude in the region above threshold. The coupling constants are determined by fitting unitarized one loop partial waves to the data and a rather decent description is obtained – we expect that the corresponding results for the total cross section would come quite close to the experimental curves in the above figures. The backside of the coin is that the representation then unavoidably fails in the subthreshold region, so that it is not possible to establish contact with the low energy theorems of chiral symmetry.

23 Analog of the Roy equations

The preceding discussion makes it evident that the chiral representation of the πN scattering amplitude to $O(q^4)$ can provide a decent approximation only in the subthreshold region – a reliable determination of the σ -term from the data in the physical region cannot be performed on this basis. Even in the case of $\pi\pi$ scattering, where the chiral representation does converge rapidly enough for the one-loop approximation to yield a decent description

of the amplitude in part of the physical region, the Roy equations provide a more accurate framework, which moreover also covers significantly higher energies [18, 19]. In the present section, we briefly outline the steps required to extend the Roy equation analysis to the case of πN scattering.

As shown by Roy [15], analyticity and crossing symmetry imply a set of integral equations for the partial waves of $\pi\pi$ scattering. The case of $\pi\pi$ scattering is special in that the s -, t - and u -channels correspond to the same physical situation, so that the partial wave decomposition is the same in all three channels. The Roy equations represent the real parts of the partial waves in terms of integrals over their imaginary parts and two subtraction constants. In the elastic region, unitarity then converts this system into a set of coupled integral equations. At low energies, the angular momentum barrier suppresses the higher partial waves, so that the amplitude is dominated by the S - and P -waves. As the pions are spinless and carry isospin 1, Bose statistics implies that there are three such waves, $t_0^0(s)$, $t_1^1(s)$, $t_0^2(s)$ (the upper index denotes the total isospin of the $\pi\pi$ state, while the lower one specifies its total angular momentum). The effects due to the higher partial waves can be accounted for in the so-called driving terms. In the elastic region, however, these are very small and can just as well be dropped. For a detailed discussion of the properties of the Roy equations, we refer to [18].

Two complications arise when extending this framework to πN scattering: The proton carries spin $\frac{1}{2}$ and, more importantly, there are now two different categories of unitarity cuts that matter at low energies: πN states, relevant for the discontinuities in the s - and u -channels, and states of the type $\pi\pi$ or $\bar{N}N$, which generate the discontinuities in the t -channel. Accordingly, we need to invoke two different partial wave decompositions. We use the notation of [28] and denote the s -channel partial waves by $f_{\ell\pm}(s)$. For $\ell = 0$ and $\ell = 1$, there are altogether 6 such waves:

$$f_1^\pm(s) \equiv f_{0+}^\pm(s), \quad f_2^\pm(s) \equiv f_{1-}^\pm(s) \quad f_3^\pm(s) \equiv f_{1+}^\pm(s). \quad (23.3)$$

The upper index refers to isospin – it is convenient to use the t -channel isospin basis, where f^+ and f^- correspond to $I_t = 0$ and $I_t = 1$, respectively.

In the t -channel, $\bar{N}N$ states of angular momentum ℓ carry parity $(-1)^{\ell+1}$. They can thus only couple to $\pi\pi$ states of total angular momentum $J = \ell \pm 1$. In the notation of ref. [28], the corresponding S - and P -waves are denoted by $f_\pm^J(t)$, where the upper index specifies the total angular momentum J , while the lower one labels the two independent partial waves occurring for $J \geq 1$. In the t -channel, the isospin quantum number is fixed by the total angular momentum: J even implies $I = 0$, J odd corresponds to $I = 1$. Ignoring terms with $J \geq 2$, the partial wave decomposition in the isospin even channel

contains a single wave, while the isospin odd channel contains two:

$$f_4^+(t) \equiv f_+^0(t), \quad f_4^-(t) \equiv f_-^1(t), \quad f_5^-(t) \equiv f_+^1(t). \quad (23.4)$$

Altogether, the discontinuities generated by the S - and P -waves thus involve 9 functions of a single variable, to be compared with the 3 functions $t_0^0(s)$, $t_1^1(s)$, $t_0^2(s)$ that occur in the case of $\pi\pi$ scattering. A closed system of integral equations for these functions is proposed in appendix K. It is of the same form as the Roy equations:

$$\begin{aligned} f_i^+(x) &= f_i^+(x)_B + k_i^+(x) + \sum_{k=1}^4 \int_{s_k}^{\infty} dy K_{ik}^+(x, y) \text{Im} f_k^+(y), \\ f_i^-(x) &= f_i^-(x)_B + k_i^-(x) + \sum_{k=1}^5 \int_{s_k}^{\infty} dy K_{ik}^-(x, y) \text{Im} f_k^-(y), \\ s_k &= \begin{cases} (m_N + M_\pi)^2, & k = 1, 2, 3 \\ 4M_\pi^2, & k = 4, 5 \end{cases} \end{aligned} \quad (23.5)$$

The first term on the right represents the partial wave projection of the pseudovector Born term, while the second contains the subtraction constants. The kernels $K_{ik}^\pm(x, y)$ are explicitly known kinematic functions. The main term on the diagonal is the familiar Cauchy kernel,

$$K_{ik}^\pm(x, y) = \frac{\delta_{ik}}{\pi(y - x - i\epsilon)} + \dots$$

In principle, only one subtraction constant is required, but additional subtractions may be introduced in order to arrive at a system of equations that is less sensitive to the contributions from higher partial waves or higher energies. In the case of $\pi\pi$ scattering, it is advantageous to work with two subtraction constants, although, in principle, one of these is superfluous: The Olsson sum rule relates a combination of the two subtraction constants to an integral over total cross sections. The specific form of the equations proposed in appendix K for the case of πN scattering involves four subtraction constants. One of these can be represented as an integral over total cross sections, while the remaining three are to be determined with the experimental information available at low energies. In particular, the beautiful data obtained from pionic atoms [43] subject these constants to a stringent constraint.

The above system of equations may be viewed as a unitarization of the low energy representation provided by chiral perturbation theory: The dispersion integrals describe the low energy singularities that necessarily accompany the

tree graph contributions, on account of unitarity. There are two differences to the one loop representation of the unitarity corrections in eqs. (16.2), (16.3): (i) That representation accounts for the imaginary parts only to first nonleading order of the chiral expansion, while the one underlying the above set of integral equations retains the full imaginary parts of the S - and P -waves. (ii) The chiral representation involves an oversubtracted set of dispersion integrals. The extra subtractions are needed, because in that representation, the energy dependence is expanded in a Taylor series. The problem does not occur in the above framework, because unitarity implies that the partial waves tend to zero at high energies.

In the case of $\pi\pi$ scattering, the integral equations can be written in exact form, where all of the partial waves are accounted for. The equations for the S - and P -waves then contain corrections from the higher angular momenta, collected in the driving terms mentioned above. We do not know of a corresponding set of exact equations for the case of πN scattering – driving terms would have to be added to convert (23.5) into an exact system. The size of these corrections depends on the number of subtractions made and on the range of energies considered. With four subtractions, they should be negligibly small in the elastic region, because the bulk of the contributions from the partial waves with $\ell \geq 2$ is then absorbed in the subtraction constants. The available detailed phenomenological information about the imaginary parts of the higher waves [28] allows an explicit evaluation of their contributions, so that this can be checked.

Alternative unitarizations are proposed in the literature [44, 45]. The advantage of the present proposal is that the resulting representation of the scattering amplitude does not introduce any fictitious singularities. In particular, once the system of equations is solved and the subtraction constants are determined, the representation yields a formula for the value of the scattering amplitude at the Cheng–Dashen point:

$$\begin{aligned} \Sigma &= F_\pi^2 \left\{ d_{00}^+ + 2M_\pi^2 d_{01}^+ + 64M_\pi^4 \int_{4M_\pi^2}^\infty dt \frac{\text{Im } f_4^+(t)}{t^2 (t - 2M_\pi^2) (4m_N^2 - t)} \right\} , \\ C &= 2F_\pi^2 \left\{ d_{00}^- + 12M_\pi^2 \int_{4M^2}^\infty dt \frac{8m_N \text{Im } f_5^-(t) - \sqrt{2} t \text{Im } f_4^-(t)}{t (t - 2M_\pi^2) (4m_N^2 - t)} \right\} . \end{aligned} \quad (23.6)$$

The approach outlined above is closely related to the one used by R. Koch [17], who relies on fixed ν dispersion relations to study the t -dependence. Also, a similar method was used in ref. [46] to extract the value of the σ -term from the data available at the time. For more recent work in this direction, we refer to [47], where hyperbolic dispersion relations [48] are used to supplement the partial wave relations [28, 16] for $K\pi$ scattering.

24 Summary and conclusion

1. We have derived a representation of the πN scattering amplitude that is valid to the fourth order of the chiral expansion. The infrared singularities occurring in that representation are stronger than for $\pi\pi$ scattering. The difference also manifests itself in the expansion of the nucleon mass or of the σ -term in powers of the quark masses, which contain contributions of $O(M_\pi^3)$ that are quite important numerically. The Goldberger-Treiman relation and the low energy theorem that relates the σ -term to the value of the scattering amplitude at the Cheng-Dashen point, on the other hand, do not contain infrared singularities, at the order considered.

2. We have shown that the Mandelstam double spectral function only contributes beyond the order of the low energy expansion examined in the present paper. The dependence of the box graph on the momentum transfer, for instance, can be expanded in powers of $t/4m_N^2$ – the cut due to $N\bar{N}$ intermediate states in the t -channel does not manifest itself at finite orders of the low energy expansion. Up to and including $O(q^4)$, the scattering amplitude can be written in terms of functions of a single variable, either s or t or u . These functions describe the singularities associated with the unitarity cuts. In the framework of the effective theory, they arise from the one loop graphs. We have given an explicit, dispersive representation for these functions, which accounts for all terms to $O(q^4)$ and sums up those higher order contributions that are generated by the threshold singularities.

3. The chiral expansion of the dispersion integrals reduces these to algebraic expressions involving elementary functions such as $\arccos(-\omega/M_\pi)$. On general grounds, the result of this expansion must agree with what is obtained in HBCHPT, where the loop integrals are expanded ab initio. That expansion, however, is a subtle matter, because the integrals contain infrared singularities. In particular, the choice of the kinematic variable to be kept fixed plays an important role. While the expansion at fixed ω/M_π does not lead to a decent description of the full loop integrals, the one at fixed ω_q/M_π does yield an approximate representation for the relativistic integrals, even above threshold.

4. While the expansion at fixed ω_q/M_π solves one problem, it generates another. To absorb the divergences of the loop integrals in the coupling constants of the effective Lagrangian, the integrals must be expanded in powers of M_π at fixed ω/M_π , so that an expansion of the subtraction terms is required, which converges only slowly. Algebraically, the accuracy of the representation does not depend on the splitting between the polynomial part

and the cut contribution, but numerically, the amplitude is very sensitive to this choice. We find it more convenient not to invoke an expansion of the integrals – the problem does not occur in the relativistic representation that forms the basis of our work.

5. We find that the dependence of the amplitude on the momentum transfer t is adequately described by the contributions from the one loop graphs, so that the extrapolation from the Cheng-Dashen point to $t = 0$ does not pose a significant problem. The representation obtained for the dependence on the variables s and u , however, has a very limited range of validity. Higher order effects, such as those due to the Δ do matter. The one loop representation does not provide the bridge needed to connect the value of the amplitude at the Cheng-Dashen point to the physical region.

6. We conclude that dispersive methods are required to obtain a reliable description of the scattering amplitude at low energies. With this in mind, we propose a system of integral equations that is analogous to the Roy equations for $\pi\pi$ scattering and interrelates the lowest partial wave amplitudes associated with the s -, t - and u -channels. The structure of the amplitude that underlies this system is very similar to the dispersive representation mentioned above, but the constraints imposed on the partial waves by unitarity are now strictly obeyed. It remains to be seen whether or not this set of equations provides a useful framework for the analysis of the low energy structure, in particular for a reliable determination of the σ -term.

Acknowledgment

We greatly profited from Jürg Gasser's knowledge of the subject. This work would not have been possible without his help and cooperation. We thank P. Büttiker and J. Stahov for making the KA84 solution available to us and G. Oades for communicating his results for the subthreshold coefficients prior to publication. Also, we acknowledge useful discussions and correspondence with B. Ananthanarayan, G. Ecker, R. Kaiser, U.G. Meissner, H. Neufeld and U. Raha. This work was supported by the Swiss National Science Foundation, and by TMR, BBW-Contract No. 97.0131 and EC-Contract No. ERBFMRX-CT980169 (EURODAΦNE).

A Notation

We use the notation of Höhler's "Collection of Pion-Nucleon Scattering Formulas". (Appendix of [28].)

Kinematics

P, q four momenta of the incoming nucleon and pion
 P', q' four momenta of the outgoing nucleon and pion

$$s = (P + q)^2, \quad t = (q - q')^2, \quad u = (P - q')^2, \quad s + t + u = 2M_\pi^2 + 2m_N^2$$

$$\omega_q = M_\pi \Omega_q = \frac{s - m_N^2 + M_\pi^2}{2\sqrt{s}} \quad \text{c. m. pion energy}$$

$$E = \frac{s + m_N^2 - M_\pi^2}{2\sqrt{s}} \quad \text{c. m. nucleon energy}$$

$$q = \sqrt{\omega_q^2 - M_\pi^2} \quad \text{c. m. momentum}$$

$$\cos \theta = 1 + \frac{t}{2q^2} \quad \text{scattering angle (c. m. system)}$$

$$\omega = M_\pi \Omega = \frac{s - m_N^2 - M_\pi^2}{2m_N} \quad \text{lab. energy of the incoming pion}$$

$$k = \sqrt{\omega^2 - M_\pi^2} \quad \text{lab. momentum of the incoming pion}$$

$$\nu = \frac{s - u}{4m_N} = \omega + \frac{t}{4m_N}$$

$$\nu_B = \frac{1}{4m_N}(t - 2M_\pi^2)$$

Isospin

We denote the amplitudes for the reactions $\pi^\pm p \rightarrow \pi^\pm p$ by A_\pm , the charge exchange reaction amplitude $\pi^- p \rightarrow \pi^0 n$ by A_0 . The amplitudes of the isospin eigenstates are denoted by A^I , $I = \frac{1}{2}, \frac{3}{2}$. The relations to the isospin

odd and even amplitudes A^\pm are

$$\begin{aligned}
A_+ &= A^{\frac{3}{2}} = A^+ - A^-, & A_- &= \frac{1}{3}(2A^{\frac{1}{2}} + A^{\frac{3}{2}}) = A^+ + A^- \\
A_0 &= \frac{\sqrt{2}}{3}(A^{\frac{3}{2}} - A^{\frac{1}{2}}) = -\sqrt{2}A^-, & A^{\frac{1}{2}} &= \frac{1}{2}(3A_- - A_+) = A^+ + 2A^- \\
A^+ &= \frac{1}{3}(A^{\frac{1}{2}} + 2A^{\frac{3}{2}}), & A^- &= \frac{1}{3}(A^{\frac{1}{2}} - A^{\frac{3}{2}})
\end{aligned}$$

Partial waves

For the partial wave decomposition, the amplitude

$$C = A + \frac{\nu}{1 - t/4m_N^2} B = D + \frac{\nu t}{4m_N^2 - t} B$$

is more convenient to work with than A or D .

In the s -channel, the decomposition reads

$$\begin{aligned}
C &= \frac{2\pi\sqrt{s}}{p_-^2} \sum_{\ell=0}^{\infty} (\ell+1) f_{\ell+}(s) \{ (E+m_N)P_\ell(z) - (E-m_N)P_{\ell+1}(z) \} \\
&\quad + \frac{2\pi\sqrt{s}}{p_-^2} \sum_{\ell=1}^{\infty} \ell f_{\ell-}(s) \{ (E+m_N)P_\ell(z) - (E-m_N)P_{\ell-1}(z) \}, \\
B &= \frac{4\pi}{q^2} \sum_{\ell=0}^{\infty} f_{\ell+}(s) \{ -(E+m_N)P'_\ell(z) + (E-m_N)P'_{\ell+1}(z) \} \\
&\quad + \frac{4\pi}{q^2} \sum_{\ell=1}^{\infty} f_{\ell-}(s) \{ (E+m_N)P'_\ell(z) - (E-m_N)P'_{\ell-1}(z) \}, \\
t &= 2q^2(z-1), \quad p_- = \sqrt{m_N^2 - \frac{1}{4}t}.
\end{aligned} \tag{A.1}$$

The t -channel partial waves are defined by

$$\begin{aligned}
C &= \frac{8\pi}{p_-^2} \sum_{J=0}^{\infty} (J + \frac{1}{2}) (p_- q_-)^J P_J(Z) f_+^J(t), \\
B &= 8\pi \sum_{J=1}^{\infty} \frac{J + \frac{1}{2}}{\sqrt{J(J+1)}} (p_- q_-)^{J-1} P'_J(Z) f_-^J(t), \\
\nu &= \frac{Z p_- q_-}{m_N}, \quad p_- = \sqrt{m_N^2 - \frac{1}{4}t}, \quad q_- = \sqrt{M_\pi^2 - \frac{1}{4}t}.
\end{aligned} \tag{A.2}$$

Threshold expansion

We write the threshold expansion of the amplitude $X \in \{D^+, D^-, B^+, B^-\}$ in the form

$$\text{Re } X(q^2, t) = X_{00} + X_{10} q^2 + X_{01} t + X_{20} q^4 + X_{11} q^2 t + X_{02} t^2 + \dots$$

The coefficients X_{nm} of this expansion are related to the scattering lengths and effective ranges. For the threshold expansion of the real part of the partial wave amplitudes

$$T_{l\pm} = q f_{l\pm} = \frac{1}{2i} (\eta_{\pm} e^{2i\delta_{l\pm}} - 1)$$

we use the notation

$$\text{Re } T_{l\pm} = q^{2l+1} (a_{l\pm} + b_{l\pm} q^2 + c_{l\pm} q^4 + \dots).$$

The lowest coefficients of the threshold expansion of the amplitudes D and B are obtained from the expansion of the partial wave amplitudes via

$$\begin{aligned} D_{00} &= 4\pi (1 + \alpha) a_{0+} \\ D_{10} &= 4\pi (1 + \alpha) \left\{ \frac{a_{0+}}{2\alpha m_N^2} + b_{0+} + a_{1-} + 2a_{1+} \right\} \\ D_{01} &= 2\pi \left\{ \frac{a_{0+}}{4m_N^2} + a_{1-} + a_{1+} (2 + 3\alpha) \right\} \\ D_{20} &= \frac{2\pi (1 + \alpha)}{\alpha m_N^2} \left\{ - (1 - \alpha + \alpha^2) \frac{a_{0+}}{4\alpha^2 m_N^2} + b_{0+} + 2\alpha m_N^2 c_{0+} + a_{1-} \right. \\ &\quad \left. + 2\alpha m_N^2 b_{1-} + 2a_{1+} + 4\alpha m_N^2 b_{1+} + 4\alpha m_N^2 a_{2-} + 6\alpha m_N^2 a_{2+} \right\} \\ D_{11} &= \frac{\pi}{2m_N^2} \left\{ - \frac{a_{0+}}{4m_N^2} + b_{0+} + a_{1-} + 4m_N^2 b_{1-} + 2(3 + 4\alpha) \frac{a_{1+}}{\alpha} \right. \\ &\quad \left. + 4(2 + 3\alpha) m_N^2 b_{1+} + 12(2 + \alpha) m_N^2 a_{2-} + 12(3 + 4\alpha) m_N^2 a_{2+} \right\} \\ D_{02} &= \frac{3\pi}{4m_N^2} \left\{ a_{1+} + 4m_N^2 a_{2-} + 2(3 + 5\alpha) m_N^2 a_{2+} \right\} \\ B_{00} &= 8\pi m_N \left\{ \frac{a_{0+}}{4m_N^2} + a_{1-} - a_{1+} \right\} \\ B_{10} &= \frac{2\pi}{m_N} \left\{ - \frac{a_{0+}}{4m_N^2} + b_{0+} + a_{1-} + 4m_N^2 b_{1-} + 2a_{1+} \right. \\ &\quad \left. - 4m_N^2 b_{1+} + 12m_N^2 a_{2-} - 12m_N^2 a_{2+} \right\} \\ B_{01} &= \frac{3\pi}{m_N} \left\{ a_{1+} + 4m_N^2 a_{2-} - 4m_N^2 a_{2+} \right\}. \end{aligned}$$

B Off-shell πN -amplitude

As discussed in the text, the off-shell amplitude of the effective theory is without physical meaning. In the underlying theory, however, an unambiguous off-shell extrapolation can be constructed from correlators of currents with the appropriate quantum numbers. For the pion field, the operator of lowest dimension is the pseudoscalar density $P^a(x)$

$$P^a(x) = \bar{q}(x) i\gamma_5 \tau^a q(x), \quad a = 1, 2, 3$$

which couples to the pion with strength G_π ,

$$\langle 0 | P^a(0) | \pi^b \rangle = G_\pi \delta^{ab}.$$

To generate nucleons, we need a three-quark operator with the correct quantum numbers. At lowest dimension, there are two independent such operators:

$$\begin{aligned} \mathbf{N}_1(x) &= \left(q_\alpha(x) i\tau^2 \mathcal{C} q_\beta(x) \right) \gamma_5 q_\gamma(x) \epsilon^{\alpha\beta\gamma} \\ \mathbf{N}_2(x) &= \left(q_\alpha(x) i\tau^2 \mathcal{C} \gamma_5 q_\alpha(x) \right) q_\gamma(x) \epsilon^{\alpha\beta\gamma} \end{aligned}$$

In $q_\alpha(x) = (u_\alpha(x), d_\alpha(x))$ we have collected the quarks with color index α . The brackets indicate a sum over Dirac and flavor indices, $i\tau^2$ stands for the antisymmetric tensor in SU(2) flavor space and $\mathcal{C} = -i\gamma_0\gamma_2$ is the charge conjugation matrix. These operators couple to the proton with coupling strength $G_{1,2}$.

$$\langle 0 | \mathbf{N}_{1,2}(x) | P, s \rangle = G_{1,2}(\mu) \mathbf{u}(P, s)$$

Since these operators carry anomalous dimension, their matrix elements depend on the running scale of QCD, but are otherwise free from ambiguities. Their Green functions contain contact terms that make it difficult to handle the corresponding generating functional – the perturbation generated by the source terms is not renormalizable. We may, however, restrict ourselves to Green functions involving only two nucleon fields, so that a finite number of counter terms suffices. The pion nucleon scattering amplitude can be extracted e. g. from the Green function

$$\langle 0 | \mathbf{T} \left[\mathbf{N}_1(x') P^{a'}(y') P^a(y) \bar{\mathbf{N}}_1(x) \right] | 0 \rangle.$$

Under a chiral transformation $q(x) \rightarrow \left\{ \frac{1}{2}(1 + \gamma_5)V_R + \frac{1}{2}(1 - \gamma_5)V_L \right\} q(x)$ the operator \mathbf{N}_1 transforms as

$$\mathbf{N}_1 \rightarrow \left\{ \frac{1}{2}(1 + \gamma_5)V_R - \frac{1}{2}(1 - \gamma_5)V_L \right\} \mathbf{N}_1$$

In our effective theory, it is easy to identify an object that transforms in the same way, namely $\Psi = u\psi_R - u^\dagger\psi_L$. If we would add a source term $\bar{\eta}_1 \mathbf{N}_1 + \bar{\mathbf{N}}_1 \eta$ to the Lagrangian of QCD, this source would couple to the field Ψ in our effective Lagrangian and we would be able to compute the above Green function with an extended version of our effective Lagrangian. Since the two fields $\Psi(x)$ and $\psi(x)$ do generate the same on-shell amplitudes we can also use the field $\psi(x)$ to extract these, as we did in our calculation.

C One-loop integrals

In this appendix, we list the integrals that occur in the evaluation of the scattering amplitude to one loop. Throughout, we use infrared regularization (for a detailed discussion of that method, we refer to [9]). We perform the tensor decomposition of the integrals with respect to the sums and the differences of the external momenta,

$$\begin{aligned}\Sigma^\mu &= (P + q)^\mu = (P' + q')^\mu \\ Q^\mu &= (P' + P)^\mu \\ \Delta^\mu &= (q' - q)^\mu = (P - P')^\mu .\end{aligned}$$

and put all external legs on their mass shell,

$$P^2 = P'^2 = m^2 , \quad q^2 = q'^2 = M^2 .$$

The coefficients represent Lorentz invariant functions of the Mandelstam variables. The squares of the vectors Σ , Δ and Q are given by

$$\Sigma^2 = s , \quad \Delta^2 = t , \quad Q^2 = 4m^2 - t$$

1 meson: $\Delta_\pi = I_{10}$

$$\Delta_\pi = \frac{1}{i} \int_I \frac{d^d k}{(2\pi)^d} \frac{1}{M^2 - k^2} = 2M^2 \lambda_\pi$$

1 nucleon: $\Delta_N = I_{01}$

$$\Delta_N = \frac{1}{i} \int_I \frac{d^d k}{(2\pi)^d} \frac{1}{m^2 - k^2} = 0$$

Note that integrals formed exclusively with nucleon propagators vanish in infrared regularization: $I_{0n} = 0$.

2 mesons: $J = I_{20}$

$$\{J, J^\mu, J^{\mu\nu}\} = \frac{1}{i} \int_I \frac{d^d k}{(2\pi)^d} \frac{\{1, k^\mu, k^\mu k^\nu\}}{(M^2 - k^2)(M^2 - (k - \Delta)^2)}$$

$$J^\mu = \frac{1}{2} \Delta^\mu J(t)$$

$$J^{\mu\nu} = (\Delta^\mu \Delta^\nu - g^{\mu\nu} \Delta^2) J^{(1)}(t) + \Delta^\mu \Delta^\nu J^{(2)}(t)$$

1 meson, 1 nucleon: $I = I_{11}$

$$\{I, I^\mu, I^{\mu\nu}\} = \frac{1}{i} \int_I \frac{d^d k}{(2\pi)^d} \frac{\{1, k^\mu, k^\mu k^\nu\}}{(M^2 - k^2)(m^2 - (\Sigma - k)^2)}$$

$$I^\mu = \Sigma^\mu I^{(1)}(s)$$

$$I^{\mu\nu} = g^{\mu\nu} I^{(2)}(s) + \Sigma^\mu \Sigma^\nu I^{(3)}(s)$$

2 mesons, 1 nucleon:

$$\{I_{21}, I_{21}^\mu, I_{21}^{\mu\nu}\} = \frac{1}{i} \int_I \frac{d^d k}{(2\pi)^d} \frac{\{1, k^\mu, k^\mu k^\nu\}}{(M^2 - k^2)(M^2 - (k - \Delta)^2)(m^2 - (P - k)^2)}$$

$$I_{21}^\mu = Q^\mu I_{21}^{(1)}(t) + \frac{1}{2} \Delta^\mu I_{21}(t),$$

$$I_{21}^{\mu\nu} = g^{\mu\nu} I_{21}^{(2)}(t) + Q^\mu Q^\nu I_{21}^{(3)} + \Delta^\mu \Delta^\nu I_{21}^{(4)}(t) + (\Delta^\mu Q^\nu + Q^\mu \Delta^\nu) \frac{1}{2} I_{21}^{(1)}(t),$$

1 meson, 2 nucleons: I_{12}, I_A, I_B .

$$\{I_{12}, I_{12}^\mu, I_{12}^{\mu\nu}\} = \frac{1}{i} \int_I \frac{d^d k}{(2\pi)^d} \frac{\{1, k^\mu, k^\mu k^\nu\}}{(M^2 - k^2)(m^2 - (P_1 - k)^2)(m^2 - (P_2 - k)^2)}$$

With $Q = P_1 + P_2$ and $\Delta = P_1 - P_2$, the tensorial decomposition reads

$$I_{12}^\mu = Q^\mu I_{12}^{(1)} + \Delta^\mu I_{12}^{(2)},$$

$$I_{12}^{\mu\nu} = g^{\mu\nu} I_{12}^{(3)} + Q^\mu Q^\nu I_{12}^{(4)} + \Delta^\mu \Delta^\nu I_{12}^{(5)} + (\Delta^\mu Q^\nu + Q^\mu \Delta^\nu) I_{12}^{(6)}.$$

Several different topologies give rise to this integral: the graphs (c), (d), (g), (h) and (m) in fig. 2. The values of P_1 and P_2 differ from graph to graph.

In all cases, however, one of the two momenta is on the mass shell – we set $P_1^2 = m^2$. The coefficients of the tensor decomposition then only depend on two variables:

$$I_{12}^{(n)} = I_{12}^{(n)}(s, t), \quad P_1^2 = m^2, \quad P_2^2 = s, \quad t = (P_1 - P_2)^2.$$

In the case of the graph (m), we have $P_1 = P$, $P_2 = P'$, so that we are dealing with the special case $s = m^2$. In the case of (c), (d), (g) and (h) on the other hand, the difference $P_1 - P_2$ represents the momentum of an on-shell pion, so that $t = M^2$. To simplify the notation, we introduce invariant functions that correspond to these two special cases and only depend on a single variable:

$$I_A(t) = I_{12}(m^2, t), \quad I_B(s) = I_{12}(s, M^2).$$

The coefficients of the decomposition of the corresponding tensorial integrals are

$$\begin{aligned} I_A^\mu(t) &= Q^\mu I_A^{(1)}(t), \\ I_A^{\mu\nu}(t) &= g^{\mu\nu} I_A^{(2)}(t) + Q^\mu Q^\nu I_A^{(3)}(t) + \Delta^\mu \Delta^\nu I_A^{(4)}(t) \\ I_B^{(n)}(s) &= I_{12}^{(n)}(s, M^2). \end{aligned}$$

1 meson, 3 nucleons:

$$\begin{aligned} \{I_{13}, I_{13}^\mu\} &= \\ & \frac{1}{i} \int_I \frac{d^d k}{(2\pi)^d} \frac{\{1, k^\mu\}}{(M^2 - k^2)(m^2 - (P - k)^2)(m^2 - (\Sigma - k)^2)(m^2 - (P' - k)^2)} \\ I_{13}^\mu(s, t) &= Q^\mu I_{13}^{(1)}(s, t) + (\Delta + 2q)^\mu I_{13}^{(2)}(s, t) \end{aligned}$$

D Results for the loop graphs

In the present appendix, we list the contributions from the various topologies shown in fig. 2. Note that the amplitude in addition contains the contributions obtained from the graphs (a)–(i) and (n)–(s) through crossing,

$$\begin{aligned} A_G^\pm(s, t) &= A_G^\pm(s, t) \pm A_G^\pm(u, t) \\ B_G^\pm(s, t) &= B_G^\pm(s, t) \mp B_G^\pm(u, t) \\ D_G^\pm(s, t) &= D_G^\pm(s, t) \pm D_G^\pm(u, t) \end{aligned} \quad G \in (a, \dots, i, n, \dots, s)$$

D.1 Loop graphs of $\mathcal{L}^{(1)}$

The contribution of the loops formed exclusively with vertices of the lowest order Lagrangian $\mathcal{L}^{(1)}$ starts at order $O(q^3)$. We give the exact result for the $\mathcal{L}^{(1)}$ loops in terms of the amplitudes $A(s, t, u)$, $B(s, t, u)$, since the corresponding expressions can be written in a more compact form. Note that the amplitude $A(s, t, u)$ does not obey the chiral power counting rules.

We use the following abbreviation:

$$F(s) = -2 M^2 I(s) + (s - m^2) I^{(1)}(s) .$$

graphs a+b

$$A_{ab}^+ = \frac{g_A^2 m F(s)}{2 F^4} \qquad B_{ab}^+ = -\frac{g_A^2}{2 F^4} \left\{ \frac{2 m^2 F(s)}{s - m^2} + M^2 I(s) + F(s) \right\}$$

$$A_{ab}^- = A_{ab}^+ \qquad B_{ab}^- = B_{ab}^+$$

graphs c+d

$$A_{cd}^+ = \frac{g_A^4 m}{8 F^4} \left\{ -2 \Delta_\pi + (s - m^2) I^{(1)}(s) - 8 m^2 \left(M^2 I_B(s) - (s - m^2) I_B^{(2)}(s) \right) \right\}$$

$$B_{cd}^+ = \frac{g_A^4}{8 F^4} \left\{ -M^2 I(s) + (s - m^2) \left(I^{(1)}(s) - 4 m^2 I_B^{(1)}(s) \right) \right. \\ \left. + \frac{4 m^2}{s - m^2} \left[\Delta_\pi + (3 m^2 + s) \left(M^2 I_B(s) - (s - m^2) I_B^{(2)}(s) \right) \right] \right\}$$

$$A_{cd}^- = A_{cd}^+ \qquad B_{cd}^- = B_{cd}^+$$

graph e

$$A_e^+ = \frac{3 g_A^4 m}{16 F^4} \left\{ \frac{4 m^2 F(s)}{m^2 - s} - (2 M^2 I(s) + 3 F(s)) \right\}$$

$$B_e^+ = \frac{3 g_A^4}{16 F^4} \left\{ F(s) + M^2 I(s) - \frac{4 m^2}{m^2 - s} \left(M^2 I(s) + 2 F(s) \right) + \frac{8 m^4 F(s)}{(m^2 - s)^2} \right\}$$

$$A_e^- = A_e^+ \qquad B_e^- = B_e^+$$

graph f

$$A_f^+ = \frac{m(s-m^2)I^{(1)}(s)}{2F^4} \quad B_f^+ = \frac{1}{8F^4} \left\{ -4M^2 I(s) - \Delta_\pi + 4(s-m^2)I^{(1)}(s) \right\}$$

$$A_f^- = \frac{A_f^+}{2} \quad B_f^- = \frac{B_f^+}{2}$$

graphs g+h

$$A_{gh}^+ = \frac{g_A^2 m}{2F^4} (s-m^2) \left\{ -2I(s) + I^{(1)}(s) + 8m^2 I_B^{(1)}(s) \right\}$$

$$B_{gh}^+ = \frac{g_A^2}{4F^4} \left\{ -M^2 I(m^2) - 2\Delta_\pi - 8m^2 M^2 I_B(s) \right. \\ \left. + 2(m^2-s) \left[I(s) - I^{(1)}(s) - 4m^2 \left(I_B^{(1)}(s) + I_B^{(2)}(s) \right) \right] \right\}$$

$$A_{gh}^- = 0 \quad B_{gh}^- = 0$$

graph i

$$A_i^+ = \frac{3g_A^4 m}{16F^4} \left\{ 2M^2 (I(m^2) - I(s)) + (s-m^2) (2I(s) + I^{(1)}(s)) \right. \\ \left. + 8m^2 \left[-M^2 I_A(t) + 4m^2 I_A^{(1)}(t) - (s-u) I_A^{(3)}(t) \right] \right. \\ \left. + M^2 \left(I_B(s) - I_B^{(1)}(s) - I_B^{(2)}(s) \right) - (m^2 + 3s) I_B^{(1)}(s) - (s-m^2) I_B^{(2)}(s) \right] \\ \left. + 32m^4 (s-m^2) I_{13}^{(1)}(s, t) \right\}$$

$$B_i^+ = \frac{3g_A^4}{16F^4} \left\{ (3m^2 + s) I(s) + 4m^2 I^{(1)}(m^2) - (m^2 + s) I^{(1)}(s) \right. \\ \left. + 4m^2 \left[M^2 I_A(t) - 2I_A^{(2)}(t) + 2M^2 I_B(s) - 2(3m^2 + s) I_B^{(1)}(s) \right] \right. \\ \left. + 2(m^2 - s) I_B^{(2)}(s) \right] + 16m^4 \left[-M^2 I_{13}(s, t) + 2(s-m^2) I_{13}^{(2)}(s, t) \right] \right\}$$

$$A_i^- = -\frac{1}{3} A_i^+ \quad B_i^- = -\frac{1}{3} B_i^+$$

graph k

$$A_k^+ = B_k^+ = A_k^- = 0 \qquad B_k^- = \frac{t J^{(1)}(t)}{F^4}$$

graph l

$$A_l^+ = \frac{g_A^2 m}{2 F^4} \left\{ 2 M^2 I(m^2) - (M^2 - 2t) \left(J(t) - 4 m^2 I_{21}^{(1)}(t) \right) \right\} \qquad B_l^+ = 0$$

$$A_l^- = -\frac{4 g_A^2 m^3}{F^4} (s - u) I_{21}^{(3)}(t) \qquad B_l^- = -\frac{g_A^2}{F^4} \left\{ t J^{(1)}(t) + 4 m^2 I_{21}^{(2)}(t) \right\}$$

graph m

$$A_m^+ = B_m^+ = 0$$

$$A_m^- = -\frac{g_A^2 m^3}{F^4} (s - u) I_A^{(3)}(t)$$

$$B_m^- = -\frac{g_A^2}{8 F^4} \left\{ \Delta_\pi - 4 m^2 \left(I^{(1)}(m^2) + M^2 I_A(t) - 2 I_A^{(2)}(t) \right) \right\}$$

graphs n - v

$$A_{no}^\pm = -\frac{g_A^2 m}{F^4} M^2 I(m^2) \qquad B_{no}^\pm = A_{no}^+ \left(\frac{2m}{m^2 - s} - \frac{1}{4m} \right)$$

$$A_{pr}^\pm = \frac{g_A^2 m \Delta_\pi}{2 F^4} \qquad B_{pr}^\pm = A_{pr}^+ \left(\frac{2m}{m^2 - s} - \frac{1}{2m} \right)$$

$$A_s^\pm = 0 \qquad B_s^\pm = 0$$

$$A_{tu}^+ = -\frac{g_A^2 m M^2 I(m^2)}{F^4} \qquad B_{tu}^+ = 0$$

$$A_{tu}^- = 0 \qquad B_{tu}^- = \frac{A_{tu}^+}{2m}$$

$$A_v^+ = 0 \qquad B_v^+ = 0$$

$$A_v^- = 0 \qquad B_v^- = \frac{5 \Delta_\pi}{8 F^4}$$

D.2 Loop graphs of $\mathcal{L}^{(2)}$

The loops which, besides vertices from $\mathcal{L}^{(1)}$, also involve one vertex from $\mathcal{L}^{(2)}$, start contributing at order q^4 . As exemplified in section (6), the fact that we only need the leading order of the expansion of these diagrams simplifies the calculation considerably. The results are given in terms of the amplitudes $\{D(s, t), B(s, t)\}$ to order $\{O(q^4), O(q^2)\}$. We define

$$Q(t) = \frac{(m^2 - s)^2 + 2 m^2 (t - 2 M^2)}{8 m^3}$$

graphs a+b

$$\begin{aligned} D_{ab}^+ &= Q(t) B_{ab}^+ & B_{ab}^+ &= \frac{8 g_A^2 m^3}{F^4 (m^2 - s)} (c_3 - c_4 (d - 2)) I^{(2)}(s) \\ D_{ab}^- &= D_{ab}^+ & B_{ab}^- &= B_{ab}^+ \end{aligned}$$

graph f

$$\begin{aligned} D_f^+ &= B_f^+ = B_f^- = 0 \\ D_f^- &= \frac{1}{2 F^4} \left\{ 4 c_1 M^2 (m^2 - s) I(s) - [8 c_1 m^2 M^2 - (c_2 + c_3) (m^2 - s)^2] I^{(1)}(s) \right. \\ &\quad \left. - 2 (c_2 + c_3) (m^2 - s) (I^{(2)}(s) + m^2 I^{(3)}(s)) \right\} \end{aligned}$$

graphs g+h

$$\begin{aligned} D_{gh}^+ &= -D_{gh}^- - \frac{8 g_A^2 c_4 (d - 2) m^3}{F^4} Q(t) I_B^{(3)}(s) \\ B_{gh}^+ &= -B_{gh}^- - \frac{8 c_4 g_A^2 m^3}{F^4} \left\{ (d - 4) I_B^{(3)}(s) + 2 m Q(0) I_B^{(5)}(s) \right\} \\ D_{gh}^- &= -\frac{8 g_A^2 m^3}{4 F^4} \left\{ 4 c_3 Q(t) I_B^{(3)}(s) + Q(0) \left[-8 c_1 M^2 I_B^{(2)}(s) \right. \right. \\ &\quad \left. \left. + \left(\frac{c_2}{m^2} (m^2 - s)^2 + 2 c_3 (2 M^2 - t) \right) I_B^{(5)}(s) \right. \right. \\ &\quad \left. \left. - 4 (c_2 + c_3) (m^2 - s) I_B^{(6)}(s) \right] \right\} \\ B_{gh}^- &= \frac{8 c_3 g_A^2 m^3 I_B^{(3)}(s)}{F^4} \end{aligned}$$

graph k

$$D_k^+ = \frac{1}{2F^4} \left\{ (M^2 - 2t) (4c_1 M^2 + c_3 (t - 2M^2)) J(t) \right. \\ \left. + 2 \left(4c_1 M^2 - \frac{2c_2 M^2}{d} - c_3 (M^2 + 2t) \right) \Delta_\pi - 2c_2 t (2t - M^2) J^{(1)}(t) \right\} \\ B_k^+ = D_k^- = 0 \\ B_k^- = \frac{4c_4 m t J^{(1)}(t)}{F^4}$$

graph m

$$D_m^+ = -\frac{3g_A^2}{8F^4} \left(c_2 (s - u)^2 - 32c_1 m^2 M^2 + 8c_3 m^2 (2M^2 - t) \right) \\ \times \left((d - 1) I_A^{(2)}(t) + t I_A^{(4)}(t) \right) \\ B_m^+ = 0 \quad D_m^- = 0 \\ B_m^- = \frac{2c_4 g_A^2 m^3}{F^4} \left\{ (d - 5) I_A^{(2)}(t) - t I_A^{(4)}(t) \right\}$$

graphs n+o

$$D_{no}^+ = Q(t) B_{no}^+ \quad B_{no}^+ = \frac{8g_A^2 m^3}{F^4 (m^2 - s)} (c_3 - c_4 (d - 2)) I^{(2)}(m^2) \\ D_{no}^- = D_{no}^+ \quad B_{no}^- = B_{no}^+$$

graph s

$$D_s^+ = Q(t) B_s^+ \quad B_s^+ = \frac{6g_A^2 m^3 M^2}{F^4 (m^2 - s)^2} \left(\frac{c_2}{d} - 2c_1 + c_3 \right) \Delta_\pi \\ D_s^- = D_s^+ \quad B_s^- = B_s^+$$

graph v

$$D_v^+ = \frac{1}{4F^4} \left\{ -40c_1 M^2 + 2c_2 \left(\frac{4M^2}{d} + \frac{(s - u)^2}{4m^2} \right) + 4c_3 (4M^2 - t) \right\} \Delta_\pi \\ B_v^+ = 0 \quad D_v^- = 0 \quad B_v^- = \frac{2c_4 m}{F^4} \Delta_\pi$$

E Renormalization of the effective couplings

The renormalization of the coupling constants l_3 and l_4 that occur in the mesonic part of the effective Lagrangian is discussed in [20]. These constants enter our amplitude when expressing the bare quantities M, F in terms of their physical values M_π, F_π and in the wave function renormalization of the pion field. The renormalization of the couplings of $\mathcal{L}_N^{(3)}$ is given in [21], where the HBCHPT formalism is used to extract the divergent part of the one loop functional. In infrared regularization, the amplitude is of the form $M^d f$, where f is a function whose chiral expansion only contains integer powers of the chiral expansion parameter. Hence the poles at $d = 4$ always appear in the combination $(d - 4)^{-1} + \ln M/\mu$. The same is true for HBCHPT, because the nonrelativistic loop integrals do not involve the nucleon mass scale. The coefficients of the chiral logarithms must be the same in the two formulations of the effective theory, because these are of physical significance and cannot depend on the regularization scheme. We conclude that the divergences encountered in our approach are the same as those occurring in HBCHPT.

As a side remark, we note that in dimensional regularization, the renormalization of the effective coupling constants is different. In that approach, the infrared regular part of the amplitude is retained. This part also contains poles at $d = 4$, but these are not accompanied by a chiral logarithm. Instead the pole terms occur in the combination $(d - 4)^{-1} + \ln m/\mu$. Also, some of the divergences contained in the regular and singular parts cancel – the dimensionally regulated amplitude contains chiral logarithms without an associated pole at $d = 4$.

We define the renormalized coupling constants by

$$l_i = l_i^r(\mu) + \gamma_i \lambda, \quad d_i = d_i^r(\mu) + \frac{\delta_i}{F^2} \lambda, \quad e_i = e_i^r(\mu) + \frac{\epsilon_i}{F^2 m} \lambda, \\ \lambda = \frac{\mu^{d-4}}{(4\pi)^2} \left\{ \frac{1}{d-4} - \frac{1}{2} \left(\ln 4\pi + \Gamma'(1) + 1 \right) \right\}.$$

For the pion couplings l_3, l_4 the coefficients are

$$\gamma_3 = -\frac{1}{2}, \quad \gamma_4 = 2.$$

Those relevant for d_1, d_2, \dots may be taken from ref. [21]:

$$\begin{array}{llll} \delta_1 = -\frac{1}{6} g^4 & \delta_2 = -\frac{1}{12} - \frac{5}{12} g^2 & \delta_3 = \frac{1}{2} + \frac{1}{6} g^4 & \delta_5 = \frac{1}{24} + \frac{5}{24} g^2 \\ \delta_{14} = \frac{1}{3} g^4 & \delta_{15} = 0 & \delta_{16} = \frac{1}{2} g + g^3 & \delta_{18} = 0 \end{array}$$

These expressions differ from those given in [7] because these authors introduce additional equation of motion terms in the Lagrangian, to arrive at a finite scattering amplitude also off the mass shell.

Finally, we list the coefficients occurring in the renormalization of the coupling constants e_1, e_2, \dots that enter the amplitude at order $O(q^4)$:

$$\begin{aligned}
\epsilon_1 &= \frac{3}{2} g^2 - \frac{3}{2} (8 c_1 - c_2 - 4 c_3) m \\
\epsilon_2 &= -\frac{3}{2} g^2 - \frac{1}{2} (c_2 + 6 c_3) m \\
\epsilon_3 &= -1 - 3 g^2 - \frac{22}{3} g^4 - 8 c_1 m - c_2 m + 4 c_3 m \\
\epsilon_4 &= 10 + 12 g^2 + \frac{52}{3} g^4 + 8 c_2 m \\
\epsilon_5 &= \frac{1}{2} + \frac{7}{2} g^2 + \frac{13}{3} g^4 - 8 c_1 m + \frac{13}{6} c_2 m + 5 c_3 m \\
\epsilon_6 &= -12 - 8 g^2 - 8 g^4 \\
\epsilon_7 &= -3 - \frac{2}{3} g^2 - \frac{11}{3} g^4 \\
\epsilon_8 &= -g^2 - \frac{1}{3} g^4 - \frac{1}{3} (c_2 + 6 c_3) m \\
\epsilon_9 &= 1 + \frac{22}{3} g^4 + 4 c_4 m + g^2 (13 + 24 c_4 m) \\
\epsilon_{10} &= -\frac{16}{3} g^4 - \frac{4}{3} g^2 (3 + 8 c_4 m) \\
\epsilon_{11} &= \frac{1}{6} - \frac{7}{6} g^2 - \frac{2}{3} g^4 + \frac{2}{3} c_4 m
\end{aligned}$$

One readily checks that these renormalizations ensure a finite result for the quantities $m_N, g_{\pi N}, M_\pi, F_\pi$, for which we listed the explicit expressions in section 8. The same holds for the coefficients occurring in the polynomial part of our representation (see appendix 12), so that the scattering amplitude approaches a finite limit when the cutoff is removed.

F Subthreshold coefficients

In this appendix, we list the explicit results obtained for the expansion of the subthreshold coefficients in powers of the quark masses. These relations specify the polynomial part of the dispersive representation (15.1) in terms of the effective coupling constants. We express the result in terms of the physical pion mass. To simplify the formulae, we set the renormalization scale μ equal to M_π and indicate this with a tilde on the renormalized couplings:

$$\begin{aligned}
\tilde{d}_i &= d_i - \frac{\delta_i}{F^2} \lambda_\pi = d_i^r(\mu) - \frac{\delta_i}{16 \pi^2 F^2} \ln \frac{M_\pi}{\mu} , \\
\tilde{e}_i &= e_i - \frac{\epsilon_i}{F^2} \lambda_\pi = e_i^r(\mu) - \frac{\epsilon_i}{16 \pi^2 F^2} \ln \frac{M_\pi}{\mu} .
\end{aligned}$$

Note that the chiral logarithms are then contained in the coupling constants.

Amplitude D^+

$$d_{00}^+ = -\frac{2(2c_1 - c_3)M_\pi^2}{F_\pi^2} + \frac{g_A^2(3 + 8g_A^2)M_\pi^3}{64\pi F_\pi^4} + M_\pi^4 \left(\frac{\tilde{e}_3}{F_\pi^2} + \frac{8c_1\tilde{l}_3}{F_\pi^4} + \frac{3(g_A^2 + 6g_A^4)}{64\pi^2 F_\pi^4 m_N} - \frac{2c_1 - c_3}{16\pi^2 F_\pi^4} \right)$$

$$d_{10}^+ = \frac{2c_2}{F_\pi^2} - \frac{(4 + 5g_A^4)M_\pi}{32\pi F_\pi^4} + M_\pi^2 \left(\frac{\tilde{e}_4}{F_\pi^2} - \frac{16c_1c_2}{F_\pi^2 m_N} - \frac{1 + g_A^2}{4\pi^2 F_\pi^4 m_N} - \frac{197g_A^4}{240\pi^2 F_\pi^4 m_N} \right)$$

$$d_{01}^+ = -\frac{c_3}{F_\pi^2} - \frac{g_A^2(77 + 48g_A^2)M_\pi}{768\pi F_\pi^4} + M_\pi^2 \left(\frac{\tilde{e}_5}{F_\pi^2} + \frac{52c_1 - c_2 - 32c_3}{192\pi^2 F_\pi^4} - \frac{g_A^2(47 + 66g_A^2)}{384\pi^2 F_\pi^4 m_N} \right)$$

$$d_{20}^+ = \frac{12 + 5g_A^4}{192F_\pi^4 M_\pi \pi} + \frac{\tilde{e}_6}{F_\pi^2} + \frac{17 + 10g_A^2}{24\pi^2 F_\pi^4 m_N} + \frac{173g_A^4}{280\pi^2 F_\pi^4 m_N}$$

$$d_{11}^+ = \frac{g_A^4}{64F_\pi^4 M_\pi \pi} + \frac{\tilde{e}_7}{F_\pi^2} + \frac{9 + 2g_A^2}{96\pi^2 F_\pi^4 m_N} + \frac{67g_A^4}{240\pi^2 F_\pi^4 m_N}$$

$$d_{02}^+ = \frac{193g_A^2}{15360\pi F_\pi^4 M_\pi} + \frac{\tilde{e}_8}{F_\pi^2} - \frac{c_2}{8F_\pi^2 m_N^2} + \frac{29g_A^2}{480\pi^2 F_\pi^4 m_N} + \frac{g_A^4}{64\pi^2 F_\pi^4 m_N} - \frac{19c_1}{480\pi^2 F_\pi^4} + \frac{7c_2}{640\pi^2 F_\pi^4} + \frac{7c_3}{80\pi^2 F_\pi^4}$$

Amplitude D^-

$$d_{00}^- = \frac{1}{2F_\pi^2} + \frac{4(\tilde{d}_1 + \tilde{d}_2 + 2\tilde{d}_5)M_\pi^2}{F_\pi^2} + \frac{g_A^4 M_\pi^2}{48\pi^2 F_\pi^4} - M_\pi^3 \left(\frac{8 + 12g_A^2 + 11g_A^4}{128\pi F_\pi^4 m_N} - \frac{4c_1 + (c_3 - c_4)g_A^2}{4\pi F_\pi^4} \right)$$

$$d_{10}^- = \frac{4 \tilde{d}_3}{F_\pi^2} - \frac{15 + 7 g_A^4}{240 \pi^2 F_\pi^4} + \frac{M_\pi (168 + 138 g_A^2 + 85 g_A^4)}{768 \pi F_\pi^4 m_N} - \frac{M_\pi (8 c_1 + 8 c_2 + 8 c_3 + 5 c_3 g_A^2 - 5 c_4 g_A^2)}{16 \pi F_\pi^4}$$

$$d_{01}^- = -\frac{2(\tilde{d}_1 + \tilde{d}_2)}{F_\pi^2} - \frac{1 + 7 g_A^2 + 2 g_A^4}{192 \pi^2 F_\pi^4} + \frac{(12 + 53 g_A^2 + 24 g_A^4) M_\pi}{384 \pi F_\pi^4 m_N} - \frac{(c_3 - c_4) g_A^2 M_\pi}{8 \pi F_\pi^4}$$

Amplitude B^+

$$b_{00}^+ = \frac{4 m_N (\tilde{d}_{14} - \tilde{d}_{15})}{F_\pi^2} - \frac{g_A^4 m_N}{8 \pi^2 F_\pi^4} + \frac{g_A^2 (8 + 7 g_A^2) M_\pi}{64 \pi F_\pi^4} - \frac{(c_3 - c_4) g_A^2 m_N M_\pi}{2 \pi F_\pi^4}$$

Amplitude B^-

$$b_{00}^- = \frac{1}{2F_\pi^2} + \frac{2 c_4 m_N}{F_\pi^2} - \frac{g_A^2 (1 + g_A^2) m_N M_\pi}{8 \pi F_\pi^4} + \frac{\tilde{e}_9 m_N M_\pi^2}{F_\pi^2} - \frac{g_A^2 (3 + 2 g_A^2 + 9 c_4 m_N) M_\pi^2}{12 \pi^2 F_\pi^4}$$

$$b_{10}^- = \frac{g_A^4 m_N}{32 F_\pi^4 M_\pi \pi} + \frac{\tilde{e}_{10} m_N}{F_\pi^2} + \frac{g_A^2 (25 + 36 g_A^2 + 80 c_4 m_N)}{120 \pi^2 F_\pi^4}$$

$$b_{01}^- = \frac{g_A^2 m_N}{96 F_\pi^4 M_\pi \pi} + \frac{\tilde{e}_{11} m_N}{F_\pi^2} - \frac{1 - 9 g_A^2 - 4 g_A^4 + 4 c_4 m_N}{192 \pi^2 F_\pi^4}$$

G t -channel partial waves

Only the two $\pi\pi$ partial waves

$$t_0^0 = \frac{2t - M_\pi^2}{32\pi F_\pi^2} \quad \text{and} \quad t_1^1 = \frac{t - 4M_\pi^2}{96\pi F_\pi^2}$$

enter the t -channel unitarity relation (14.5) at the one loop level. The imaginary parts of the amplitudes D , B can thus be constructed from the three lowest partial waves f_+^0 , f_\pm^1 of the tree level πN amplitude:

$$\begin{aligned} \text{Im}_t D^+ &= \frac{16\pi}{4m_N^2 - t} \text{Im} f_+^0, & \text{Im}_t D^- &= \frac{24\pi\nu}{4m_N^2 - t} \left\{ 2m_N \text{Im} f_+^1 - \frac{t}{2\sqrt{2}} \text{Im} f_-^1 \right\}, \\ \text{Im}_t B^+ &= 0, & \text{Im}_t B^- &= 6\pi\sqrt{2} \text{Im} f_-^1. \end{aligned}$$

The Born term contribution to the relevant t -channel partial waves reads

$$\begin{aligned} f_{B^+}^0(t) &= \frac{g_{\pi N}^2 m_N}{4\pi} \left\{ f(\kappa) - \frac{t}{4m^2} \right\}, \\ f_{B^+}^1(t) &= \frac{g_{\pi N}^2 m_N}{\pi} \left\{ 1 - \frac{f(\kappa)}{(t - 2M_\pi^2)\kappa^2} - \frac{1}{24m_N^2} \right\}, \\ f_{B^-}^1(t) &= \frac{g_{\pi N}^2}{\sqrt{2}\pi} \left\{ \frac{(1 + \kappa^2)f(\kappa) - 1}{(t - 2M_\pi^2)\kappa^2} - \frac{1}{12m_N^2} \right\}, \end{aligned}$$

while the one generated by $\mathcal{L}_N^{(2)}$ is linear in t :

$$\begin{aligned} f_+^0(t) &= \frac{m^2}{24\pi F^2} \{-24M^2 c_1 + (4M^2 - t)c_2 + 6(2M^2 - t)c_3\} + O(q^3), \\ f_+^1(t) &= \frac{m + c_4 t}{24\pi F^2}, & f_-^1(t) &= \frac{1 + 4m_N c_4}{12\sqrt{2}\pi F_\pi^2}. \end{aligned}$$

The function $f(\kappa)$ stands for

$$f(\kappa) = \frac{\arctan \kappa}{\kappa}, \quad \kappa = \frac{\sqrt{(t - 4M_\pi^2)(4m_N^2 - t)}}{t - 2M_\pi^2}.$$

Note that the chiral expansion of this function does not converge at $t = 4M_\pi^2$: Since κ counts as a quantity of $O(q^{-1})$, the arctan is replaced by its Taylor series in inverse powers of κ . The point $t = 4M_\pi^2$ corresponds to $\kappa = 0$ and is thus outside the radius of convergence of that series. The infrared singularities occurring in the scalar form factor in the vicinity of the t -channel threshold are discussed in detail in ref. [9] – the scattering amplitude exhibits essentially the same structure there.

H Imaginary parts of the loop integrals

In this section we give the exact low energy imaginary part of the loop integrals defined in Appendix C. We can distinguish three different types of singularities:

1. Singularities in the low energy region,
2. Physical singularities in the high energy region,
3. Unphysical singularities generated by the regularization.

The singularities of the first kind are those generated by intermediate states that involve at most one nucleon. They are identical in dimensional and infrared regularization. The singularities of type (2) and (3) are absent at any finite order of the chiral expansion. An example for type (2) is the t -channel cut due to $\bar{N}N$ intermediate states in the triangle integral with two nucleon- and one pion-propagator. This integral develops an imaginary part for $t > 4m^2$, which can be obtained from the elastic unitarity relation in the t -channel. In the chiral expansion, the corresponding contribution is converted into a Taylor series in t . In infrared regularization, the loop integrals contain further singularities, which are not related to physical intermediate states. The infrared part of the self energy integral $I(s)$, for instance, has a cut for $s < 0$ and a pole at $s = 0$. Singularities of this type do not occur in dimensional regularization. In the following, we only list the imaginary parts of type (1) – only these are relevant for the low energy structure of the scattering amplitude.

1 meson, 1 nucleon

The dimensionally regularized self energy integral has a right hand cut starting at $s = (m + M)^2$. Its discontinuity is given by

$$\text{Im } H(s) = \frac{\rho(s)}{16 \pi s} \theta(s - s_+) , \quad s_{\pm} = (m \pm M)^2$$

and $\rho(s) = \sqrt{(s - s_+)(s - s_-)} = 2m \sqrt{\omega^2 - M^2}$.

The regular part of $H(s)$ has a pole at $s = 0$ and a cut for $s < 0$. The imaginary part of R is

$$\text{Im } R(s) = \frac{\rho(s)}{32 \pi s} \theta(-s)$$

The infrared part is given by the difference $I(s) = H(s) - R(s)$ and hence has a cut on the left as well as on the right. The left hand cut lies outside the

low energy region and is absent to any order of the chiral expansion. Note that the right hand cut is the same in both regularizations. The imaginary part of the coefficients of the vector and tensor integrals reads

$$\begin{aligned} 2 s \operatorname{Im} I^{(1)}(s) &= (s - m^2 + M^2) \operatorname{Im} I(s) \\ 12 s \operatorname{Im} I^{(2)}(s) &= -\rho(s)^2 \operatorname{Im} I(s) \\ 3 s^2 \operatorname{Im} I^{(3)}(s) &= \left((s - m^2 + M^2)^2 - M^2 s \right) \operatorname{Im} I(s) \end{aligned}$$

2 mesons

$$\operatorname{Im} J(t) = \frac{1}{16\pi} \sqrt{1 - \frac{4M^2}{t}} \theta(t - 4M^2) ,$$

$$4 \operatorname{Im} J^{(2)}(t) = \operatorname{Im} J(t) , \quad 12 t \operatorname{Im} J^{(1)}(t) = (t - 4 M^2) \operatorname{Im} J(t) .$$

2 mesons, 1 nucleon

For $t < 4 m^2$ the imaginary part of the scalar triangle integral is given by

$$\operatorname{Im} I_{21}(t) = \frac{\theta(t - 4M^2)}{8\pi \sqrt{t(4M^2 - t)}} \arctan \frac{\sqrt{(t - 4M^2)(4m^2 - t)}}{t - 2M^2} .$$

$\operatorname{Im} I_{21}^{(n)}(t)$ can be expressed in terms of $\operatorname{Im} I_{21}(t)$ and $\operatorname{Im} J(t)$:

$$\begin{aligned} 2 Q^2 \operatorname{Im} I_{21}^{(1)}(t) &= (2 M^2 - t) \operatorname{Im} I_{21}(t) + 2 \operatorname{Im} J(t) , \\ 8 \operatorname{Im} I_{21}^{(2)}(t) &= (4 M^2 - t) \operatorname{Im} I_{21}(t) + 2 (t - 2 M^2) \operatorname{Im} I_{21}^{(1)}(t) , \\ 8 Q^2 \operatorname{Im} I_{21}^{(3)}(t) &= 6 (2 M^2 - t) \operatorname{Im} I_{21}^{(1)}(t) + (t - 4 M^2) \operatorname{Im} I_{21}(t) , \\ 8 t \operatorname{Im} I_{21}^{(4)}(t) &= 2 (2 M^2 - t) \operatorname{Im} I_{21}^{(1)}(t) + (3 t - 4 M^2) \operatorname{Im} I_{21}(t) , \end{aligned}$$

where $Q^2 = 4 m^2 - t$.

1 meson, 2 nucleons

We restrict ourselves to the two special cases

$$I_A(t) = I_{12}(m^2, t) , \quad I_B(s) = I_{12}(s, M^2) .$$

The functions $I_A^{(n)}(t)$ are analytic in the low energy region,

$$\text{Im } I_A^{(n)}(t) = 0 \quad \text{for } t < 4m^2 .$$

For $s > 0$ the absorptive part of $I_B(s)$ is given by

$$\text{Im } I_B(s) = \frac{\theta(s - s_+)}{16 \pi \rho(s)} \ln \left\{ \frac{(2m\omega - M^2)s}{m^2s - (m^2 - M^2)^2} \right\}$$

The imaginary part of the coefficients of the tensorial decomposition can be obtained from the relations

$$2\rho(s)^2 \text{Im } I_B^{(1)}(s) = (m^2 - M^2 - s) \times ((m^2 - s + 2M^2) \text{Im } I_B(s) + \text{Im } I(s)) ,$$

$$2\rho(s)^2 \text{Im } I_B^{(2)}(s) = (m^2 - s) (3m^2 + s - 3M^2) \text{Im } I_B(s) + (m^2 + 3s - M^2) \text{Im } I(s) ,$$

$$4 \text{Im } I_B^{(3)}(s) = 2M^2 \text{Im } I_B(s) - (2m\omega + 3M^2) \text{Im } I_B^{(1)}(s) - (2m\omega + M^2) \text{Im } I_B^{(2)}(s) ,$$

$$4\rho(s)^2 \text{Im } I_B^{(4)}(s) = 4M^2 \text{Im } I_B^{(3)}(s) - (2m\omega + 2M^2) \text{Im } I^{(1)}(s) + 4(2m^2\omega^2 + M^2m\omega - M^4) \text{Im } I_B^{(1)}(s) ,$$

$$4\rho(s)^2 \text{Im } I_B^{(5)}(s) = -4(2m^2 + m\omega - M^2)(2m\omega + M^2) \text{Im } I_B^{(2)}(s) + 4(4m^2 + 4m\omega + M^2) \text{Im } I_B^{(3)}(s) + 2(2m^2 + 3m\omega + M^2) \text{Im } I^{(1)}(s) ,$$

$$4M^2 \text{Im } I_B^{(6)}(s) = 2(2m\omega + M^2) \left(\text{Im } I_B^{(1)}(s) - 2 \text{Im } I_B^{(4)}(s) \right) - \text{Im } I^{(1)}(s) .$$

1 meson, 3 nucleons

The absorptive part of the box integral $I_{13}(s, t)$ is a function of t . For $t < 4m^2$, it is given by

$$\text{Im } I_{13}(s, t) = \frac{1}{4\pi\sqrt{4\zeta(s) - t\rho(s)^2}} \frac{1}{\sqrt{-t}} \text{arcsinh} \left\{ \frac{\sqrt{-t}\rho(s)}{2\sqrt{\zeta(s)}} \right\},$$

$$\zeta(s) = (2m\omega - M^2)(m^2s - (m^2 - M^2)^2)$$

$$4(\rho(s)^2 + st) \text{Im } I_{13}^{(1)}(s, t) = (m^2 - M^2 - s) \left\{ 2 \text{Im } I_B(s) \right. \\ \left. + (2m^2 - 2s + 4M^2 - t) \text{Im } I_{13}(s, t) \right\}$$

$$4(\rho(s)^2 + st) \text{Im } I_{13}^{(2)}(s, t) = 2(m^2 - M^2 + s) \text{Im } I_B(s) \\ + ((m^2 - s)(4m^2 - 2M^2 - t) - M^2(2M^2 - t)) \text{Im } I_{13}(s, t)$$

Note, that the tensor integrals are not singular at $\rho(s)^2 + st = 0$. This can e.g. be seen by using the relation

$$\text{Im } I_B(s) = \frac{\sqrt{4s\zeta(\omega) + \rho(\omega)^4}}{2s} \text{Im } I_{13}(s, -\frac{\rho(\omega)^2}{s})$$

To the accuracy of our calculation, we need only the first two terms of the Taylor expansion of these integrals in t (see section 14.3).

I Low energy expansion of the loop integrals

We give the explicit form of the coefficients of the tensor decomposition of the loop integrals to next-to-leading order. The result is expressed in terms of the dimensionless variables

$$\Omega = \frac{s - m^2 - M^2}{2mM}, \quad \tau = \frac{t}{M^2}, \quad \text{and} \quad \alpha = \frac{M}{m}.$$

It involves the three functions

$$\begin{aligned}
f(\Omega) &= \frac{1}{8\pi^2} \sqrt{1 - \Omega^2} \arccos(-\Omega) , \\
\bar{J}(\tau) &= J(t) - J(0) = \frac{1}{8\pi^2} \left\{ 1 - \sqrt{\frac{4 - \tau}{\tau}} \arcsin \frac{\sqrt{\tau}}{2} \right\} , \\
g(\tau) &= \frac{1}{32\pi\sqrt{\tau}} \ln \frac{2 + \sqrt{\tau}}{2 - \sqrt{\tau}} - \frac{1}{32\pi} \ln \left\{ 1 + \frac{\alpha}{\sqrt{4 - \tau}} \right\} \\
&\quad + \frac{\alpha}{32\pi^2} \left\{ 1 + \frac{\pi}{\sqrt{4 - \tau}} + \frac{2(2 - \tau)}{\sqrt{\tau(4 - \tau)}} \arcsin \frac{\sqrt{\tau}}{2} \right\} .
\end{aligned}$$

The function $f(\Omega)$ is associated with the scalar self energy integral and $g(\tau)$ is related to the triangle integral with two meson and a single nucleon propagator. Note that $g(\tau)$ contains arbitrarily high orders of the expansion parameter α . It is constructed in such a way that the representations for $I_{21}^{(n)}(\tau)$ also cover the region around $\tau = 4$, where the chiral expansion of these integrals breaks down (see section 18 and ref. [9]).

2 mesons: $J = I_{20}$

$$\begin{aligned}
J(t) &= \bar{J}(\tau) - \frac{1}{16\pi^2} - 2\lambda_\pi \\
J^{(1)}(t) &= \frac{\tau - 4}{12\tau} \bar{J}(\tau) - \frac{1}{576\pi^2} + \left(\frac{1}{\tau} - \frac{1}{6}\right) \lambda_\pi \\
J^{(2)}(t) &= \frac{1}{4} \bar{J}(\tau) - \frac{1}{64\pi^2} - \frac{2 + \tau}{2\tau} \lambda_\pi
\end{aligned}$$

1 meson, 1 nucleon: $I = I_{11}$

$$\begin{aligned}
I(s) &= -\alpha (1 - 2\alpha\Omega) f(\Omega) + \frac{\alpha(\Omega - \alpha)}{16\pi^2} - 2\alpha (\Omega + \alpha - 2\alpha\Omega^2) \lambda_\pi + O(\alpha^3) \\
I^{(1)}(s) &= -\alpha^2 (\Omega + \alpha - 4\alpha\Omega^2) f(\Omega) + \frac{\alpha^2\Omega^2 (1 - 2\alpha\Omega)}{16\pi^2} \\
&\quad + \alpha^2 (1 - 2\Omega^2 - 6\alpha\Omega + 8\alpha\Omega^3) \lambda_\pi + O(\alpha^4)
\end{aligned}$$

$$I^{(2)}(s) = \frac{m^2 \alpha^3}{3} (1-4\alpha\Omega) (\Omega^2-1) f(\Omega) + \frac{m^2 \alpha^3 \Omega}{144 \pi^2} (6-5\Omega^2-15\alpha\Omega+14\alpha\Omega^3) \\ - \frac{1}{3} m^2 \alpha^3 (3\Omega - 2\Omega^3 + 3\alpha - 12\alpha\Omega^2 + 8\alpha\Omega^4) \lambda_\pi + O(\alpha^5)$$

$$I^{(3)}(s) = \frac{\alpha^3}{3} (1-4\Omega^2-12\alpha\Omega+24\alpha\Omega^3) f(\Omega) + \frac{\alpha^3 \Omega}{72 \pi^2} (7\Omega^2-3+18\alpha\Omega-30\alpha\Omega^3) \\ + \frac{2}{3} \alpha^3 (3\Omega - 4\Omega^3 + 3\alpha - 24\alpha\Omega^2 + 24\alpha\Omega^4) \lambda_\pi + O(\alpha^5)$$

2 mesons, 1 nucleon

$$I_{21}(t) = \frac{1}{m^2 \alpha} (g(\tau) + \alpha \lambda_\pi) + O(\alpha)$$

$$I_{21}^{(1)}(t) = \frac{1}{8m^2} \left\{ \alpha (2-\tau) g(\tau) + 2\bar{J}(\tau) - \frac{1-\pi\alpha}{8\pi^2} - 4\lambda_\pi \right\} + O(\alpha^2)$$

$$I_{21}^{(2)}(t) = \frac{\alpha}{16} \left\{ 2(4-\tau) g(\tau) + \alpha(\tau-2) \bar{J}(\tau) + \frac{4\pi + \alpha(\tau-4)}{16\pi^2} \right. \\ \left. + 4\alpha(4-\tau) \lambda_\pi \right\} + O(\alpha^3)$$

$$I_{21}^{(3)}(t) = \frac{1}{64m^2} \left\{ 2\alpha(\tau-4) g(\tau) + 3\alpha^2(2-\tau) \bar{J}(\tau) - \frac{\alpha(4\pi - \alpha\tau)}{16\pi^2} \right. \\ \left. + 8\alpha^2(\tau-4) \lambda_\pi \right\} + O(\alpha^3)$$

$$I_{21}^{(4)}(t) = \frac{1}{16m^2 \alpha \tau} \left\{ 2(3\tau-4) g(\tau) + (2-\tau)\alpha \bar{J}(\tau) + \frac{4\pi + \alpha(8-\tau)}{16\pi^2} \right. \\ \left. + 8\alpha\tau \lambda_\pi \right\} + O(\alpha)$$

1 meson, 2 nucleons

$$I_{12}(s, t) = -\frac{1}{4m^2 \Omega^2} (2\Omega - \alpha - 2\alpha\Omega^2) f(\Omega) - \frac{1}{m^2} (1 - \alpha\Omega) \lambda_\pi \\ + \frac{1}{64m^2 \pi^2 \Omega^2} (2\pi\Omega + 2\Omega^2 - \pi\alpha - 2\alpha\Omega + 2\alpha\Omega^3) + O(\alpha^2)$$

$$I_{12}^{(1)}(s, t) = -\frac{\alpha}{24 m^2 \Omega} (6 \Omega + \alpha - 16 \alpha \Omega^2) f(\Omega) + \frac{\alpha}{1152 m^2 \pi^2 \Omega} (18 \Omega^2 + 3 \pi \alpha - 21 \alpha \Omega - 8 \alpha \Omega^3) - \frac{1}{12 m^2} \alpha (6 \Omega + 9 \alpha - 16 \alpha \Omega^2) \lambda_\pi + O(\alpha^3)$$

$$I_{12}^{(2)}(s, t) = -\frac{\alpha}{12 m^2 \Omega^2} (2 + \Omega^2) f(\Omega) + \frac{\alpha}{576 \pi^2 m^2 \Omega^2} (6 \pi + 12 \Omega - \Omega^3) - \frac{\alpha \Omega}{6 m^2} \lambda_\pi + O(\alpha^2)$$

$$I_{12}^{(3)}(s, t) = \frac{\alpha^2}{12 \Omega^2} (\Omega^2 - 1) (2 \Omega - \alpha - 6 \alpha \Omega^2) f(\Omega) + \frac{\alpha^2}{576 \pi^2 \Omega^2} \left\{ 2 \Omega (3 \pi + 6 \Omega - 5 \Omega^3) - \alpha (3 \pi + 6 \Omega + 13 \Omega^3 - 18 \Omega^5) \right\} - \frac{\alpha^2}{6} (3 - 2 \Omega^2 - 8 \alpha \Omega + 6 \alpha \Omega^3) \lambda_\pi + O(\alpha^4)$$

$$I_{12}^{(4)}(s, t) = \frac{\alpha^2}{48 m^2 \Omega^2} \left\{ 2 \Omega - 8 \Omega^3 - \alpha (1 + 14 \Omega^2 - 36 \Omega^4) \right\} f(\Omega) - \frac{\alpha^2}{2304 m^2 \pi^2 \Omega^2} \left\{ 2 \Omega (3 \pi + 6 \Omega - 14 \Omega^3) - \alpha (3 \pi + 6 \Omega + 22 \Omega^3 - 72 \Omega^5) \right\} + \frac{\alpha^2}{12 m^2} (3 - 4 \Omega^2 - 16 \alpha \Omega + 18 \alpha \Omega^3) \lambda_\pi + O(\alpha^4)$$

$$I_{12}^{(5)}(s, t) = O(\alpha^2)$$

$$I_{12}^{(6)}(s, t) = -\frac{\alpha^2}{24 m^2 \Omega} (1 + 2 \Omega^2) f(\Omega) + \frac{\alpha^2}{1152 m^2 \pi^2 \Omega} (3 \pi + 6 \Omega + 4 \Omega^3) - \frac{\alpha^2 \Omega^2}{6 m^2} \lambda_\pi + O(\alpha^3)$$

1 meson, 3 nucleons

$$I_{13}(s, t) = \frac{1}{128 m^4 \pi^2 \alpha \Omega^3} \left\{ 2 \Omega (\pi + 2 \Omega) - \alpha (2 \pi + 4 \Omega - \pi \Omega^2 - 4 \Omega^3) \right\} - \frac{\Omega - \alpha}{4 m^4 \alpha \Omega^3} f(\Omega) + O(\alpha)$$

$$I_{13}^{(1)}(s, t) = -\frac{1}{24 m^4 \Omega^2} (3 \Omega - 2 \alpha - 4 \alpha \Omega^2) f(\Omega) - \frac{3 - 4 \alpha \Omega}{12 m^4} \lambda_\pi$$

$$+ \frac{1}{1152 m^4 \pi^2 \Omega^2} \left\{ 9 \Omega (\pi + \Omega) - 2 \alpha (3 \pi + 6 \Omega - 5 \Omega^3) \right\} + O(\alpha^2)$$

$$I_{13}^{(2)}(s, t) = -\frac{1}{24 m^4 \Omega^3} (2 + \Omega^2) f(\Omega) - \frac{1}{12 m^4} \lambda_\pi$$

$$+ \frac{1}{1152 m^4 \pi^2 \Omega^3} (6 \pi + 12 \Omega - \Omega^3) + O(\alpha)$$

J Low energy expansion of the amplitude

The representation of the amplitude given in sections 15 and 16 consists of the Born term, a set of dispersive contributions that account for the cuts in the s -, t - and u -channels and a polynomial. The dispersive part is described by the functions $D_1^\pm(s), \dots, B_2^\pm(t)$, which can be expressed as integrals over the corresponding imaginary parts, according to (16.2) and (16.3). As discussed in section 18, the first few terms of the chiral expansion of these integrals can be evaluated in closed form. In the present appendix, we give the corresponding explicit expressions.

The chiral expansion of the scattering amplitude involves a choice of kinematic variables to be kept fixed. As discussed in section 18, the convergence of the expansion improves considerably if the lab. energy $\Omega = \omega/M_\pi$ is replaced by the c.m. energy $\Omega_q = \omega_q/M_\pi$. At the same time, however, the change of variables generates bookkeeping problems, because polynomials in Ω_q do not represent polynomials in ν, t . For this reason, we work with the variables ω, t in the s -channel and use ν, t for the t -channel. The corresponding expansion at fixed Ω_q is readily obtained from the expressions given below: It suffices to express ω in terms of Ω_q and to expand the result in powers of α at fixed Ω_q .

When combined with the chirally expanded polynomial part specified in appendix F the expressions given below can be used to work out the chiral expansion of the scattering lengths and effective range parameters, for instance. As discussed in section 18, the expansion of observables that involve derivatives of the amplitude converges only extremely slowly because of the strong infrared singularities generated by the s - and u -channel cuts. For numerical analysis, we strongly recommend the use of the dispersive representation specified in sections 15 and 16.

The functions $D_1^\pm(s)$, $D_2^\pm(s)$, $B_1^\pm(s)$

For all of the expanded one-loop graphs that contain a cut in the s -channel, the discontinuity across the cut is given by a polynomial in ω and t times the factor $\sqrt{\omega^2 - M_\pi^2}/\omega^3$, where ω is the pion lab momentum. The factor $\sqrt{\omega^2 - M_\pi^2}$ represents the imaginary part of the elementary function

$$f(\omega) = \frac{1}{8\pi^2} \sqrt{1 - \frac{\omega^2}{M_\pi^2}} \arccos\left(-\frac{\omega}{M_\pi}\right),$$

which does develop the required square root discontinuity: Approaching the real axis from above, we have

$$f(\omega) = \frac{1}{8\pi^2} \sqrt{\left|1 - \frac{\omega^2}{M_\pi^2}\right|} \begin{cases} -\operatorname{arccosh}\left(-\frac{\omega}{M_\pi}\right) & \text{for } \omega < -M_\pi \\ \arccos\left(-\frac{\omega}{M_\pi}\right) & \text{for } -M_\pi < \omega < M_\pi \\ \operatorname{arccosh}\left(\frac{\omega}{M_\pi}\right) - i\pi & \text{for } \omega > M_\pi \end{cases}$$

The imaginary part determines the real part up to a polynomial. In fact, in the normalization specified in section 16, the real part is fully determined by the imaginary part, through the condition that the Taylor series expansion of the functions $D_1^\pm(s)$, $D_2^\pm(s)$, $B_1^\pm(s)$ in powers of ω does not contribute to the subthreshold coefficients listed in eq. (16.4). It therefore suffices to list the contributions proportional to $f(\omega)$, which we denote by $\hat{D}_1^\pm(s)$, $\hat{D}_2^\pm(s)$, $\hat{B}_1^\pm(s)$, respectively. The explicit expressions read:

$$\begin{aligned} \hat{D}_1^+(s) &= \frac{M_\pi}{12F_\pi^4 m_N \omega^3} \{ \Delta_1^+ + g_A^2 \Delta_2^+ + g_A^4 \Delta_3^+ \} f(\omega) \\ \Delta_1^+ &= 12\omega^4 (-m_N \omega + 3\omega^2 - M_\pi^2) \\ \Delta_2^+ &= 24\omega^4 (\omega^2 - M_\pi^2) \\ \Delta_3^+ &= 8(\omega^2 - M_\pi^2)^2 (-m_N \omega + 3\omega^2 + M_\pi^2) \\ \hat{D}_2^+(s) &= \frac{M_\pi (\omega^2 - M_\pi^2)}{12F_\pi^4 m_N \omega^3} \{ 2g_A^2 \omega^2 + g_A^4 (-4m_N \omega + 5\omega^2 + 4M_\pi^2) \} f(\omega) \\ \hat{B}_1^+(s) &= \frac{g_A^2 M_\pi (\omega^2 - M_\pi^2)}{3F_\pi^4 \omega^3} \{ 2\omega^2 + g_A^2 (-m_N \omega + 2\omega^2 + M_\pi^2) \\ &\quad - 8(c_3 - c_4)m_N \omega^2 \} f(\omega) \end{aligned}$$

$$\hat{D}_1^-(s) = \frac{M_\pi}{12 F_\pi^4 m_N \omega^3} \{ \Delta_1^- + g_A^2 \Delta_2^- + g_A^4 \Delta_3^- + \Delta_4^- \} f(\omega)$$

$$\begin{aligned} \Delta_1^- &= 6 \omega^4 (-m_N \omega + 3 \omega^2 - M_\pi^2) \\ \Delta_2^- &= 6 \omega^2 (2 \omega^4 - 2 \omega^2 M_\pi^2 + M_\pi^4) \\ \Delta_3^- &= 2 (-m_N \omega + 3 \omega^2 + M_\pi^2) (\omega^2 - M_\pi^2)^2 \\ \Delta_4^- &= -48 m_N \omega^4 \{ (c_2 + c_3) \omega^2 - 2 c_1 M_\pi^2 \} \\ &\quad - 16 g_A^2 (c_3 - c_4) m_N \omega^2 (\omega^2 - M_\pi^2)^2 \end{aligned}$$

$$\hat{D}_2^-(s) = \frac{g_A^2 M_\pi (\omega^2 - M_\pi^2)}{12 F_\pi^4 m_N \omega^3} \{ 3 \omega^2 + g_A^2 (-m_N \omega + 3 \omega^2 + M_\pi^2) - 8 (c_3 - c_4) m_N \omega^2 \} f(\omega)$$

$$\hat{B}_1^-(s) = \frac{g_A^2 M_\pi (\omega^2 - M_\pi^2)}{3 F_\pi^4 \omega^3} \{ 2 g_A^2 (-m_N \omega + 2 \omega^2 + M_\pi^2) + 3 \omega^2 + 8 c_4 m_N \omega^2 \} f(\omega)$$

Note that the expressions contain fictitious singularities at $\omega = 0$. These drop out when evaluating the functions $D_1^\pm(s)$, $D_2^\pm(s)$, $B_1^\pm(s)$, which are obtained by simply removing the leading terms in the expansion in powers of ω :

$$\begin{aligned} \hat{D}_1^\pm(s) &= \sum_{n=-3}^4 d_{1,n}^\pm \omega^n + D_1^\pm(s) , \\ \hat{D}_2^\pm(s) &= \sum_{n=-3}^2 d_{2,n}^\pm \omega^n + D_2^\pm(s) , \\ \hat{B}_1^\pm(s) &= \sum_{n=-3}^2 b_{1,n}^\pm \omega^n + B_1^\pm(s) . \end{aligned}$$

The functions $D_3^\pm(t)$, $B_2^\pm(t)$

Only the diagrams belonging to the topologies (k) and (l) have a branch point at $t = 4M_\pi^2$. Note that in the case of (k), the two-pion-vertices from $\mathcal{L}_N^{(1)}$ are relevant as well as those from $\mathcal{L}_N^{(2)}$, which are proportional to c_1 , c_2 , c_3 , c_4 . Explicit representations for the contributions from these graphs are given in appendix D. Those of type (k) may be expressed in terms of the familiar loop integral $\bar{J}(t)$. The low energy structure of the vertex diagrams (l) is discussed in detail in [9]. To the order we are considering here, the corresponding integrals may be expressed in terms of $\bar{J}(t)$ and of

the function $g(t)$ which is the expanded version of the triangle integral $I_{21}(t)$ with two mesons and one nucleon. In the t -channel, we thus encounter two functions that play the same role as the quantity $f(\omega)$ used for the s -channel. Again, it suffices to list the contributions proportional to these functions (the explicit expressions for $\bar{J}(t)$ and $g(t)$ are given in section 18):

$$\hat{D}_3^+(t) = \frac{M_\pi^2 - 2t}{12 F_\pi^4} \left\{ \left(24 c_1 M_\pi^2 + c_2 (t - 4 M_\pi^2) \right. \right. \\ \left. \left. + 6 c_3 (t - 2 M_\pi^2) + \frac{3 g_A^2 t}{2 m_N} \right) \bar{J}(t) + \frac{3 g_A^2 (2 M_\pi^2 - t)}{M_\pi} g(t) \right\}$$

$$B_2^+(t) = 0$$

$$\hat{D}_3^-(t) = \frac{1}{12 F_\pi^4} \left\{ t - 4 M_\pi^2 + g_A^2 (5t - 8 M_\pi^2) \right\} \bar{J}(t) \\ - \frac{g_A^2}{8 F_\pi^4 m_N M_\pi} (3t^2 - 12t M_\pi^2 + 8 M_\pi^4) g(t)$$

$$\hat{B}_2^-(t) = \frac{1}{12 F_\pi^4} \left\{ 2 g_A^2 (5M_\pi^2 - 2t) + (1 + 4 c_4 m_N)(t - 4 M_\pi^2) \right\} \bar{J}(t) \\ + \frac{g_A^2 m_N}{2 F_\pi^4 M_\pi} (t - 4 M_\pi^2) g(t)$$

The functions $D_3^\pm(t)$ and $B_2^-(t)$ are then obtained by subtracting from the above expressions the first few terms of their expansion in t :

$$\hat{D}_3^+(t) = d_{3,0}^+ + d_{3,1}^+ t + d_{3,1}^+ t^2 + D_3^+(t) \\ \hat{D}_3^-(t) = d_{3,0}^- + d_{3,1}^- t + D_3^-(t) \\ \hat{B}_2^-(t) = b_{2,0}^- + B_2^-(t)$$

K Integral equations for πN scattering

In section 23, we briefly described a system of integral equations for the partial waves of πN scattering, which is analogous to the Roy equations for the $\pi\pi$ scattering amplitude. The present appendix provides the technical details needed to explicitly work out the kernels that occur in these equations.

Our starting point is the hypothesis that, at low energies, the properties of the scattering amplitude are governed by the pole from the Born term and

by the unitarity cuts in the s -, t - and u -channels and that only the S - and P -waves generate a significant contribution to the latter. In the s -channel partial wave decomposition, the terms from these waves read

$$\begin{aligned} A^\pm &= 4\pi \left\{ \frac{(\sqrt{s} + m_N)(f_{0+}^\pm + 3z f_{1+}^\pm)}{E + m_N} - \frac{(\sqrt{s} - m_N)(f_{1-}^\pm - f_{1+}^\pm)}{E - m_N} + \dots \right\}, \\ B^\pm &= 4\pi \left\{ \frac{f_{0+}^\pm + 3z f_{1+}^\pm}{E + m_N} + \frac{f_{1-}^\pm - f_{1+}^\pm}{E - m_N} + \dots \right\}, \end{aligned} \quad (\text{K.1})$$

where $z = \cos\theta$ is related to the momentum transfer, $t = 2q^2(z - 1)$. The variables q and E denote the momentum and the energy of the nucleon in the centre of mass system, respectively. The analogous terms from the lowest t -channel partial waves read

$$\begin{aligned} A^+ &= \frac{16\pi f_+^0}{4m_N^2 - t} + \dots, & A^- &= -\frac{24\pi m_N \nu (\sqrt{2} m_N f_-^1 - 2f_+^1)}{4m_N^2 - t} + \dots, \\ B^+ &= 0 + \dots, & B^- &= 6\sqrt{2}\pi f_-^1 + \dots, \end{aligned} \quad (\text{K.2})$$

where the dots stand for contributions with $J \geq 2$.

This shows that the relevant contributions from the singularities in the s - and u -channels are linear in t , while those from the t -channel are linear in ν . The above hypothesis is thus equivalent to the assumption that the invariant amplitudes A^\pm and B^\pm may be described in terms of functions of a single variable, which moreover only have a right hand cut:⁷

$$\begin{aligned} A^+ &= A_{pv}^+ + A_1^+(s) + A_1^+(u) + t A_2^+(s) + t A_2^+(u) + A_3^+(t) + A_p^+, \\ A^- &= A_{pv}^- + A_1^-(s) - A_1^-(u) + t A_2^-(s) - t A_2^-(u) + \nu A_3^-(t) + A_p^-, \\ B^+ &= B_{pv}^+ + B_1^+(s) - B_1^+(u) + t B_2^+(s) - t B_2^+(u) + B_p^+, \\ B^- &= B_{pv}^- + B_1^-(s) + B_1^-(u) + t B_2^-(s) + t B_2^-(u) + B_3^-(t) + B_p^-. \end{aligned} \quad (\text{K.3})$$

The first terms on the right denote the pseudovector Born contributions, while A_p^\pm and B_p^\pm stand for polynomials in the Mandelstam variables. The imaginary parts of the functions $A_1^+(s), \dots, B_3^-(t)$ are determined by those of the 9 partial waves occurring in (K.1), (K.2): In the notation of eqs. (23.3),

⁷In the present context, the invariant amplitudes A^\pm are more convenient to work with than D^\pm , because the P -waves f_{1+}^\pm give rise to a quadratic t -dependence in D^\pm .

(23.4), the discontinuities of $A_1^\pm(s)$, $A_2^\pm(s)$, $B_1^\pm(s)$, $B_2^\pm(s)$ are given by

$$\begin{aligned}
\text{Im}A_1^\pm &= 4\pi \frac{(\sqrt{s} + m_N)(\text{Im}f_1^\pm + 3\text{Im}f_3^\pm)}{E + m_N} - 4\pi \frac{(\sqrt{s} - m_N)(\text{Im}f_2^\pm - \text{Im}f_3^\pm)}{E - m_N}, \\
\text{Im}A_2^\pm &= 6\pi \frac{(\sqrt{s} + m_N)\text{Im}f_3^\pm}{(E + m_N)^2(E - m_N)}, \\
\text{Im}B_1^\pm &= 4\pi \frac{\text{Im}f_1^\pm + 3\text{Im}f_3^\pm}{E + m_N} + 4\pi \frac{\text{Im}f_2^\pm - \text{Im}f_3^\pm}{E - m_N}, \\
\text{Im}B_2^\pm &= 6\pi \frac{\text{Im}f_3^\pm}{(E + m_N)^2(E - m_N)},
\end{aligned} \tag{K.4}$$

while those of $A_3^\pm(t)$, $B_3^\pm(t)$ are determined by the t -channel partial waves:

$$\begin{aligned}
\text{Im}A_3^+ &= 16\pi \frac{\text{Im}f_4^+}{4m_N^2 - t}, \quad \text{Im}A_3^- = -24\pi m_N \frac{\sqrt{2} m_N \text{Im}f_4^- - 2\text{Im}f_5^-}{4m_N^2 - t}, \\
\text{Im}B_3^+ &= 0, \quad \text{Im}B_3^- = 6\sqrt{2}\pi \text{Im}f_4^-.
\end{aligned} \tag{K.5}$$

We can now set up the analogon of the Roy equations. In order not to burden the discussion with problems of technical nature, we first disregard subtractions. The dispersion relations obeyed by the functions associated with the s -channel cuts then read

$$G(s) = \frac{1}{\pi} \int_{(m_N + M_\pi)^2}^{\infty} \frac{ds' \text{Im}G(s')}{s' - s - i\epsilon}, \quad G = A_1^\pm, A_2^\pm, B_1^\pm, B_2^\pm, \tag{K.6}$$

while those related to the t -channel singularities are of the form

$$H(t) = \frac{1}{\pi} \int_{4M_\pi^2}^{\infty} \frac{dt' \text{Im}H(t')}{t' - t - i\epsilon}, \quad H = A_3^\pm, B_3^\pm. \tag{K.7}$$

The above equations specify the amplitude in the low energy region, in terms of the imaginary parts of the 9 relevant partial waves and of the constants occurring in the polynomial parts A_p^\pm, B_p^\pm of the representation (K.3). In particular, the real parts of those partial waves may be worked out from the s - and t -channel partial wave decompositions of that representation.

To extract the s -channel partial waves, we need to perform the integrals

$$\alpha_\ell^\pm(s) = \int_{-1}^{+1} dz A^\pm(s, t) P_\ell(z), \quad \beta_\ell^\pm(s) = \int_{-1}^{+1} dz B^\pm(s, t) P_\ell(z), \tag{K.8}$$

where t is to be expressed in terms of s and z , with $t = 2q^2(z - 1)$. The

partial waves of interest are then given by

$$\begin{aligned}
f_1^\pm(s) &= \frac{E + m_N}{16\pi\sqrt{s}} \{ \alpha_0^\pm(s) + (\sqrt{s} - m_N) \beta_0^\pm(s) \} \\
&\quad + \frac{E - m_N}{16\pi\sqrt{s}} \{ -\alpha_1^\pm(s) + (\sqrt{s} + m_N) \beta_1^\pm(s) \} , \\
f_2^\pm(s) &= \frac{E + m_N}{16\pi\sqrt{s}} \{ \alpha_1^\pm(s) + (\sqrt{s} - m_N) \beta_1^\pm(s) \} \\
&\quad + \frac{E - m_N}{16\pi\sqrt{s}} \{ -\alpha_0^\pm(s) + (\sqrt{s} + m_N) \beta_0^\pm(s) \} , \\
f_3^\pm(s) &= \frac{E + m_N}{16\pi\sqrt{s}} \{ \alpha_1^\pm(s) + (\sqrt{s} - m_N) \beta_1^\pm(s) \} \\
&\quad + \frac{E - m_N}{16\pi\sqrt{s}} \{ -\alpha_2^\pm(s) + (\sqrt{s} + m_N) \beta_2^\pm(s) \} .
\end{aligned} \tag{K.9}$$

In order to extract the t -channel partial waves, we need to expand the amplitude in powers of ν at fixed t . Concerning the contribution from the t -channel cuts, the operation is trivial, because these are linear in ν . Those arising from the cuts in the s -channel represent a superposition of terms of the form

$$\frac{1}{s' - s} = \frac{1}{s' - m_N^2 - M_\pi^2 - 2m_N \nu + \frac{1}{2} t}$$

with $s' \geq (m_N + M_\pi)^2$. The relevant angular variable is given by

$$Z = \frac{m_N \nu}{p_- q_-} = -\cos \theta_t , \quad p_- = \sqrt{m_N^2 - \frac{1}{4} t} , \quad q_- = \sqrt{M_\pi^2 - \frac{1}{4} t} ,$$

so that the partial wave expansion amounts to the series

$$\begin{aligned}
\frac{1}{s' - s} &= \frac{1}{2 p_- q_-} \sum_{\ell=0}^{\infty} (2\ell + 1) P_\ell(Z) Q_\ell(Z') , \\
Z' &\equiv \frac{2s' - 2m_N^2 - 2M_\pi^2 + t}{4 p_- q_-} .
\end{aligned} \tag{K.10}$$

In the Z -plane, the expansion converges in an ellipse that has the foci at $Z = \pm 1$ and passes through the point $Z = Z'$. In the context of our system of integral equations, we need the t -channel partial waves for $t > 4M_\pi^2$. For real values of Z and $t < 4m_N^2$, the variable ν is then purely imaginary and the denominator $s' - s$ is different from zero, in the entire range of integration over s' . Hence the partial wave expansion converges and can be inverted without problems.

In fact, in the case of the amplitude C , we may apply the formula (A.2) to convert the dispersive representation into a series of Legendre polynomials of the form (A.2) and read off the coefficients. For the amplitude B , however, the partial wave decomposition involves the first derivative of the Legendre polynomials. The corollary of (K.10) that is relevant in this case reads:

$$\frac{1}{s' - s} = \frac{1}{2p_- q_-} \sum_{\ell=1}^{\infty} P'_\ell(Z) \{Q_{\ell-1}(Z') - Q_{\ell+1}(Z')\} . \quad (\text{K.11})$$

This then allows us to read off the contributions to t -channel partial waves that are generated by the s - and u -channel cuts.

For the specific partial waves of interest, we may also write down explicit projection formulae analogous to (K.8) and (K.9):

$$\begin{aligned} f_4^+(t) &= \frac{p_-}{8\pi} \int_{-1}^1 dZ \{p_- A^+(\nu, t) + q_- m_N Z B^+(\nu, t)\} , \\ f_4^-(t) &= \frac{\sqrt{2}}{16\pi} \int_{-1}^1 dZ (1 - Z^2) B^-(\nu, t) , \\ f_5^-(t) &= \frac{1}{8\pi q_-} \int_{-1}^1 dZ Z \{p_- A^-(\nu, t) + q_- m_N Z B^-(\nu, t)\} , \end{aligned} \quad (\text{K.12})$$

with $\nu = Z p_- q_- / m_N$. Note that, for $4M_\pi^2 < t < 4m_N^2$, the integral extends over purely imaginary values of ν .

Collecting the various pieces, the system of equations takes the form (23.5): The S - and P -waves are expressed as linear superpositions of contributions from the Born term, from the polynomial and from the imaginary parts of these waves. The advantage of working in the t -channel isospin basis is that the system does not intertwine the partial waves with even and odd isospin. For the t -channel partial waves, the unitarity condition is also diagonal in these variables:

$$\begin{aligned} \text{Im} f_4^+(t) &= \{1 - 4M_\pi^2/t\}^{-\frac{1}{2}} t_0^0(t)^* f_4^+(t) , \\ \text{Im} f_i^-(t) &= \{1 - 4M_\pi^2/t\}^{-\frac{1}{2}} t_1^1(t)^* f_i^-(t) , \quad i = 4, 5 \end{aligned} \quad (\text{K.13})$$

In the s -channel, however, unitarity does connect the two sets of amplitudes. The relation (14.4) applies to the partial waves of a given s -channel isospin:

$$f_i^{\frac{1}{2}} = f_i^+ + 2f_i^- , \quad f_i^{\frac{3}{2}} = f_i^+ - f_i^- , \quad i = 1, 2, 3 . \quad (\text{K.14})$$

Expressed in terms of the amplitudes $f_1^\pm, f_2^\pm, f_3^\pm$, elastic unitarity requires

$$\begin{aligned} \text{Im} f_i^+(s) &= q |f_i^+(s)|^2 + 2q |f_i^-(s)|^2 , \\ \text{Im} f_i^-(s) &= q f_i^+(s) f_i^-(s)^* + q f_i^-(s) f_i^+(s)^* + q |f_i^-(s)|^2 . \end{aligned} \quad (\text{K.15})$$

Finally, we need to specify the polynomial part of the representation (K.3), which accounts for the contributions from the higher partial waves. This part is intimately connected with the issue of subtractions, because the contributions from the subtraction constants amount to a polynomial. Note also that the decomposition of the amplitude in eq. (K.3) is not unique. We may, for instance, add a constant to the functions $A_1^-(s)$, $A_2^-(s)$, $B_1^+(s)$, $B_2^+(s)$, without changing the scattering amplitude.

While the imaginary parts of the functions $B_i^\pm(s)$ fall off sufficiently fast at high energies for the integrals in eq. (K.6) to converge, the dispersion relations for the functions $A_i^\pm(s)$ need to be subtracted at least once. In order to suppress the contributions of the higher partial waves we oversubtract and introduce two subtractions for the amplitudes $A_1^\pm(s)$ and one for $B_1^\pm(s)$. Since the contributions of $A_2^\pm(s)$ and $B_2^\pm(s)$ are suppressed by a factor of t , we use the minimal number of subtractions for these. Crossing symmetry reduces the number of subtraction constants by a factor of two, so that the eight subtractions lead to four subtraction constants. We identify these with the subthreshold parameters d_{00}^+ , d_{10}^+ , d_{00}^- , b_{00}^- , so that we can write the polynomial part of the amplitude as

$$\begin{aligned} A_p^+ &= d_{00}^+ + t d_{10}^+ , & B_p^+ &= 0 \\ A_p^- &= \nu (d_{00}^- - b_{00}^-) , & B_p^- &= b_{00}^- , \end{aligned} \quad (\text{K.16})$$

Since the amplitude B^+ is odd under crossing, we can perform an additional subtraction in $B_2^+(s)$, without introducing a new subtraction constant. Subtracting at $s_0 = m_N^2 + M_\pi^2$, the dispersion relations in the variable s take the form

$$G_n(s) \equiv \frac{(s - s_0)^n}{\pi} \int_{(m_N + M_\pi)^2}^{\infty} \frac{ds' \text{Im}G(s')}{(s' - s_0)^n (s' - s)} , \quad (\text{K.17})$$

with $n = 2$ for $A_1^\pm(s)$ and $n = 1$ for $A_2^\pm(s)$, $B_1^\pm(s)$, $B_2^+(s)$. Only the one for $B_2^-(s)$ remains unsubtracted, $n = 0$. The analogous dispersion relations in the variable t read

$$H_n(t) = \frac{t^n}{\pi} \int_{4M_\pi^2}^{\infty} \frac{dt' \text{Im}H(t')}{t'^n (t' - t)} , \quad (\text{K.18})$$

with $n = 2$ for $A_3^+(t)$ and $n = 1$ for $A_3^-(t)$, $B_3^-(t)$.

This then completes our system of equations. In order to solve it, the system must be iterated. Starting with a given input for $\text{Im}f_n^\pm$, the relations (23.5) determine the corresponding real parts. The unitarity conditions (K.13), (K.15) then yield a new set of imaginary parts, etc. Note that the

outcome is meaningful only at low energies, whereas the dispersion integrals extend to infinity. Also, elastic unitarity is valid only at low energies – we need experimental information for the behaviour of the imaginary parts of the partial waves in the inelastic region, $s > (m_N + 2M_\pi)^2$, $t > 16M_\pi^2$.

In the case of $\pi\pi$ scattering, the mathematics of the Roy equations has been explored in detail and it has been shown that two subtractions suffice to arrive at a remarkably accurate representation in the elastic region [18]. For πN scattering, the properties of the corresponding system of equations yet need to be explored. Concerning the behaviour of the imaginary parts at higher energies, as well as the contributions from higher partial waves, the phenomenological information is much better than in the case of $\pi\pi$ scattering. Also, the $\pi\pi$ phase shifts, which enter the t -channel unitarity condition, are now known very accurately [19]. We are confident that the proposed system of equations will indeed provide the required link between the physical region and the Cheng-Dashen point and thus allow an accurate determination of the σ -term.

References

- [1] E.M. Henley and W. Thirring, *Elementary Quantum Field Theory*, (McGraw-Hill, New York 1962), Part III. Pion Physics.
- [2] J. Gasser, M. E. Sainio and A. Švarc, Nucl. Phys. B **307** (1988) 779.
- [3] E. Jenkins and A. V. Manohar, Phys. Lett. B **255** (1991) 558.
- [4] G. Ecker, Czech. J. Phys. **44** (1994) 405.
- [5] V. Bernard, N. Kaiser and U.-G. Meissner, Int. J. Mod. Phys. **E4** (1995) 193.
- [6] M. Mojžiš, Eur. Phys. J. C **2** (1998) 181.
- [7] N. Fettes, U. Meissner and S. Steininger, Nucl. Phys. A **640** (1998) 199.
- [8] N. Fettes and U. Meissner, Nucl. Phys. A **676** (2000) 311.
- [9] T. Becher and H. Leutwyler, Eur. Phys. J. C **9** (1999) 643.
- [10] J. L. Goity, D. Lehmann, G. Prezeau and J. Saez, hep-ph/0101011.
D. Lehmann and G. Prezeau, hep-ph/0102161.

- [11] J. Schweizer, "Low energy representation for the axial form factor of the nucleon", Diploma thesis, University of Bern, 2000.
- [12] B. Kubis and U. G. Meissner, Nucl. Phys. A **679** (2001) 698; Eur. Phys. J. C **18** (2001) 747.
S. Zhu, S. Puglia and M. J. Ramsey-Musolf, Phys. Rev. D **63** (2001) 034002.
- [13] J. Kambor and M. Mojžiš, JHEP **04** (1999) 031.
- [14] V. Bernard, N. Kaiser and U. Meissner, Phys. Lett. B **389** (1996) 144.
- [15] S.M. Roy, Phys. Lett. **36B** (1971) 353
- [16] R. Oehme, Phys. Rev. **100** (1955) 1503; *ibid.* **102** (1956) 1174.
R. H. Capps and G. Takeda, Phys. Rev. **103** (1956) 1877.
G. F. Chew, M. L. Goldberger, F. E. Low and Y. Nambu, Phys. Rev. **106** (1957) 1345.
F. Steiner, Fortsch. Physik **18** (1970) 43; *ibid.* **19** (1971) 115.
J. Baacke and F. Steiner, Fortsch. Physik **18** (1970) 67.
- [17] R. Koch, Nucl. Phys. A **448** (1986) 707.
- [18] B. Ananthanarayan, G. Colangelo, J. Gasser and H. Leutwyler, hep-ph/0005297, Phys. Reports, in print.
- [19] G. Colangelo, J. Gasser and H. Leutwyler, Phys. Lett. B **488** (2000) 261;
G. Colangelo, J. Gasser and H. Leutwyler, Nucl. Phys. B **603** (2001) 125
- [20] J. Gasser and H. Leutwyler, Ann. Phys. **158** (1984) 142.
- [21] G. Ecker, Phys. Lett. B **336** (1994) 508.
G. Ecker and M. Mojžiš, Phys. Lett. B **365** (1996) 312.
- [22] V. Bernard, N. Kaiser, J. Kambor and U.-G. Meissner, Nucl. Phys. B **388** (1992) 315.
- [23] J. Gasser, H. Leutwyler and M. E. Sainio, Phys. Lett. B **253** (1991) 252 and 260.
- [24] J. Gasser and H. Leutwyler, Ann. Phys. **158** (1984) 142.

- [25] C. A. Dominguez, *πNN form-factor, chiral symmetry breaking and three - pion resonances*, Phys. Rev. D **27** (1983) 1572.
 C. A. Dominguez, *The Goldberger-Treiman relation: A probe of the chiral symmetries of quantum chromodynamics*, Riv. Nuovo Cim. **8N6** (1985) 1.
 P. A. Guichon, G. A. Miller and A. W. Thomas, *The axial form-factor of the nucleon and the pion - nucleon vertex function*, Phys. Lett. B **124** (1983) 109.
 P. M. Gensini, *Strangeness in the proton wave function ?*, Nuovo Cim. A **102** (1989) 75 [Erratum-ibid. A **102** (1989) 1181].
- [26] N. F. Nasrallah, Phys. Rev. D **62** (2000) 036006
- [27] M.L. Goldberger and S.B. Treiman, Phys. Rev. **110** (1958) 1178.
- [28] G. Höhler, in Landolt-Börnstein, **9b2**, ed. H. Schopper (Springer, Berlin, 1983).
- [29] T.P. Cheng and R. Dashen, Phys. Rev. Lett. **26** (1971) 594.
- [30] L.S. Brown, W.J. Pardee and R.D. Peccei, Phys. Rev. D **4** (1971) 2801.
- [31] H. Pagels and W.J. Pardee, Phys. Rev. D **4** (1971) 3335.
- [32] M. E. Sainio, πN Newslett. **13** (1997) 144.
- [33] R. A. Arndt, R. L. Workman, I. I. Strakovsky and M. M. Pavan, nucl-th/9807087.
- [34] J. Stahov, πN Newslett. **15** (1999) 13.
- [35] G. C. Oades, πN Newslett. **15** (1999) 307. Note that some of the numerical values listed in this reference are incorrect. We thank G. Oades for providing us with the corrected values.
- [36] J. Gasser, Nucl. Phys. **B279** (1987) 65.
- [37] M. Knecht, B. Moussalam, J. Stern and N.H. Fuchs, Nucl. Phys. B **457** (1995) 513; *ibid.* **471** (1996) 445.
- [38] E. Jenkins and A. V. Manohar, Phys. Lett. B **259** (1991) 353.
 E. Jenkins and A. V. Manohar, *Effective Theories of the Standard Model*, ed. U.-G. Meissner, (World Scientific, Singapore 1991).

- J. Kambor, in Proc. Workshop on *Chiral Dynamics: Theory and Experiment*, Mainz, Germany (1997), eds. A. Bernstein, D. Drechsel, T. Walcher, Lecture Notes in Physics, **513**, Springer-Verlag, 1998.
- T. R. Hemmert, B. R. Holstein and J. Kambor, Phys. Lett. B **395** (1997) 89; Phys. Rev. **D55** (1997) 5598; J. Phys. G **24** (1998) 1831.
- P. J. Ellis and H.-B. Tang, Phys. Rev. C **57** (1998) 3356.
- N. Fettes and U. G. Meissner, Nucl. Phys. A **679** (2001) 629.
- [39] V. Antonelli, A. Gall, J. Gasser, A. Rusetsky, Annals Phys. **286** (2001) 108.
- [40] S. Weinberg, Phys. Rev. Lett. **17** (1966) 616.
- [41] Proc. 8th Symposium on Meson - Nucleon Physics and the Structure of the Nucleon (MENU 99), Zuoz, Switzerland (1999), πN Newslett. **15** (1999).
- [42] R. Koch, Z. Phys. C **29** (1985) 597.
- [43] H. J. Leisi, πN Newslett. **15** (1999) 258.
H. C. Schröder *et al.*, Phys. Lett. B **469** (1999) 25.
- [44] G. F. Chew and S. Mandelstam, Phys. Rev. **119** (1960) 467.
T. N. Truong, Phys. Rev. Lett. **61** (1988) 2526, **67** (1991) 2260.
E. Oset, J. A. Oller, J. R. Pelaez and A. Ramos, Acta Phys. Polon. B **29** (1998) 3101.
U. Meissner and J. A. Oller, Nucl. Phys. A **673** (2000) 311.
A. Gomez Nicola, J. Nieves, J. R. Pelaez and E. Ruiz Arriola, Phys. Lett. B **486** (2000) 77.
- [45] P. F. A. Goudsmit, H. J. Leisi, E. Matsinos, B. L. Birbrair and A. B. Gridnev, Nucl. Phys. A **575** (1994) 673.
A. Gashi, E. Matsinos, G. C. Oades, G. Rasche and W. S. Woolcock, hep-ph/9902207, hep-ph/0009081.
- [46] J. Gasser, H. Leutwyler, M.P. Locher and M.E. Sainio, Phys. Lett. B **213** (1988) 85.
J. Gasser, H. Leutwyler and M.E. Sainio, Phys. Lett. B **253** (1991) 252, 260.

- [47] B. Ananthanarayan and P. Büttiker, *Eur. Phys. J. C* **19** (2001) 517.
- [48] G.Hite and F. Steiner, *Nuovo Cim.* **18A** (1973), 237